



Successful Tests of Adaptive Optics

F. MERKLE, ESO

P. KERN, P. LÉNA, F. RIGAUT, Observatoire de Paris, Meudon, France

J. C. FONTANELLA, G. ROUSSET, ONERA, Châtillon-Sous-Bagneux, France

C. BOYER, J. P. GAFFARD, P. JAGOUREL, LASERDOT, Marcoussis, France

An old dream of ground-based astronomers has finally come true, thanks to the joint development of a new technique in astronomical imaging – called *adaptive optics* –, by ESO and Observatoire de Paris, ONERA (Office National d'Etudes et de Recherches Aérospatiales), LASERDOT (formerly CGE) in France.

It has been demonstrated that this technique effectively eliminates the adverse influence of atmospheric turbulence on images of astronomical objects, yielding images almost as sharp as if the telescope were situated in space.

A Break-through in Optical Technology

In a major technological breakthrough in ground-based astronomy the VLT Adaptive Optics Prototype System (also referred to as Come-On) has now proved its ability to overcome this natural barrier during a series of successful tests in the period 12–23 October 1989. They were performed at the coudé focus of the 1.52-m telescope at the Observatoire de Haute-Provence (OHP), France.

The extensive tests showed that it was possible to effectively “neutralize” the atmospherically induced smearing of a stellar image by a closed-loop correction system. In this way stellar images were obtained at infrared wavelengths whose sharpness was only limited by the telescope aperture, i.e. diffraction limited images.

On each of the ten nights, infrared exposures were made of about 10 bright stars ranging from the visible magnitude 0.7 to 4.7 (including Capella, Deneb, Betelgeuse, γ^1 And, and others). The

Why Adaptive Optics?

Ever since the invention of the telescope in the early 17th century; astronomers have had to accept that the quality of astronomical images obtained with ground-based instruments is severely limited by a factor which is beyond their control, that is the turbulence in the Earth's atmosphere.

For a long time it was thought impossible to avoid this natural limit. Now, for the first time, this old problem has been demonstrably solved.

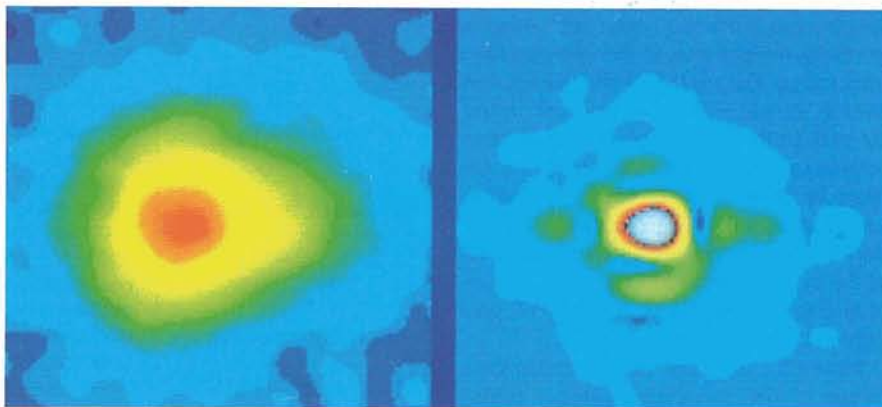


Figure 1: Imaging of Deneb in the K-Band without and with adaptive feedback loop activated. The image diameter shrinks from 1.0 arcsec to 0.37 arcsec which is the diffraction limit in the K-Band ($2.2 \mu\text{m}$).

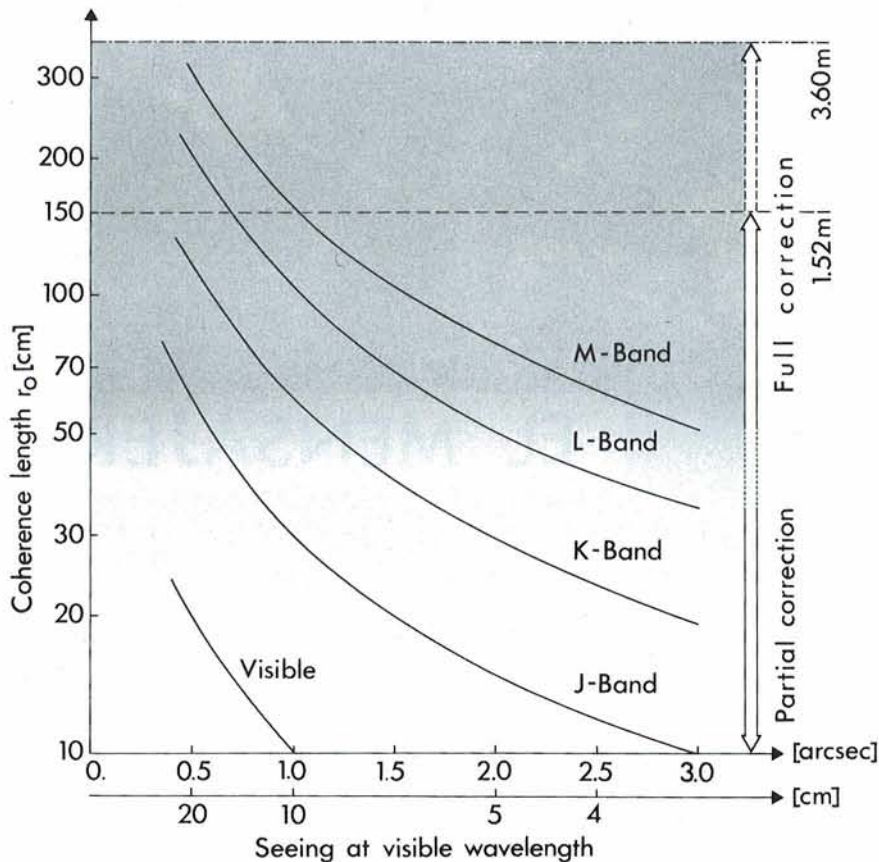


Figure 2: The application range of this prototype adaptive system is marked as the shaded zone in the diagram for different wavelengths bands (Visible, J-, K-, L-, and M-band). The coherence length r_0 for the various wavelengths is plotted as a function of the seeing disk diameter at visible wavelength. When r_0 exceeds approximately 40 cm, which corresponds to the mean actuator spacing on the deformable mirror, then full correction is obtained. Below this value only partial correction is possible. When r_0 reaches the diameter of the telescope, then the telescope is only limited by its optical quality and adaptive optics is not required.

infrared images have been taken in the J, H, K, L, and M bands. Several integrations were made through each filter without the adaptive feed-back, immediately followed by an equal number with the device activated. Depending on the brightness of the observed star, each exposure lasted between 10 and 100 seconds. At this time the prototype system is not optimized in light efficiency. For wavelengths of $3.5 \mu\text{m}$ and longer, the diffraction limit was always reached, irrespective of the atmospheric turbulence. During the observations, the seeing in the visible wavelength band ranged from 0.7 arcsec to 2.5 arcsec with equivalent seeing cell sizes (coherence lengths) r_0 of 14 to 4 cm. During the phases with better seeing, diffraction limited imaging was even reached at $2.2 \mu\text{m}$ (0.3 arcseconds) and a noticeable improvement was seen at $1.2 \mu\text{m}$. Figure 1 shows an example.

Figure 2 displays the application range of this prototype system under various seeing conditions. The diagram shows for the 4 infrared wavelengths ranges the relation between the image

size in the visible and the coherence length r_0 at infrared wavelengths. This adaptive optics prototype system is capable to fully correct the atmospheric turbulence if the seeing conditions are such that the coherence length r_0 in the infrared range is larger than 30 to 50 cm. 30 to 50 cm corresponds to the mean actuator spacing on the deformable mirror. If the operation falls in an r_0 range below this value, the correction is only

TABLE: Technical Data.

| | |
|---------------------|---|
| Deformable mirror: | 19 piezoelectric actuators +/- 7.5 micrometre stroke |
| Tip/tilt mirror: | gimbal mount |
| Wavefront sensor: | piezoelectric actuators Shack-Hartmann principle 5 x 5 and 10 x 10 subapertures 100 x 100 intensified Reticon detector built-in reference source additional field selection mirror |
| Wavefront computer: | dedicated electronics host computer based on Motorola 68020 |
| Control algorithm: | modal correction scheme mirror eigenmodes |
| Camera: | 32 x 32 InSb array camera (SAT detector) additional chopping mirror |

partial. Are the application conditions above the dashed line, then no improvement can be achieved, because the telescope (in case it is of perfect quality and well aligned) is by itself diffraction limited. A first analysis of the results confirmed the theoretical expectations. Whenever the observing conditions were in the operation range of the system, perfect image quality was reached, as demonstrated by the well-known Airy ring around the star image.

How Does it Work?

Adaptive Optics is based on an optical/electronic feed-back loop. In its physical principles it is equivalent to *active optics* as it is applied in the ESO New Technology Telescope (NTT) (see *Messenger* Nos. 53 and 56). But for the compensation of the atmospheric turbulence, the system has to correct much faster than in the active case and therefore the wavefront correction cannot be done by the primary mirror. Therefore,



Figure 3: The adaptive system at the coude focus of the 1.52-m telescope at OHP.



Figure 4: The control panel of the adaptive prototype system. The large rack in the upper left contains the wavefront computer. It is based on dedicated processors for a fast wavefront analysis.

the optical system must include an additional, small deformable mirror which can change its surface profile fast enough in a way that exactly compensates for the distortions of the wavefront after it has passed through the atmosphere.

In the present prototype system the mirror surface is deformed by 19 piezoelectric actuators. The information about how to deform the mirror comes from a wavefront sensor which allows to measure the shape of the distorted light wavefront sampled in 5 by 5 sub-apertures. It requires a very fast and powerful computer to calculate how the actuators located behind the deformable mirror have to push and pull the mirror surface. Figures 3, 4, and 5 show the system installed at the coudé focus of the 1.52-m telescope, its control panel, and a close-up view of the optomechanics and its principle. The main data of the prototype system are given in the Table. The major components of this system and the system in the

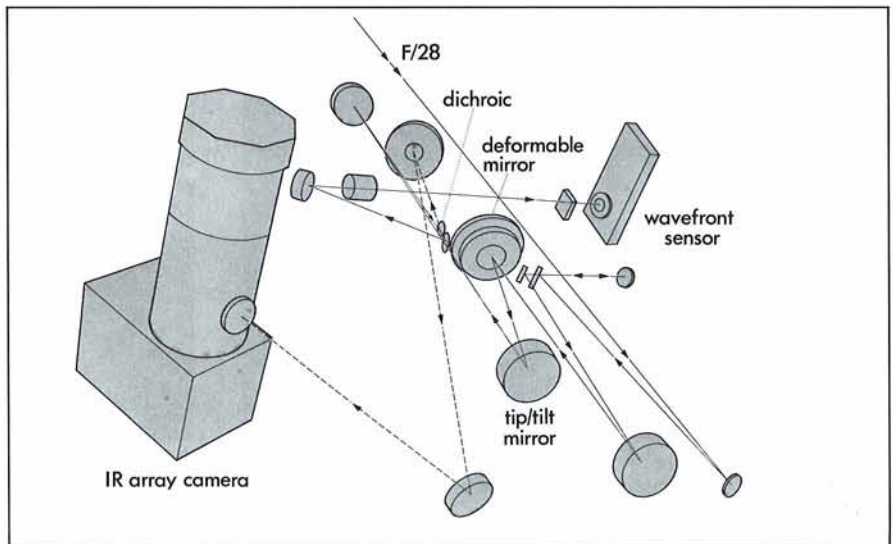
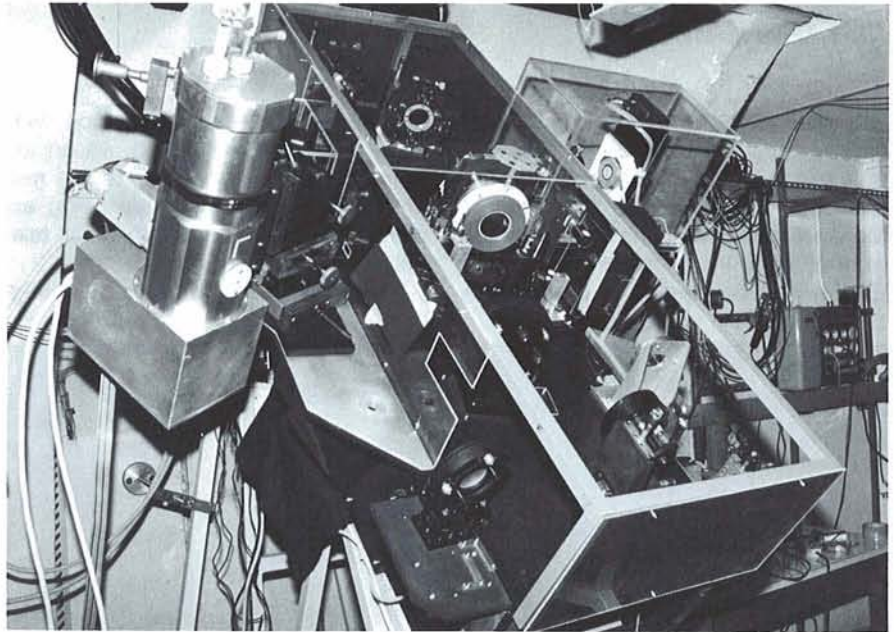


Figure 5: Close-up view of the adaptive system (upper) and schematics of the optical lay-out (lower). The F/28 beam enters from the top, a focal reducer changes the ratio to F/8 (for the ESO 3.6-m telescope), and an off-axis parabola in front of the deformable mirror collimates the beam. After the deformable mirror, the beam is reflected at a gimbal mounted mirror for tilt correction and then a second off-axis parabola refocusses it. The infrared and visible part are separated by a dichroic mirror. The infrared part is relayed to the IR array camera, while the visible part is reflected to the wavefront sensor. ▶

laboratory has been described earlier in *Messenger* Nos. 52 and 57.

Future Plans

This prototype system will soon be installed at the ESO 3.6-m telescope at La Silla. The encouraging results represent a first, major step on the way towards an adaptive system for the 16-m Very Large Telescope (VLT). An upgrade of the deformable mirror to approximately 50 actuators, a wavefront sensor with 10 by 10 sub-apertures, and an even faster computer system will be the next step. Such a system could then be designed and built for the NTT.

The new technology makes it possible to achieve the theoretical limits for optical imaging in the infrared wavelength range by means of a medium-sized telescope. Further developments will aim at perfecting the technique for larger telescopes and at shorter wavelengths. Not only will present-day telescopes benefit,

but this technique will revolutionize the exploitation of the next-generation telescopes, such as the ESO VLT, and, in many cases, compete with observations carried out by telescopes deployed in space.

A scientific-technical paper, describing the first adaptive optics results, is expected to appear soon in *Astronomy & Astrophysics*.

Acknowledgements

The design and construction of this system is the product of a three-year effort, involving a collaboration between the European Southern Observatory (ESO), Observatoire de Paris, the Office National d'Etudes et de Recherches Aérospatiales, and LASERDOT.

The project received support from ESO, the Ministère de la Recherche et de la Technologie (France), Ministère de l'Education Nationale, Direction de la Recherche (France), Université Paris VII, Centre National de la Recherche Scientifique (CNRS) and Institut National des Sciences de l'Univers (INSU).

The early development of critical optical components of the system has been independently supported by La Direction des Recherches et Etudes Techniques (DRET), Ministère de la Défense, France.

References

For additional references the following papers are recommended:

- F. Merkle (1988), "Adaptive Optics Development at ESO", Proceedings of the ESO Conference on "Very Large Telescopes and their Instrumentation", Garching 21-24 March, 1988.
- P. Kern, P. Léna, G. Rousset, J.C. Fontanella, F. Merkle, J.P. Gaffard (1988), "Prototype of an adaptive optical system for infrared astronomy", ref. as above.
- F. Merkle (1988), in SPIE Proceedings 1013: "Optical Design Methods, Applications and Large Optics", Hamburg, F.R.G., September 1988.
- P. Kern, P. Léna, J.C. Fontanella, G. Rousset, F. Merkle, J.P. Gaffard (1989) in SPIE Proceedings 114: Symposium on "Aerospace Sensing", Orlando, FL, March 1989.

Astronomical Observations With the NTT During Commissioning

M. TARENGHI, ESO

It was with particular pleasure and emotion that I received the first astronomical images obtained with the NTT from Chile. As the NTT Project Manager it was satisfying to see that the work of many – both inside and outside ESO – had converged to produce an

instrument whose performance was even better than expected. As an astronomer it was fascinating to see new details of objects which are being explored by many of us with other telescopes but at lower resolution.

The illustrations of 4 images (Fig-

ures 1-4) are spectacular examples of the possibilities of the new telescope.

It is important to understand the value and limits of these observations obtained during the commissioning phase of the NTT which represents a complex and delicate period for a new telescope.

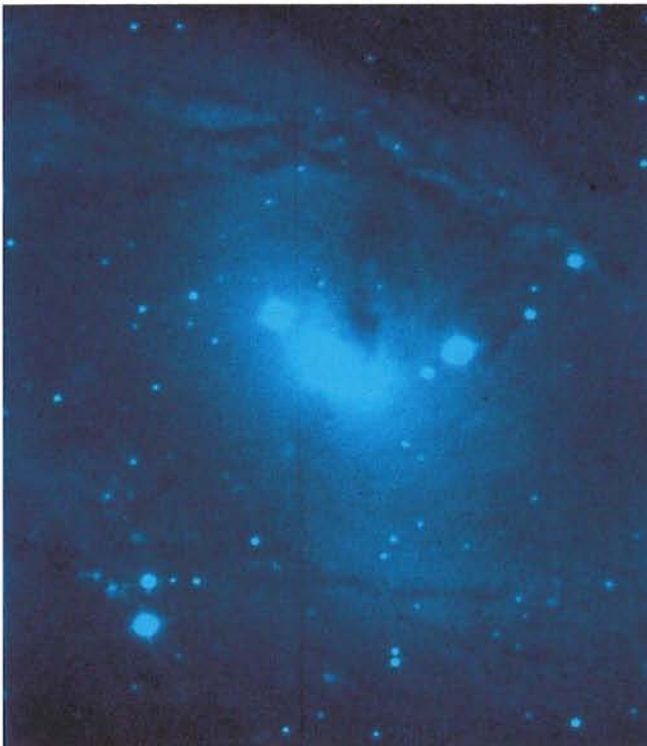


Figure 1: NGC 6300. The short exposure of only 30 seconds of this SB galaxy shows dust features in the inner part and on the nucleus that resemble the horse head in the Orion nebula. Seeing is 0.7 arcsec.

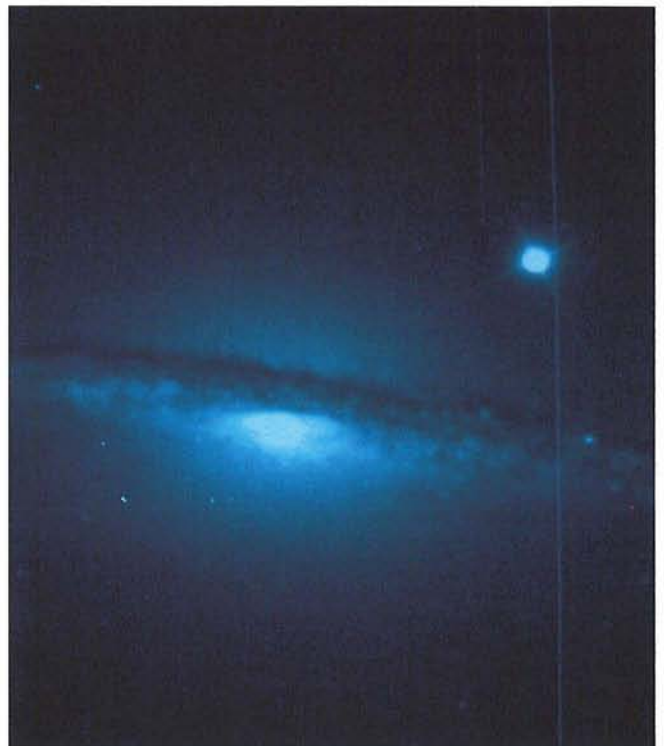


Figure 2: NGC 681. An edge-on dust spiral.

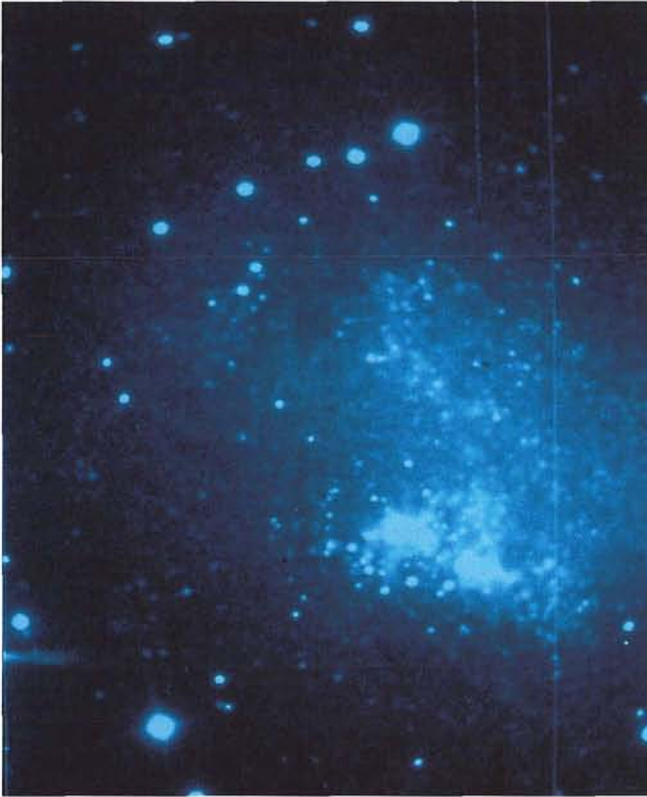


Figure 3: IC 4662. Magellanic Cloud type irregular galaxy at the distance of 4 Mpc studied with ESO telescopes in 1983 by M. Rosa and G. Schnur. Evidence of violent star formation activities was detected. The galaxy is resolved in this NTT image which shows very clearly the two giant HII regions embedded in a super association. Seeing 0.65 arcsec.



Figure 4: NGC 613. The spectacular bar spiral SBb in which – thanks to the high resolution in this NTT picture – one can detect the detailed structure of dust filaments. Two major dust lanes extend along the bar into the nuclear region.

All images were obtained without the adapter/rotator, therefore without the on-line active optics system. Moreover the modifications of the support system with the activation of the three fixed points was not implemented. Except for the region around the zenith, the optical quality was not optimal and we expect to be able to guarantee perfect images all over the sky only with the full implementation of the adapter/rotator and its image analyzer.

In the course of the last months many experiments have been performed on the seeing of the NTT. Studies of the behaviour of the rotating building, its flaps and windscreen, clearly indicate the advantages of this new design and the importance of the flaps to the

point that the observer will be discouraged to operate the NTT with the flaps closed.

The commissioning work is proceeding actively and the adapter/rotator No. 1 was mechanically and electronically installed on the NTT in October. During the month of November the modifications of the fixed points were started and the implementation of the image analyser and guiding system initiated. For the second half of December the NTT will perform in its complete configuration with EFOSC 2 at the Nasmyth focus.

The 9 months from the first light obtained on 23 March to the first deep exposure seems at first sight to be very long but the complexity of the NTT and the need to cope with a seeing better

than that forecast required greater tuning.

The first visiting astronomer is expected mid-January and we are impatient to receive constructive criticism to make even greater improvements on the NTT. In April 1990 the second adapter/rotator will be implemented and May/June will see the integration of EMMI. It will be commissioned during the European summer.

I would not like to complete this report without taking the opportunity to thank all those who have observed with the NTT in this critical period, for their unremitting passion and understanding for the inevitable number of difficulties and conflicts between technical necessity and astronomical dreams.

The First Observations With the NTT

J. MELNICK, ESO

1. Introduction

The NTT was used for astronomical observations during two runs in May and August 1989. Both the telescope and the instrument (EFOSC2) worked

remarkably well during both runs, so there was ample time for astronomical observations.

EFOSC2 was bolted onto the tele-

scope without the instrument rotator/adapter and this meant that for most positions on the sky the exposure times could not exceed a few minutes.

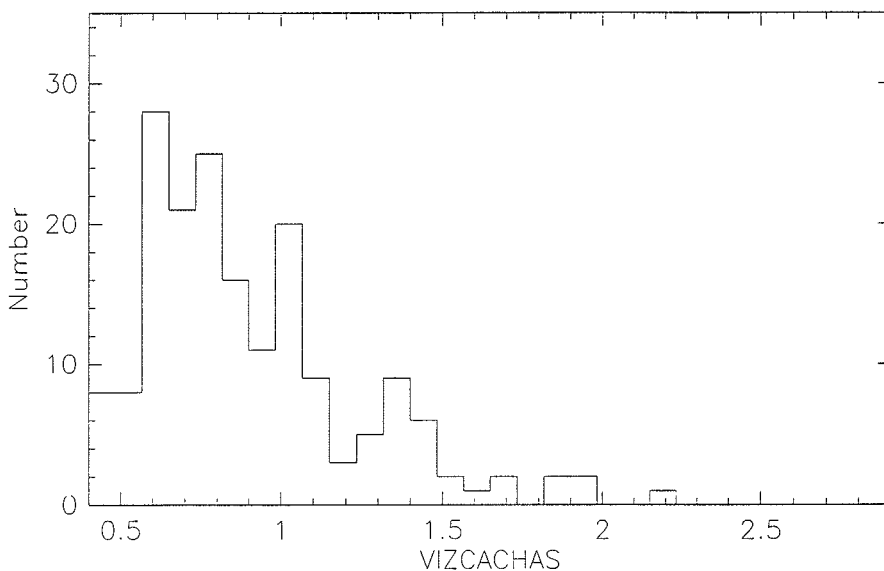
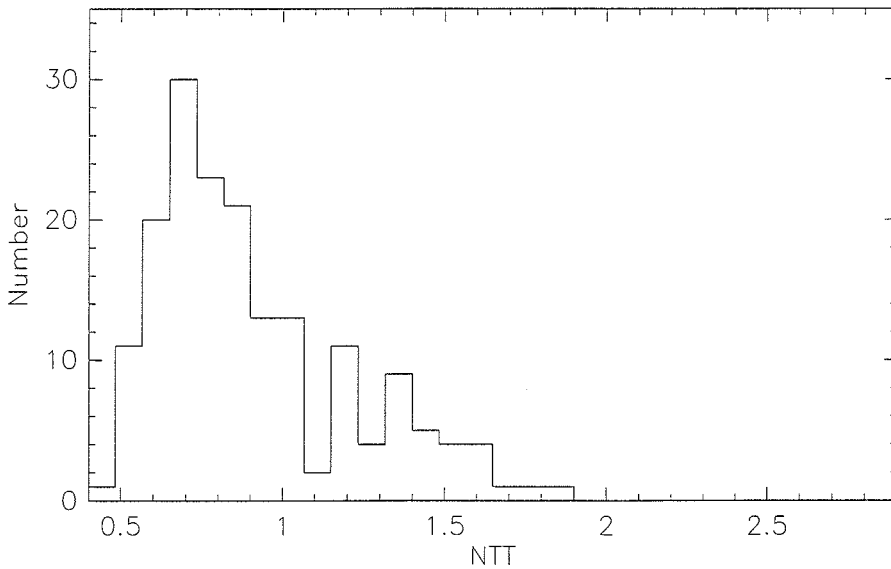


Figure 1: *Distribution of seeing at the NTT (top). Seeing measured at Vizcachas during the NTT run (bottom).*

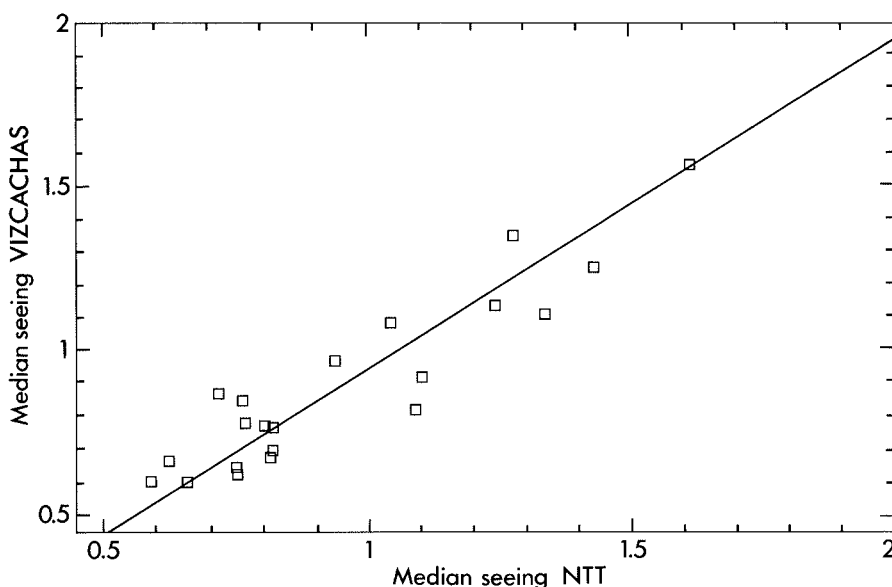


Figure 2: *Night to night comparison between the seeing recorded at the NTT and Vizcachas.*

2. Seeing

The superb optical quality of the telescope and the careful design of the dome allow the NTT to fully exploit the excellent quality of the La Silla sky.

During the second test run (August 4 to September 9), an effort was made to record the seeing systematically, every thirty minutes whenever possible. In this way, 345 seeing measurements were accumulated. For 224 of these observations, simultaneous measurements from the seeing monitor on Vizcachas were also recorded. The results are presented in Figure 1. The median seeing values are $0''.76$ at Vizcachas and $0''.80$ at the NTT (FWHM of stellar images referred to the zenith at 500 nm). The difference is not significant if one considers that the active optics system was not operational during the run, and the loads on the actuators were adjusted for positions close to the zenith.

3. First Scientific Results

The good seeing conditions which prevailed during the tests allowed us to tackle several interesting scientific problems in spite of the limitations imposed by field rotation. A “flexible scheduling” scheme was implemented where the telescope was allocated according to seeing. In fact, an important fraction of the observations were done by the telescope operators who selected the observing programmes according to the seeing conditions.

Figures 3 and 4 illustrate two results from these observations. Figure 3 shows a V frame of the compact globular cluster M80. The FWHM of the stellar images is about $0''.5$ in this image. Images of a number of compact clusters were obtained under very good seeing conditions aimed at investigating the colour-magnitude diagrams in the central regions of very compact clusters.

Figure 4 shows an R frame of the gravitationally lensed quasar Q 2237 + 0305 (Einstein’s cross). The four images of the QSO plus a fifth faint one, located near the centre of the cross (possibly the nucleus of the lensing galaxy), can be clearly seen in this image taken with $0''.65$ seeing. The QSO was systematically monitored during the run to search for microlensing effects.

A number of early type spirals were imaged under very good seeing conditions in order to investigate the structure of their central regions.

Acknowledgements

It is a pleasure to thank all the TRS people who participated in the NTT project for helping us to learn how to oper-

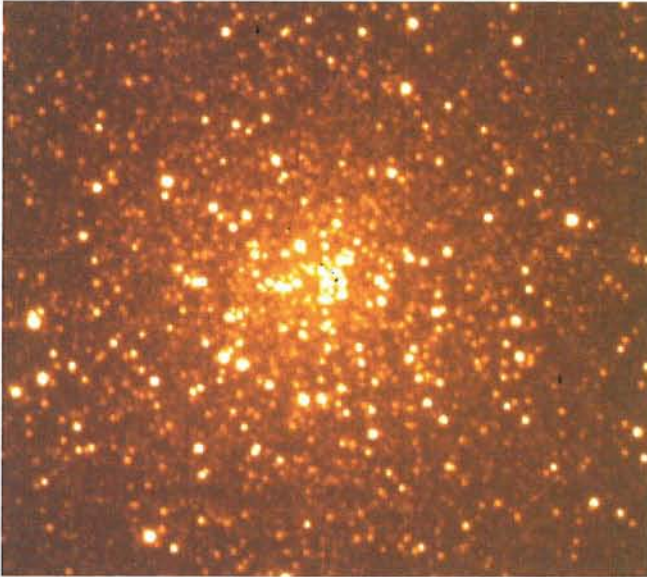


Figure 3.

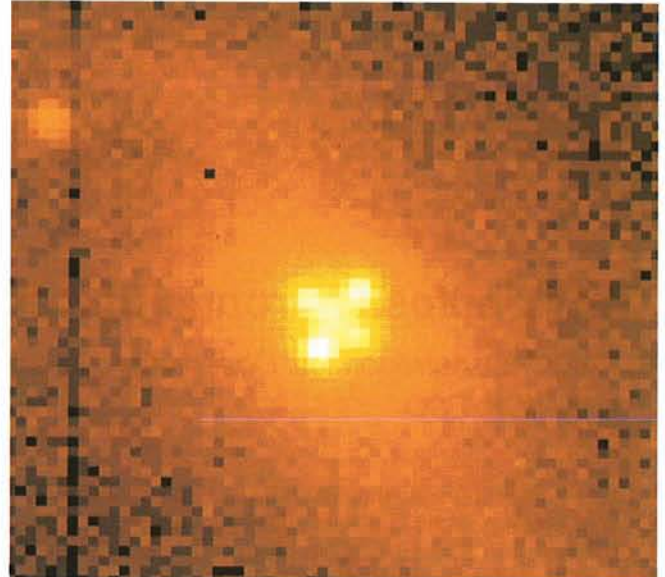


Figure 4.

ate the telescope. In particular we would like to thank Mr. Gaetano Andreoni for his help with the software and with the active optics system.

Special thanks are due to the night

assistants, Messrs. Jorge Miranda and Manuel Pizarro for their skill and patience to master the still unfinished telescope and building control system. They performed a large fraction of the

observations very efficiently, and their work was instrumental in allowing us to compile large catalogues of planetary nebulae, QSOs, and galaxies observed with unprecedented spatial resolution.

Spatially Resolved Images of the Optical Counterpart to Circinus X-1

A. MONETI, ESO

We have obtained high resolution images in which the optical counterpart to the X-ray binary Circinus X-1 is resolved. The images were obtained on 16 and 18 August 1989 using EFOSC2 in direct imaging mode on the ESO New Technology Telescope (NTT). A $30'' \times 30''$ portion of each image, centred on Cir X-1, is shown in Figure 1. The V and R images obtained on 16 August are reproduced in panels a and b, while the R and I images obtained on 18 August are reproduced in panels c and d. The integration time was 60 sec for all images; and all images have been bias corrected and flat fielded. The FWHM of the stellar profiles was $0''.5$ on 16 August and $0''.9$ on 18 August.

Argue et al. (1984) presented B and R images obtained in $\sim 1''.5$ seeing in which the position of Cir X-1, accurately determined by the authors from radio VLBI during a flare, is shown to be located at the southern end of an extended structure. In the NTT images, that extended structure is resolved into three separate stars, and the position of Cir X-1 coincides with the southernmost of these stars. Accurate photometric

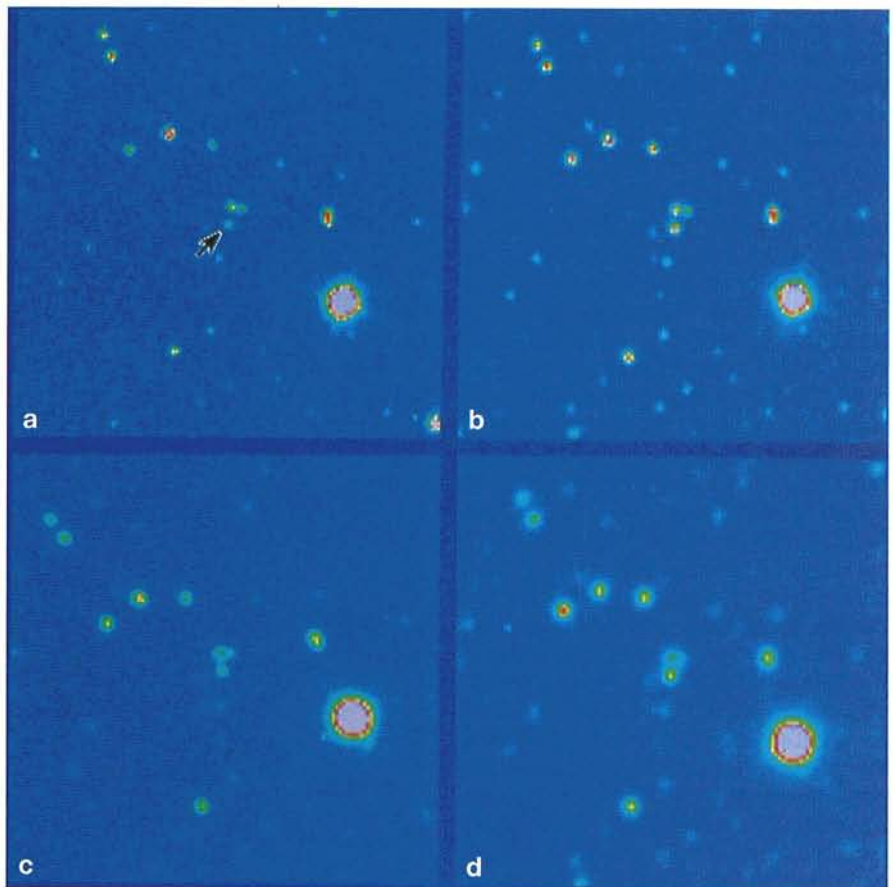


Figure 1: Images of Cir X-1 in V, R (upper panels), and R, I (lower panels). North is up and East is to the left. Cir X-1 is identified with the southernmost of the three stars in the centre of the field. The FWHM of the stellar profiles is $0''.5$ in the top panels, and $0''.9$ in the lower panels.

measurements are in progress, but a comparison of our V, R, and I images shows that this star is quite red. This is a well-known property of Cir X-1 (Whelan et al. 1977), and corroborates our identification of this star with Cir X-1. For

further confirmation, we will attempt to monitor the optical source during a flare. The detection of such a flare in the visible will further secure the identification of the aforementioned source with the X-ray source.

References

- Argue, A.N., Jauncey, D.L., Morabito, D.L., and Preston, R.A., 1984: *Mon. Not. R.A.S.*, **209**, 11 p.
 Whelan, J.A.J., et al., 1977: *Mon. Not. R.A.S.*, **181**, 259.

The Nebulosity Around BL Lac Objects

R. FALOMO, *Astronomical Observatory, Padova, Italy*

J. MELNICK, *ESO*

BL Lac objects (hereinafter BLL) are a class of active galactic nuclei which exhibit strong non thermal emission from radio to X-ray frequencies. Strong and rapid variability, together with optical polarization and very weak or absent emission/absorption features, are defining properties of the class.

In several cases BLL are surrounded by a nebulosity; however, for only 7 objects, out of the ~ 100 currently attributed to this class, the nebulosity has been studied in detail and has been shown to be consistent with an elliptical galaxy. In a dozen other cases, only indirect evidence of the presence of a galaxy, either from the detection of so-called *fuzz* or marginal detection of stellar absorption lines in the spectra, has been reported. Moreover, in some cases the shape of the nebulosity does not conform with that of a normal elliptical: asymmetries and/or complex structures are visible.

The detailed study of these nebulosities (and of the close environment of BLL), a key tool for understanding the nature of this intriguing class of objects, requires the ability to detect faint features very close to bright point-like sources. This is not an easy task.

With the ESO New Technology Telescope in operation, this requirement is met. In fact, several images of selected BLL (in all ten objects) have now been obtained with the NTT (+ EFOSC2 + CCD No. 5 with R filter) in good seeing conditions (0.6 to 0.8 arcsec) during the commissioning time. A wealth of information about the nebulosity surrounding the observed objects is present in the frames and is now subject to detailed analysis. We can anticipate that for a substantial fraction of the objects the presence of previously undetected nebulosities or faint structures or companions, only a few arcseconds apart, can be clearly demonstrated. A full report on these results will be presented in a forthcoming paper (Falomo and Melnick, in preparation).

As an example of the results obtained

so far, we here mention the case of the well studied BL Lac object PKS 2155-30, one of the brightest of its class. The V-magnitude varies from 12.8 to 14.0, and it was discovered as the counterpart of the X-ray source H2155-30 by Griffiths et al. (1979). These authors reported the presence of an east-west asymmetric nebulosity around the object (slightly extended to the east) on a red plate which was exposed for 30 minutes. By analogy with other BLL, they concluded that *the nebulosity is very likely the image of an elliptical galaxy*. Five years later Bowyer et al.

(1984) obtained spectra of the nebulosity through a 2 arcsec slit centred 3 and 4 arcsec east of the nucleus (on the side of the reported diffuse elongation). In the latter position, absorption features due to a stellar population were detected at redshift $z = 0.117$. This redshift is however difficult to reconcile with absorption features observed in the X-ray (Canizares and Kruper, 1984; Treves et al. 1989) and UV spectra (Maraschi et al. 1988).

In order to verify the presence of the nebulosity around this object and investigate its nature we obtained two short

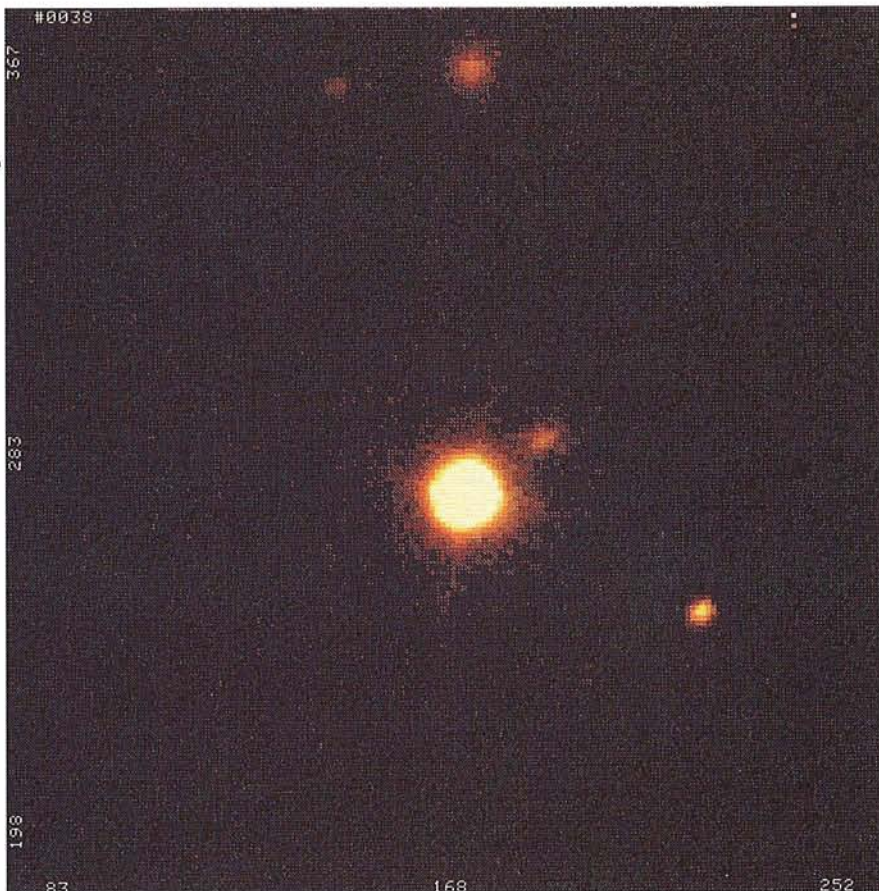


Figure 1: An NTT (EFOSC 2 + CCD No. 5) 2-minute exposure behind an R filter showing the bright BL Lac object PKS 2155-30 (centre) together with the newly discovered extended object at an angular distance of 4.5 arcsec.

exposures (30 sec and 2 min, R filter) of the source near minimum brightness ($V = 13.8$) on August 12, 1989. No evidence of nebulosity around PKS 2155-30, down to a surface brightness of $m_R \approx 23$ mag/sq. arcsec is present, but in both images, a relatively faint ($m_R \approx 19$) object, about 4.5 arcsec east of the nucleus, is clearly seen (Fig. 1). This object is marginally resolved with

some elongation in the east-west direction.

Thus the redshift reported by Bowyer et al. (1984), according to the quoted slit position, is more likely attributable to the angularly close object, now seen in our CCD frames, rather than to the BLL itself. Spectroscopy of the newly discovered object around PKS 2155-30 is being obtained.

References

- Bowyer, S., Brodie, J., Clarke, J.T., and Henry, J.P., 1984, *Ap. J.*, **278**, L 103.
 Canizares, C. and Kruper, J., 1984, *Ap. J.*, **278**, L 99.
 Griffiths, R.E., Tapia, S., Briel, U., and Chaisson, 1979, *Ap. J.*, **234**, 810.
 Maraschi, L., Blades, J.C., Calachi, C., Tanzi, E.G., and Treves, A., 1988, *Ap. J.*, **333**, 660.
 Treves, A. et al. 1989, *Ap. J.*, **341**, 733.

Possible Transition Objects Discovered with the NTT

H. E. SCHWARZ, ESO

The 3.5-m NTT with EFOSC2 has been used to make images of about 280 planetary nebulae (PN) in two narrow passbands centred on $H\alpha$ and [OIII] 5007. These data will be published in the near future in the form of a pictorial atlas. Since both [OIII] and $H\alpha$ images were taken, a map of the high excitation gas can be made by dividing the frames; an example has been presented by (1).

Previously unknown faint haloes around PN have also been found during our survey. These haloes are important for the "missing mass" problem in PN: the mass of an average AGB (Asymptotic Giant Branch) star is greater than the combined masses of the central star (white dwarf) and nebula of typical PN. Haloes can contain up to ten times more mass than the bright central nebula (2).

There are many other interesting problems which can be addressed using these images, especially when combined with other data. Here I will discuss one application: the study of transition objects or proto-PN. Transition objects or TOBs are those rare objects that are in the rapid evolutionary phase between upper AGB and PN. They have started to produce a fast, tenuous wind which interacts with the old, slow and dense wind to form shocked ansae and bubbles. The importance that the study of these TOBs has, lies in the possible impact on our ideas about PN formation and, more generally, on the poorly understood final evolutionary stages of all intermediate mass stars. Observationally, these objects are characterized by a bipolar shape, usually with ansae formed by shocked gas, a strong far IR, and a smaller optical or near IR excess and emission lines at very high velocities.

Several such objects have been found using the NTT/EFOSC2 combination, mainly due to the superb seeing at this telescope. Figure 1 shows an $H\alpha$ image of He2-1312, a PN which was previously classified as stellar. The seeing was

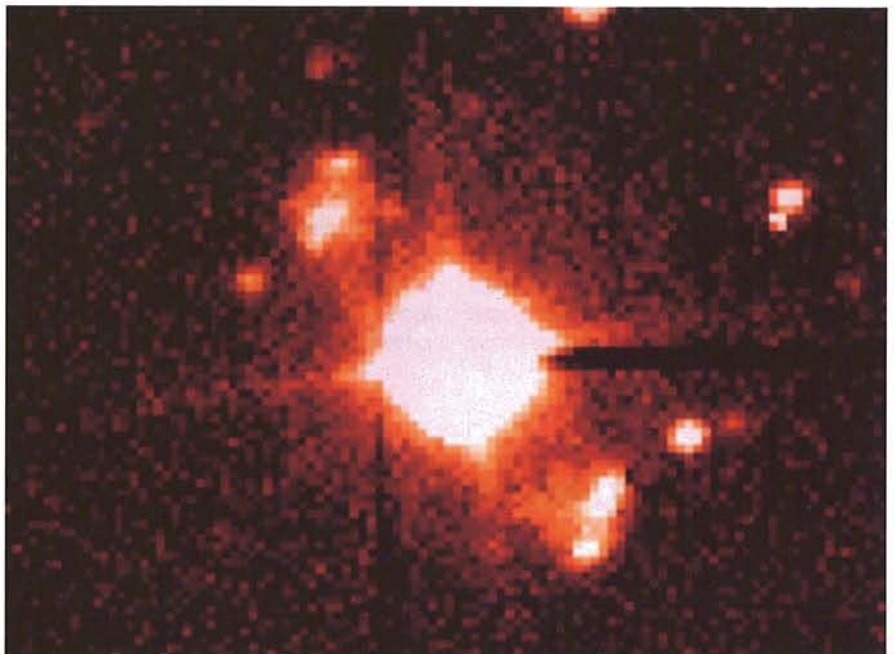


Figure 1: A 2-min $H\alpha$ exposure of He2-1312. Seeing is about 0.75 arcsec FWHM. This object was previously classified as a point source.

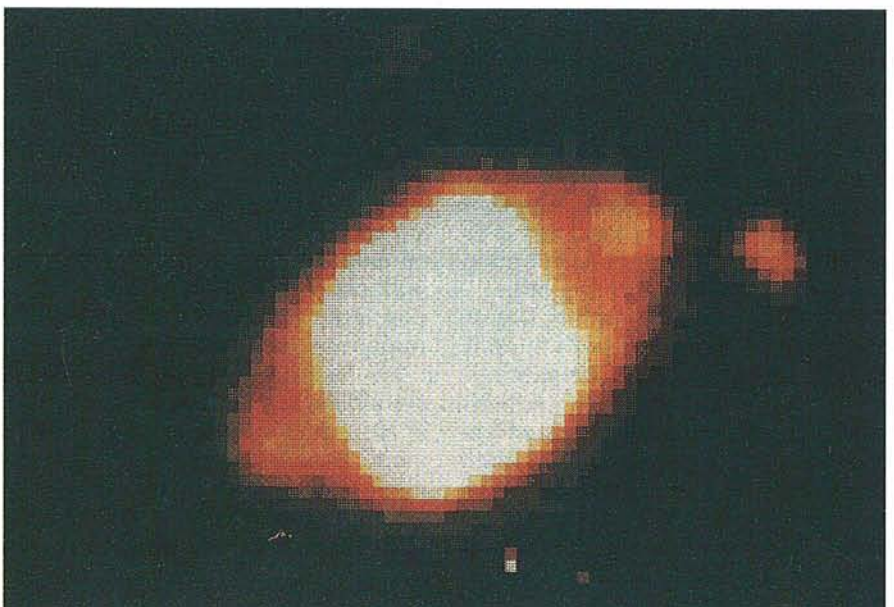


Figure 2: A 10-min $H\alpha$ exposure of 19+501. Seeing is 0.8 arcsec FWHM. Note the faint, high excitation blobs.

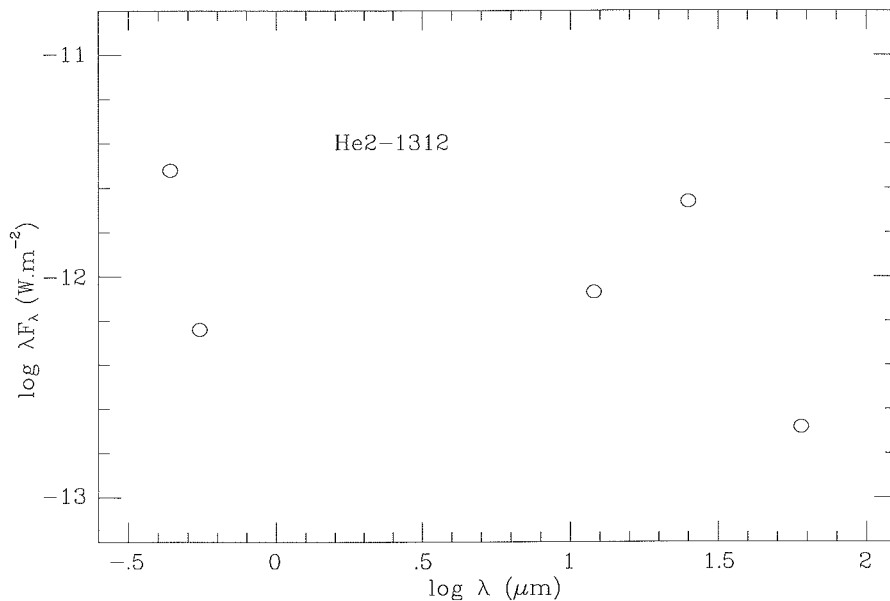


Figure 3: The energy distribution of He2-1312. Note the strong far IR excess.

about $0''.75$ FWHM. Figure 2 is a recently discovered PN ($19+5^{\circ} 1$) which was described as having a FWHM of $3''.5$ with $2''.2$ field stars (3)! In the NTT image, with a seeing of $0''.8$, the object shows intricate structure consisting of two ansae connected by faint emission to a cross

shaped central structure. The overall size is about $10''$.

Spectroscopy of both sources, again using the NTT/EFOSC2, indicates a complicated velocity structure with velocity differences of up to 560 km s^{-1} . Emission lines typical of PN are present,

with strong [O III], H β , [N II] lines and H α . In He2-1312, [O III] is absent in the outer ansae.

The sources are both in the IRAS PSC and the partial energy distribution of He2-1312 is shown in Figure 3, and is typical of this kind of object.

More data are clearly needed, kinematic mapping, near IR photometry, optical photometry and CO measurements are all useful to characterize these sources. On the basis of the evidence collected so far, I will stick my neck out and say that $19+5^{\circ} 1$ and He2-1312 are transition objects.

Considering the preliminary state of the NTT/EFOSC2 at the time of observing (no instrument rotator, no active optics operative, no spectral calibration lamps), the high quality of the obtained data points to a very rosy future for what without a doubt now is the best telescope in the world.

References

- (1) Schwarz, H.E., Melnick, J., 1989, in "From Miras to PN", in press.
- (2) Machado, A., Pottasch, S.R., 1989, *Astron. Astrophys.* **222**, 219.
- (3) Cappellaro, E., Turatto, M., Sabbadin, F., 1989, *Astron. Astrophys.* **218**, 241.

Narrow-Band Imaging of M87 with the NTT

B. JARVIS, ESO

Already during the current installation phase (August 1989), ESO's New Technology Telescope (NTT) presents an opportunity for useful science due to its large aperture and good tracking (no autoguider yet) on a site of excellent seeing. The greatest limitation is the lack of a field rotator which severely limits the maximum exposure times possible without obtaining unacceptably trailed images. Over most of the observable sky, this maximum exposure time is less than 5 minutes if one is to avoid more than 1 arcsecond of trailing one arcminute from the field centre.

With these points in mind, in August 1989, EFOSC 2, equipped with an RCA CCD ($0''.259 \text{ pixel}^{-1}$) was used to image the peculiar galaxy M87 (Virgo A, NGC 4486, and whose nuclear spectrum has similarities to a Seyfert galaxy's nucleus) through narrow-band filters centred at the galaxy's redshifted wavelengths of [O III] (5007 \AA), [N I] (5200 \AA), H α (6563 \AA), and [S II] ($6716 + 6731 \text{ \AA}$). Spectra of the core region of M87 taken earlier by the author with EFOSC 1 at the 3.6-m also showed the presence of

strong [N II] (6584 \AA) lines. Since the FWHM of the H α filter was about 70 \AA , centred at redshifted H α , the light of [N II] was also passed, making it difficult to separate the relative contributions from these two lines (see note 1).

Figure 1 shows the average of two 5-minute exposures of M87 (lightly smoothed) in the light of H α + [N II]. The background galaxy has been removed by the subtraction of a near continuum image taken at 6480 \AA . Note that due to the late time of the year at which these observations were made, the altitude of M87 was never more than 25° . However, even at this extreme airmass, the seeing was still better than $1''$!

The interesting feature in Figure 1 is the extensive fine filamentary structure of H α + [N II], which, although concentrated towards the centre of M87, extends more than $1'$ to the southeast of the nucleus terminating in a bright three knot structure. There is also a bright

"jet-like" feature pointing in a NW direction from the core and inclined about 20° to the N of the well-known radio and optical jet.

The [O III] emission, shown in Figure 2, is also very interesting. This figure is the same as Figure 1 except that the [O III] emission is shown as an insert as observed relative to the H α + [N II] features. The [O III] is extended symmetrically about the broadband photometric centre of M87 and very closely aligned with the H α + [N II] feature and not the radio structure. This is very curious in view of recent work by Haniff, Wilson and Ward (1988) and also by Wilson and Baldwin (1989). Haniff et al. found that in a sample of 10 galaxies with "linear" radio sources, *all* showed alignment (within measurement errors) of the [O III] emission line region and the radio structures. Wilson and Baldwin's observations of another Seyfert galaxy, 0714-2914 showed the same effect, i.e. alignment of [O III] emission with the radio. Moreover, Whittle et al. showed in a sample of 11 Seyferts that several showed clear evidence for double-lobe

Note 1: Meisenheimer and Hippelein (*Sterne und Weltraum*, May, 1989, p. 292) report that $I([\text{NII}])/I(\text{H}\alpha) \approx 2$.

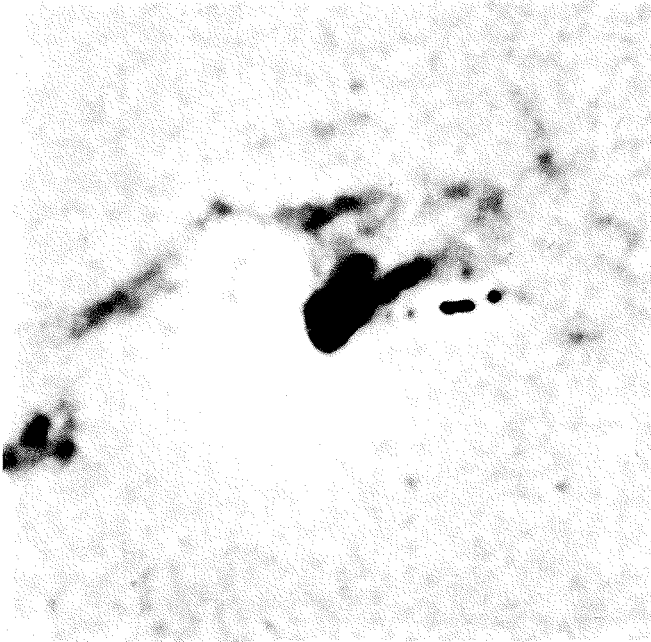


Figure 1.

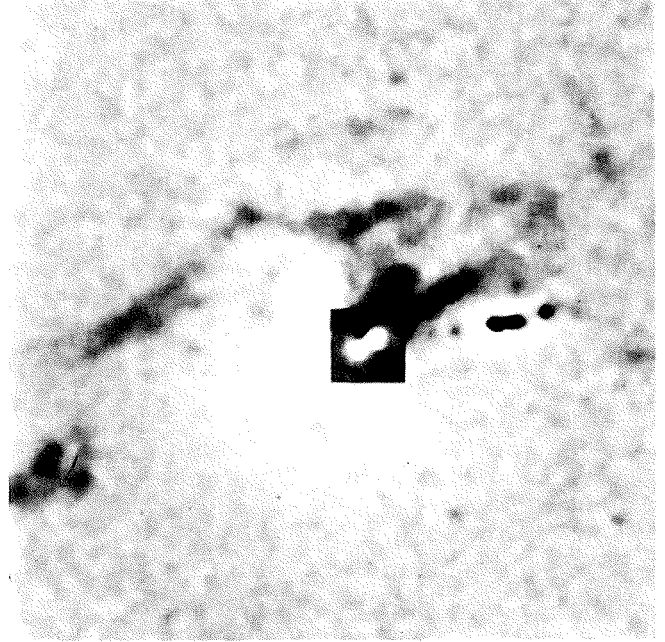


Figure 2.

substructure in the [OIII] emission. This is also clearly seen in the case of M87 (see Fig. 2) except that the circumnuclear [OIII] is aligned with the $H_\alpha + [NII]$ jet and not the well-known radio jet! How and if these features are related is currently unclear but may be associated with shock excitation and acceleration of the emission line region clouds by the radio jets, or, some mechanism for particle beaming of ionizing radiation along

the radio ejection axis (see e.g. Wilson et al., 1988).

During the next observing season for M87 by which time the field rotator should be fully functional, it is planned to extend these observations, under much more favourable conditions as well as imaging in the other known emission lines, notably [O I] and H_β . These better signal-to-noise images from longer exposures will hopefully

lead to a better understanding of what is really happening at the centre of M87.

References

- Wilson, A.S., Baldwin, J.A., 1989, preprint.
 Haniff, C.A., Wilson, A.S., and Ward, M.J., 1988, *Ap. J.*, **334**, 104.
 Wilson, A.S., Ward, M.J., and Haniff, C.A., 1988, *Ap. J.*, **334**, 121.

NTT Images of SN 1987A

G. GOUIFFES, E. J. WAMPLER, D. BAADE and L.-F. WANG, ESO

The fine optical quality of the NTT telescope, together with the good dome design and excellent La Silla site permit routine observing in conditions of sub-arcsec seeing. We have used the NTT and an RCA CCD on August 27, 1989 UT to obtain new direct images of SN 1987A. These images have a sampling of 0.26 arcsec per $30 \mu\text{m}$ CCD pixel and are described below.

Figure 1a–b reproduces two images taken through narrow band interference filters, one centred on [OIII] and the other in the neighbouring continuum at $\lambda 5118 \text{ \AA}$. Gaussian fits to the star images in the CCD frames showed that the seeing disks are slightly less than 0.5 arcsec full width at half maximum (FWHM).

With such good imaging it is possible to explore the circum-supernova environment in detail. It has been known for some time that the supernova is

surrounded by a small nebula that was initially excited by a UV flash which accompanied the supernova explosion. Evidence for the nebula was first seen in IUE spectra taken several months after the explosion (Wamsteker et al., 1987; Fransson et al., 1989). Later, narrow optical lines from the nebula appeared in spectra obtained in Dec. 1987 (Wampler and Richichi, 1989). Crotts et al. (1989) have given results of images taken in late 1988 and early 1989 with seeing of 0.68–0.84 arcsec FWHM. On April 1 of this year, an ESO image of the nebula around SN 1987A was obtained in seeing conditions of 0.85 arcsec. That ESO data were published in an earlier *Messenger* article (D’Odorico and Baade, 1989).

Despite the fact that the airmass for our observations was nearly two, the seeing conditions for the narrow-band images shown here are better than any

reported to date for SN 1987A. In addition to the better seeing, the continuing decline in the brightness of the supernova reduces the contamination of faint, nearby features by scattered supernova light. Thus, these data show the nebulosity near the supernova with unprecedented clarity. Ghost reflections in the equipment are not a problem since field star images are sharp, with no evidence of halos or extraneous images.

It is clear from Figure 1 that there is extended nebulosity in a “C” shaped arc running from 2 arcsec north of the supernova, through the east to about 2 arcsec south of the Supernova. The nebula is well marked in [OIII] light and is also faintly seen in the $\lambda 5118 \text{ \AA}$ continuum exposure. The knotty structure of this nebula was noticed in April 1989 by D’Odorico and Baade (1989) although they could not rule out its being an artefact of the extensive deconvolu-

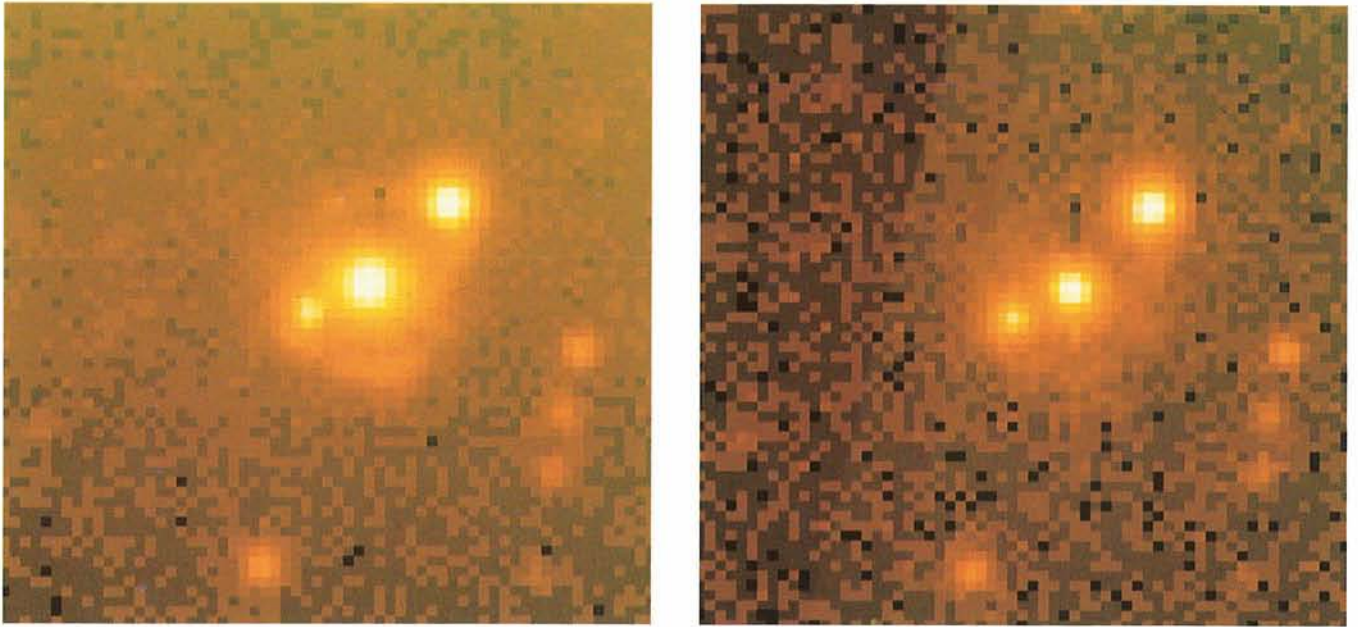


Figure 1 **a:** (left) Image of SN 1987A neighbourhood taken with an interference filter centred at λ 5007 Å. **b:** (right) the same region with a filter centred at λ 5118 Å. For both pictures north is up and east is left. The supernova is the bright image located between two stars in the centre of the picture.

tion applied to their (lower-resolution) data. The nebula was clearly detected by Crotts et al. (1989), and is attributed by them to a light echo from a dust sheet located behind the supernova.

This interpretation may not be correct, since our images show that the distribution of [OIII] light is about the same as the distribution of continuum light. If the light echo explanation is correct, very rapid recombination of O^{++} would be required for the emission line light distribution to track the continuum light echo. Furthermore, the differences seen when comparing the Crotts et al. (1989) data with the NTT images do not confirm the general expansion that would be predicted by their light echo model; the morphology of the arcs near star 2 (the brighter, NW star) reveal little, if any, change between March and August 1989. By contrast, 2 arcsec to the south of the supernova a new patch has appeared (which is even brighter than any of its northern counterparts). The observations of D'Odorico and Baade (1989) further support these conclusions. A comparison between line and continuum images suggests that the outer nebula is a mixture of gas and dust. Clearly, light travel delays in the nebula must influence the appearance of the structures, but the observed changes indicate that the geometry is more complicated than the simple model given by Crotts et al. (1989).

Within the outer nebula, and approximately centred on the supernova, is a bright, smooth, oval nebula with radii of about 1.3 arcsec E-W and 0.9 arcsec N-S. The E-W elongation of the central part of the O[III] nebula was earlier noted

by D'Odorico and Baade (1989). The elongation of the circumstellar nebula shows that the progenitor red supergiant wind was not symmetrical. Fig-

ure 2 gives two views of perspective plots of the raw images in continuum and [OIII] light. It can be seen that, when compared to the continuum exposure,

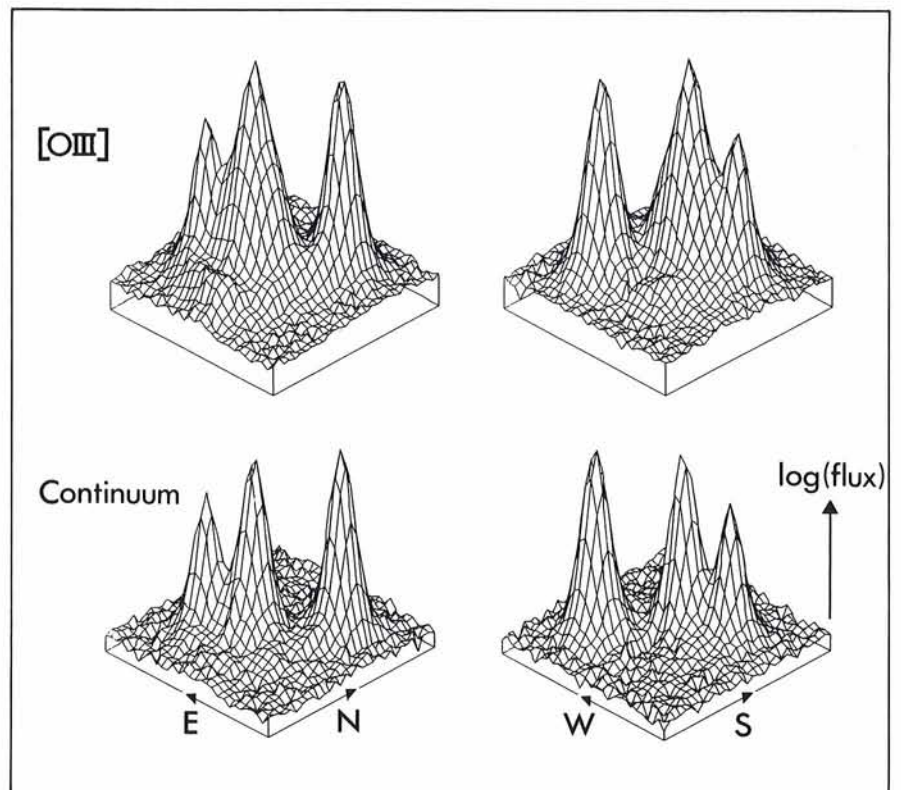


Figure 2: Three-dimensional views of the images shown in Figure 1. For both the [OIII] and continuum images two views, 180° apart, are shown. Note that the intensity is plotted on a logarithmic (magnitude) scale in order to show faint, outlying features. The upper plot is in [OIII] light and shows excess emission around the (central) supernova image. The two outlying star images show little change between the upper [OIII] plot and the lower continuum plot. Thus there was little change in the seeing during the 7 minutes that separated these two short exposures.

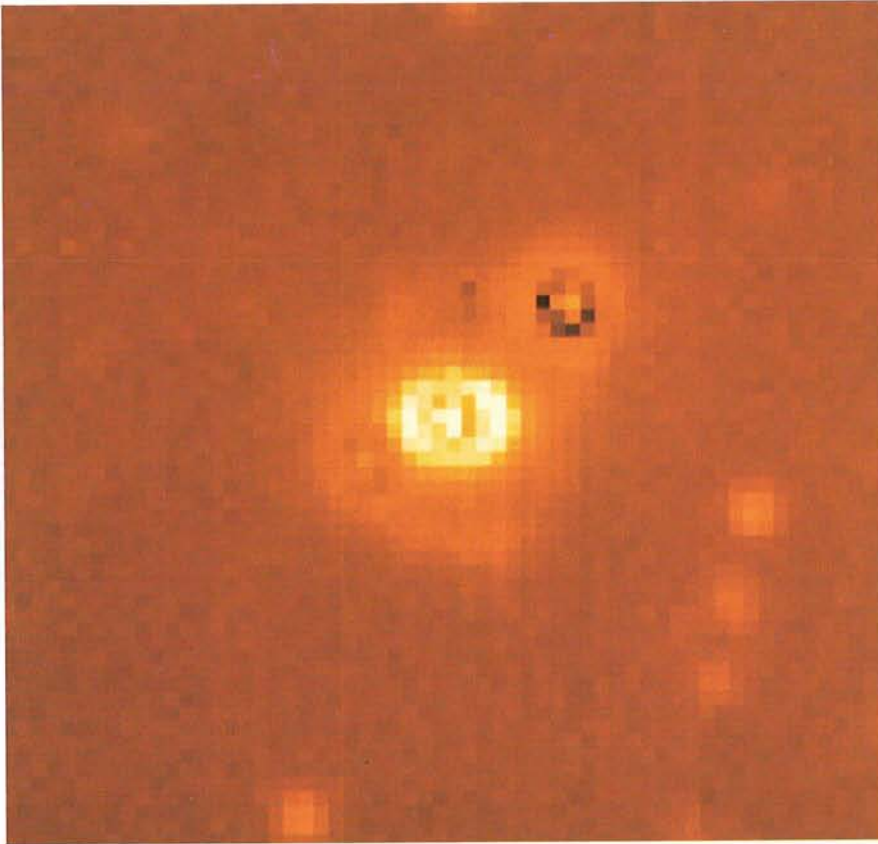


Figure 3: The nebulosity around SN 1987A after model star images, centred on the real stars, were subtracted from the frame. Because the Gaussian profiles used to model the star images only approximately match the real stellar profiles, rather large residuals remain.

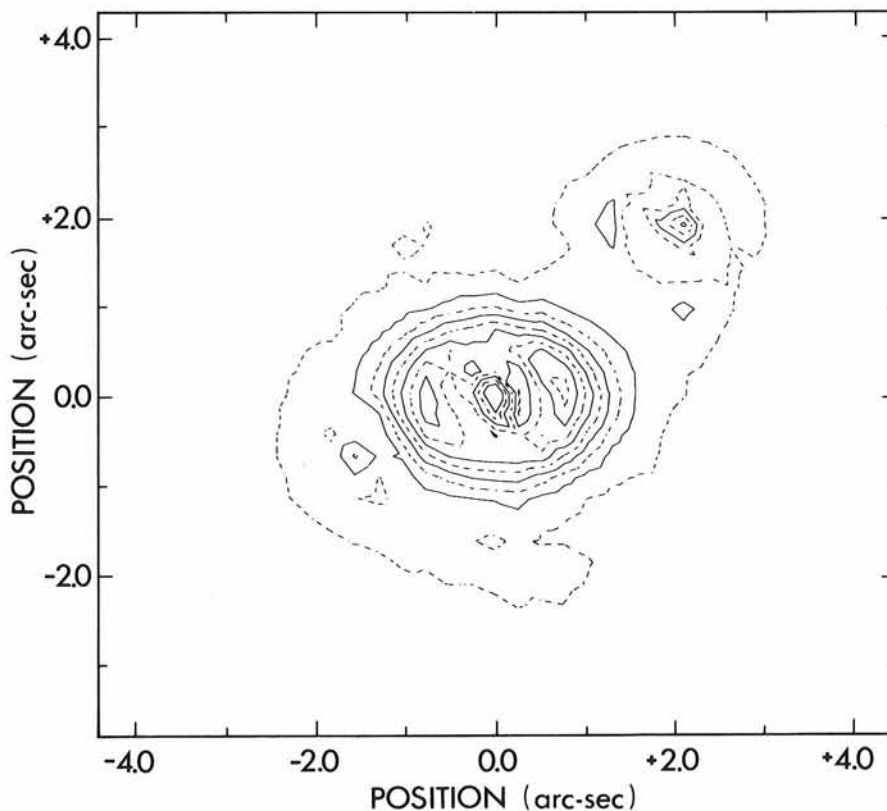


Figure 4: A contour plot of Figure 3. Outside of the central region where data are confused by uncertain subtraction of the supernova's stellar core, the oval shape of the nebula is maintained over several contours.

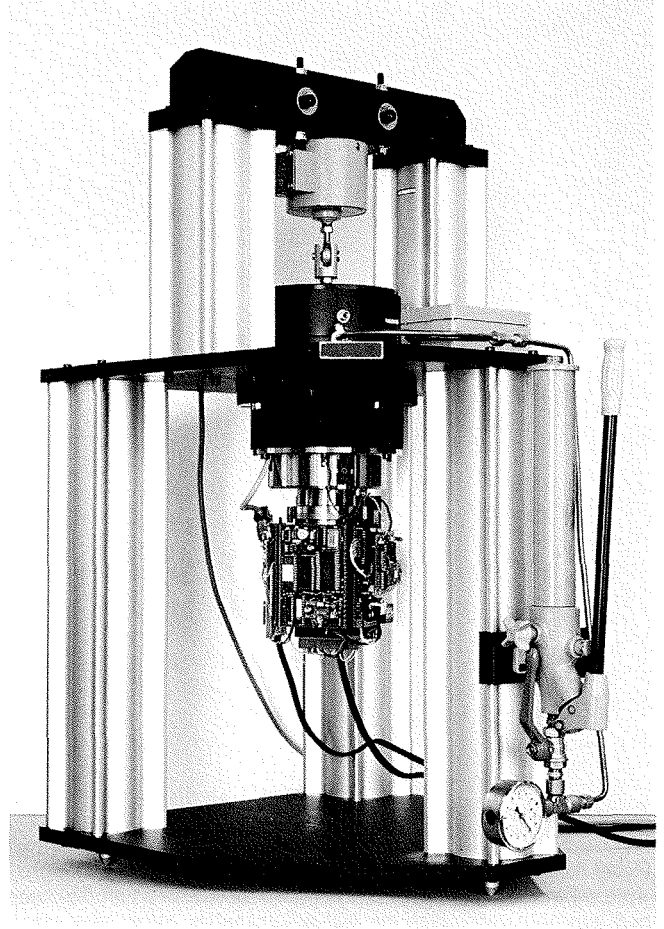
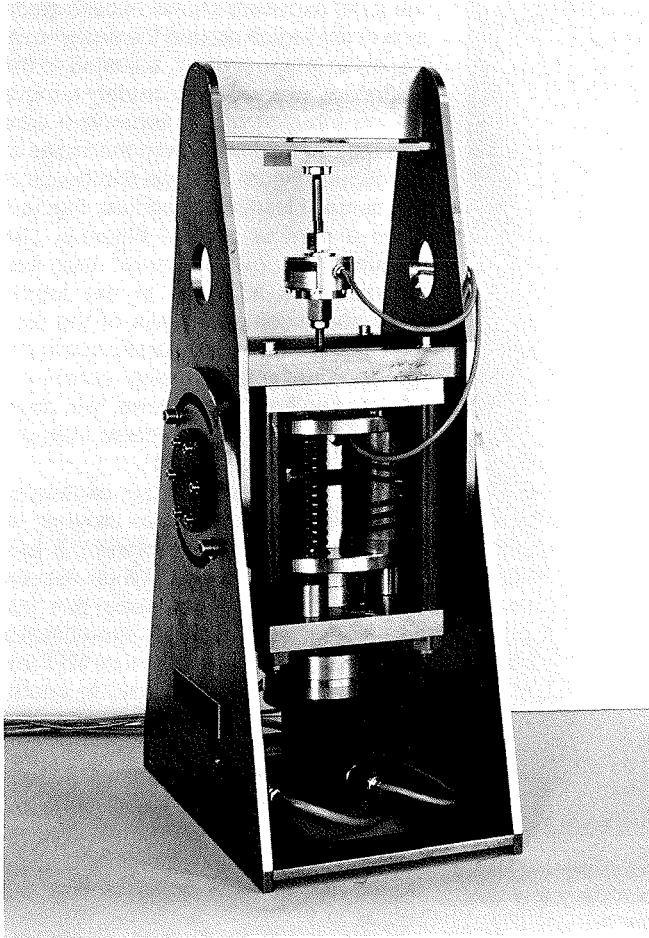
the [O III] exposure shows excess emission in the region around the supernova. Gaussian image profiles, adjusted to the field stars, were used to crudely remove the contribution of the supernova core and the two field stars from the image of the nebula. Figure 3 shows the results of this simple cleaning procedure. Figure 4 gives a contour plot of Figure 3. The amount of "supernova core" that was subtracted is arbitrary. In the future, more sophisticated models of the seeing images and a more careful scaling of the supernova core, using continuum information from slit spectra, will allow better separation of the nebula from the star images.

If the outer parts of the expanding supernova envelope are moving at 0.1 c, that gas would subtend 0.5 arc-sec at the present time. When the expanding supernova envelope gas begins to interact with the circumstellar material one might expect that NTT images taken of the supernova in conditions of excellent seeing would show a bright, new nebula appearing in the core region. The pixel size of the CCD used for these observations is too large for good sampling of very small images, but a camera with a different scale should be capable of detecting the nebula.

The first indication of an interaction between the supernova envelope and the surrounding nebula could be a sudden increase in X-ray emission from the region since the collision of the rapidly expanding envelope with circumstellar gas will generate a strong X-ray flux. The NTT images will be important, since they will show if the expanding supernova envelope is also asymmetrical and how its asymmetry relates to that of the circumstellar cloud. Early polarization measurements in the I band (Schwarz 1987) indicate intrinsic polarization with a position angle near 0° .

References

- Crotts, A.P.S., Kunkel, W.E., McCarthy, P.W. 1989, *Ap. J. Letters*, (LASP Preprint No. 89-10).
- D'Odorico, S. and Baade, D. 1989, *The Messenger*, **56**, 35.
- Fransson, C., Cassatella, A., Gilmozzi, R., Kirshner, R.P., Panagia, N., Sonneborn, G. and Wamsteker, W. 1989, *Ap. J.*, **336**, 429.
- Schwarz, H.E. 1987, in *Proc. ESO Workshop on SN 1987A*, ed. I.J. Danziger, Garching, p. 167.
- Wamsteker, W., Gilmozzi, R., Cassatella, A. and Panagia, N. 1987, *IAU Circ.*, No. 4410.
- Wampler, E.J. and Richichi, A. 1989, *Astron. Astrophys.*, **217**, 31.



Axial Support Prototypes for the VLT

Two prototypes of axial support for the primary mirror of the VLT are currently under evaluation tests in Garching. These actuators can produce push or pull forces in the range of ± 1000 Newtons with a sensitivity of 0.03 N. 150 similar actuators will support each of the primary mirrors and correct low frequency aberrations of the reflecting surface. In each support, an integrated force sensor measures the actual force applied to the mirror through a local electronic control loop receiving force commands from the telescope computer. A final prototype, taking advantage of the evaluation, will be developed at ESO in 1990. It represents one of the major elements of the active optics principle.

S. Prat (ESO)

Visitor Facilities and User Support at ESO-Garching

D. BAADE, ESO

1. Introduction

Every year, nearly 200 Visiting Astronomers come to the ESO Headquarters in Garching in order to reduce their observations obtained at La Silla, to prepare such observations, or as of more recently also to do the observations under remote control. As this is a sizeable fraction of the total ESO users community, the equipment available for these purposes and the operational procedures followed perhaps do not require much of a description to the readers of the *Messenger*. On the other hand, a broad overview has not appeared before, and, more importantly, ESO's policy for the operation and usage of the visitor facilities has not

been comprehensively described elsewhere. The following therefore tries to be reasonably complete in the latter area and purposely pays only little attention to technical information which, however, is detailed in various dedicated operating manuals (cf. below).

2. Who is Supported?

The user facilities in Garching are offered for the preparation and reduction of observations at La Silla only and if applicable to the type of data. Other users may be considered, depending on the availability of resources.

The person coming to Garching should be one of the applicants named

on the proposal for the observing programme concerned. Experience has furthermore shown that, unless a meticulous log has been kept of the observations, much time can be wasted if the data reduction is not done by the observer. Likewise, the preparation of observations, e.g. for Optopus, is also best done by the observer. Normally, the number of people invited to Garching will be limited to one per observing programme, regardless of the task to be performed.

3. How Much Does it Cost?

To Visiting Astronomers who at the time of their visit to Garching are affili-

ated to an astronomical institute in one of the ESO member countries, the user facilities are made available free of charge (only in connection with an observing programme at La Silla). ESO will cover their travel expenses (round trip; first-class train or lowest air fare and transportation to and from the railway station or airport) between that institute and Garching and pay them a daily subsistence allowance (at present DM 50) in addition to providing free accommodation. This support is given only once per observing trip to La Silla (or Garching, in case of Remote Control observations).

In all other cases, ESO does not make any financial contributions. One of the guest rooms in the ESO building may be provided if available, for which there will be a nominal charge of presently DM 20 per night. The usage of computers, measuring machines, etc. normally is free.

Consumables (magnetic tapes, hard-copies, etc.) will always have to be paid for if their usage considerably exceeds the average level.

4. For How Long are the Facilities Made Available?

With the exception of Remote Control observations, the length of the stay in Garching will depend on the type and amount of data and the experience of the visitor. A typical duration is one week.

Whenever possible, the PDS and Optonics plate measuring engines are allocated to only one user per day in order to minimize the need for recalibrations. IHAP and MIDAS users can book as much time on the respective computers as they think they can stand in a 24-hour period. However, time in the afternoon may be reserved only one day in advance and for a maximum of two hours per day. This rule is the only way to ensure that users who may, e.g., wish only to look at an image can do so without having to wait unreasonably long for a work station with image display.

5. When Can Visiting Astronomers Come?

We aim at making our equipment available 365 days per year, 24 hours a day. However, technical support and scientific assistance are provided only during normal working hours (Remote Control observations are, of course, excepted from this rule).

If you have a strong preference for certain dates of your stay in Garching, it is important that you contact us 4–6 weeks in advance. This is particularly important if additionally you need an

**CNRS – Observatoire de Haute-Provence and
European Southern Observatory**

**2nd ESO/OHP Summer School
in Astrophysical Observations**

**Observatoire de Haute-Provence, France
16–26 July 1990**

The rapid advances made in the area of astronomical instrumentation had the side effect that fewer students have ready access to up-to-date observing facilities. As a contribution to reducing this imbalance in the training of young astronomers, the ESO/OHP Summer School offers the opportunity to gain practical experience under realistic conditions.

In groups of three students, each guided by an experienced observer, the participants will use the equipment of the OHP to carry out a small observing programme with telescopes of 1.2–1.9 m aperture (direct imaging or spectroscopy, both with a CCD detector), to reduce the data with a modern image processing system (MIDAS or IHAP), to extract relevant additional information from the astronomical literature, and to describe the results in a brief summary which is to be presented to the other participants at the end of the school.

In order to prepare and supplement the practical work, there will be one 90-minute lecture per day by invited specialists. The subjects foreseen include (a) modern telescope layout, (b) high-sensitivity detectors, (c) design of high-throughput optical instruments, photometry with (d) photomultipliers and (e) CCD's, high-resolution (f) spectroscopy and (g) imaging, (h) fiber applications in low-resolution spectroscopy, (i) infrared observations, and (k) data reduction techniques. All courses, etc. will be given in the English language. (A report on the 1st ESO/OHP Summer School appeared in the *Messenger* No. 53, p. 11.)

Applications are invited from graduate students working on an astronomical Ph.D. thesis at an institute in one of the ESO member countries. Application forms are available from the organizers and have to be returned by March 31st, 1990. A letter of recommendation by a senior scientist who is familiar with the applicant's work is additionally required. Up to eighteen participants will be selected and have their travel and living expenses fully covered by ESO or OHP.

The Organizers:

| | |
|---|---|
| M.P. Véron Observatoire de Haute-Provence F-04870 Saint-Michel-l'Observatoire France | D. Baade European Southern Observatory Karl-Schwarzschild-Str. 2 D-8046 Garching F.R. Germany |
| EARN/Bitnet: MIRA@FRONI51 X25: PSI%0208004042183::MIRA SPAN: 29240::MIRA | VISAS@DGAESO51 PSI%0262458900924::VISAS ESOMC1::VISAS |

introduction or have special requirements. Requests communicated to us with less than 10 days notice will be considered only in exceptional cases.

If known in advance, Visiting Astronomers may arrive at any time on any day of the week. However, unless you are very familiar with the tools you intend to use and have also handled them relatively recently, we strongly advise you against coming to Garching shortly before a weekend or public holiday. If there is a problem in getting started, it would take the whole weekend before a solution can be attempted.

6. Where will Visiting Astronomers be Accommodated?

Together with some other research institutes, the ESO building is situated about 2 kilometres outside Garching, a town of 15,000 inhabitants and 15 kilometres from Munich. To the extent possible, we therefore try to accommodate Visiting Astronomers in one of the four guest rooms in the ESO building. For Remote Control observers, special arrangements have been made with a guest house in Garching for a room that offers a maximum of quiescence also

during the day. Remote Control observers will always be offered a car for transportation between the guest house and ESO whereas all others may use an ESO car only after office hours and if it is not needed otherwise.

7. What Kind of Work is Possible?

We aim at supporting the reduction of data obtained with all major observing modes of the standard instruments used at La Silla (take the latest call for proposals to see how long the list has grown). Only sub-mm observations, polarimetry and photoelectric photometry (optical and infrared) are currently excluded because there are no adequate high-level command procedures available in either IHAP or MIDAS. This is not to say that the reduction of such data is not possible in principle. But it is not very efficient in practice, and ESO does not provide any recipes as to how to proceed. For the full 2-D reduction of long-slit spectra and the calibration of slitless spectra only limited means exist at the moment. The handling of IR data is particularly intimately connected with the advances made in the understanding of the often delicate instrumentation; optimization of observing, calibration, and reduction procedures are still going on.

Photographic plates (direct images or spectra) can be digitized with the PDS and the Optronics measuring machines. Astrometry – also in preparation of Optopus observations – is possible with the Optronics; the reduction software is currently being ported to the MIDAS environment.

The instruments which can be used under remote control from Garching are presently the Boller & Chivens spectrograph with CCD and the direct CCD camera at the 2.2-m telescope and both Short and Long Camera (with CCD only!) at the CAT/CES.

Computers are made available for the usage of ESO software only, i.e. Visiting Astronomers wishing to run their own software first have to seek ESO's approval.

Whenever you are not sure if your requirements are satisfied by standard procedures, contact us as early in advance as possible so that we can think about alternatives.

8. How is the Work Done?

Remote Control observers are assisted during their entire observing run by a Remote Control Operator whose task it is to ensure the smooth functioning of the system in general and the link to La Silla in particular. The observer will, as on La Silla, command

the instrument and is also in charge of the on-line data reduction with IHAP for quality control, etc.

With this partial exception of the Remote Control Facility, it is expected that all equipment whose usage has been authorized is operated by the visitors themselves.

Instruction manuals are available for all standard tasks. However, anyone who has ever been alone with a new piece of software or hardware and its user guide knows that often this is not sufficient to get quickly started. Therefore, we offer a personal introduction to everyone who asks for it. The introducing astronomer will stay with you until at least one cycle of operations has been completed and will also be available to answer questions during (most of) the rest of your stay.

Usually, the introduction is given by one of the ESO students or postdoctoral fellows. They stay for only two, at most three, years at ESO. On the other hand, the spectrum of possible applications of the facilities available is both very broad and dense, and nearly every set of observations is different from the others. Therefore, it is hardly avoidable that almost all introductions include a learning phase also for the introducing astronomer. We do have to ask for your patience.

Kindly note that an introduction can be arranged for only if we know about your needs at least 10 days in advance.

The importance of careful preparations also on the part of the visitor cannot be overemphasized. This already applies to observations under local control on La Silla. Under remote control, the bandwidth of the data link

imposes limitations which are not very important in every single case. However, if one starts random experiments, the time lost will rapidly accumulate. For data reduction, although (unlike observing) not tied to a rigid external clock, a detailed work plan is perhaps even more critical because it must be realized that for most observations their proper processing is much more complex a task than their acquisition. It is important that you come with a clear idea of what shall be extracted from the data and what steps are, therefore, needed. Our introduction aims at helping you to use efficiently the software pertaining to your problem. It cannot, however, serve as a substitute for your carefully studying the relevant parts of the MIDAS (or IHAP) manual.

Another point that should be given consideration in advance (in most cases that is: prior to the observations) is the need for calibration data such as standard star fluxes, laboratory wavelengths, etc. For standard La Silla instrument configurations the necessary data are available in Garching, but it is the responsibility of the user to verify that they satisfy his needs and to be able to find alternatives if necessary.

9. What Technical Information is Available?

As stated in the Introduction, this summary has attempted to stay clear of technical details. This type of information is collected in a fair number of user guides. The ones most relevant for the work of Visiting Astronomers in Garching are:

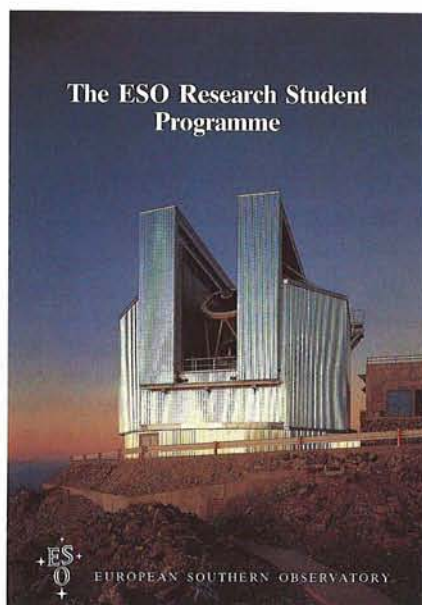
The ESO Research Student Programme:

Change of Deadline

This new programme was described in some detail in an earlier issue of the *Messenger* (55, p. 12). The corresponding brochure was announced in the last issue (57, p. 38), but for various reasons the printing was delayed until late October.

The brochure has in the meantime been sent to all institutes in the ESO member countries. Since the next-following application deadline stated therein (December 1, 1989) would be too short, it has been decided to extend it to **January 15, 1990**.

Thereafter, the normal deadlines will be as indicated, that is on May 1 and December 1.



● A short guide to ESO-Garching for Visiting Astronomers tries to set pointers to possible answers for most of the practical questions which Visiting Astronomers may foreseeably have. It is automatically sent to every new visitor prior to his/her travel to Garching.

● The *Remote Control User Guide* describes the design and performance of the RC system. It assumes that the reader is already familiar with the instrument to be used. For the time being, ESO's policy is to offer RC observations only to observers who have already obtained some experience on La Silla with comparable equipment although this is in no way necessitated by the functionality of the RC system. The document is mailed to new users at the time when they are informed that Remote Control observations will be offered to them.

● User guides for remotely controllable La Silla instruments (see Sect. 7).

● The *Local Guide for New VAX/VMS Users* tries to get people started who on the ESO VAX computers wish to use functions of the VMS operating system that are not covered by MIDAS.

● Similarly, three documents (i) *Introduction to Portable MIDAS*, (ii) *Getting started with UNIX*, and (iii) *Introduction to the X11 Window System* have been prepared in order to provide the necessary ancillary information to users of the Portable MIDAS on one of the workstations with the UNIX operating system. (The first of the three documents is of course useful with any installation of the Portable MIDAS.)

● Updates to the *MIDAS User Guide* are released twice a year by the ESO Image Processing Group. Appendix D of Vol. A also describes the peripheral devices that are available to MIDAS users in Garching. Sending the full two-volume user guide to Visiting Astronomers who will reduce only one type of data is not a very efficient use of our resources. We are, therefore, studying how best to compile instrument-specific MIDAS documentation kits.

● A cookbook which only describes how to operate the MIDAS Echelle Package and the relevant devices (the first version pertains only to the VAX) is in preparation.

● Copies of the *IHAP* manual are available on request. A new (and presumably also the last) edition is in preparation.

● The *Atlas of the Thorium-Argon Spectrum for the ESO Echelle Spectrograph in the $\lambda\lambda$ 3400–9000 Å Region* (ESO Scientific Report No. 6) is useful not only for CASPEC but also for ECHELEC data and CES spectra. An identification of the He-Ar spectrum at low resolution is given in an appendix of the IHAP manual.

First Announcement of the 2nd ESO/ST-ECF

Data Analysis Workshop

ESO, Karl-Schwarzschild-Str. 2

D-8046 Garching, FRG

April 24–26, 1990

The aim of the Workshop is to provide a forum for discussions of astronomical software techniques and algorithms. It is held annually during the spring (April/May) and centres on a different astronomical area each time. Due to available space, participation will be limited to 80 people. Last year it was necessary to reject some people and we therefore recommend that you send in the corresponding participation and accommodation forms well before the deadline.

The topic for the 1990 Data Analysis Workshop is the analysis of spectral data. The scientific section of the meeting will consist of three sessions, each starting with a main talk after which papers of 5–10 minutes duration can be presented. The last day is reserved for general user meetings for MIDAS and ST-ECF.

The tentative agenda is:

Analysis of Spectral Data

April 24: 14:00–18:00: Standard Spectra

April 25: 09:00–12:30: Long Slit Spectra

14:00–17:30: Echelle Spectra

April 26: 09:00–12:00: MIDAS users' meeting

12:00–12:30: European FITS Committee

14:00–17:30: ST-ECF users' meeting

We especially welcome contributions on algorithms and techniques for: extraction of spectral data, analysis of line profiles, estimates of the continuum, rebinning and instrumental response. We encourage people to present their work in these areas even if it is only ideas. After each introductory talk, we will have a more informal discussion where such contributions can be made. We also plan to have a poster session where people can present short contributions. Proceedings of the scientific sessions will be published.

The scientific organizing committee includes:

P. Grosbøl (Chairman) P. Benvenuti

D. Baade S. D'Odorico

M. Rosa J. Wampler

Contact address: Ms. Susan Lively, Image Processing Group, European Southern Observatory, Karl-Schwarzschild-Str. 2, D-8046 Garching, FRG.

EARN : SUSAN@DGAESO51

SPAN : ESOMC1::SUSAN

● The user guide for the *Measuring Machine Facility* (MMF) will soon have to be re-written when the central HP computer has been replaced by a *Stellar* machine. It is applicable anyway only to the PDS as the Grant machine has been taken out of service and the Optronics has already undergone some changes (cf. below). New users of the MMF will automatically receive this manual and the one of the measuring machine concerned (see below).

● The user guide for the PDS probably is one of the oldest ones in the organization that continue to be valid.

● Of the manual for the Optronics machine, only a draft version is available at the moment. In this machine, the

photo-multiplier tube has been replaced by a linear multi-channel Reticon array in order to enable faster scans of larger fields.

● The *Optopus* user guide not only describes this instrument and its operation but it also details how to prepare the input data required for the drilling of the star plates. Some modifications of this chapter will become necessary once the software has been ported to the MIDAS environment. New users of *Optopus* will receive this manual automatically prior to their visit to Garching.

● STARCAT will eventually hold all observations obtained with ESO telescopes or the Hubble Space telescope. Currently, a fair number of all kinds of

astronomical catalogues have been loaded and can be accessed by everyone. There are a STARCAT user guide and a regularly updated documentation of the on-line available data bases.

● For the future, off-prints of the article will be prepared and updated as the need arises.

Please note that the above list only comprises ESO documents for facilities that can be used at or from Garching; there is also an extensive set of user guides for La Silla equipment. The compilation of a completely revised all-ESO manual is in progress. Finally, all Visiting Astronomers have access to ESO's library.

10. How Can a Visit to Garching be Organized?

If you need more information, e.g. one of the documents listed above, or wish to arrange your stay and work in Garching, kindly contact Ms. Elisabeth Hoppe. She will also try to help you with all practical aspects of your stay in Garching. Inquiries concerning observations on and travel to and from La Silla will as

before be handled by Mrs. Christa Euler. They can be reached

- by phone:
 - +40-89-32006-223 (Euler)
 - 473 (Hoppe)
- by ordinary mail:
 - European Southern Observatory
 - Karl-Schwarzschild-Str. 2
 - D-8046 Garching
 - Fed. Rep. Germany
- by electronic mail:
 - ESOMC1::VISAS (SPAN)
 - VISAS@GAESO51 (EARN/Bitnet)
 - PSI%0262458900924::VISAS (X25)
- by telex:
 - 52828220 eo d
- by telefax:
 - +49-89-3202362
- in person:
 - office No. 222 (Euler)
 - 225 (Hoppe)

For the preparation of your stay in Garching we need to know:

- the name of the person who will come and, if different, the name of the Principal Investigator of the programme;
- the intended dates of your visit;
- the equipment to be used;
- the identification number that has

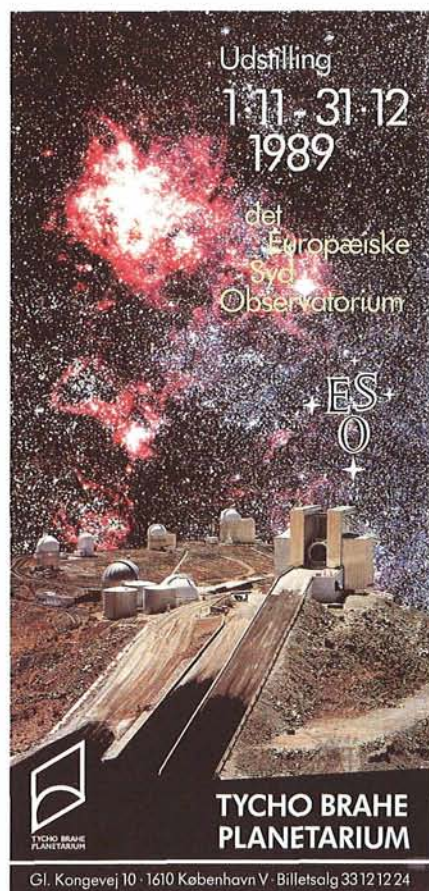
been assigned to the observing programme concerned and the number of the period when the observations were carried out;

- a precise description of the data type (e.g., EFOSC slit spectra, not just EFOSC);
- any special requirements;
- if you already have the operating manual(s) which are necessary for the preparation of your visit (check the document list given above);
- if you need an introduction by an ESO astronomer.

11. Can Things be Improved?

We try to expose you to a minimum of bureaucracy, to be flexible in the application of the rules outlined above, and to be efficient in the scientific-technical support we provide. Nevertheless, there will always be situations where you think we could have done better. Please bring such cases to our attention. Either we succeed in convincing you that there were no practical alternatives or we will have to improve our standards so that we can serve you better next time.

ESO Exhibition Opens in Copenhagen's New Tycho Brahe Planetarium



After more than five years' hard work of preparations and construction, one of the largest and most modern planetaria in Europe has now opened its doors to the public. On October 31, 1989, the new "Tycho Brahe Planetarium" was inaugurated in Copenhagen, in the presence of the Danish head of state, H.M. Queen Margrethe II, and nearly 300 other distinguished guests, comfortably seated in reclining chairs under the tilted 23-metre dome. An ESO Exhibition had been set up in the new planetarium and was officially opened at the same time.

The Queen, who was accompanied by her husband, Prince Henrik of Denmark, and the Danish Minister of Education, Mr. Bertil Haarder, activated the new Zeiss VI TD projector with a well-placed shot from a laser pistol. Not unexpectedly, the first programme was devoted to her famous countryman of the 16th century. The title is "Tycho's Star", referring to the supernova that deeply impressed young Tycho in November 1572 and which led him to the construction of more accurate instruments. The ESO people present at the inauguration were pleased to witness the projection of a magnificent

panorama of La Silla under the southern sky in connection with the presentation of the more recent SN 1987A.

The Queen then visited the exhibition area, where she was shown the ESO photos and models by the Director General, Professor Harry van der Laan, assisted by some Danish members of his staff. The Queen was particularly interested in the Very Large Telescope project and its astronomical possibilities. The Minister of Education was pleased to learn about the associated prospects for Danish science and industry.

The realization of the first large planetarium in Scandinavia is the fulfillment of an old dream by a Copenhagen amateur astronomer, Helge Pedersen and his equally energetic wife, Bodil Pedersen. Now in their eighties, the handsome couple created in 1984 the "Urania-foundation" with an initial donation of 50 million DKK. Helge Pedersen was on a trip to Indonesia to watch the solar eclipse the year before when the idea first came to his mind. The naming reflects his life-long admiration of the famous Danish astronomer and his wish to contribute to the "rehabilitation" of Tycho Brahe in the country which the



Professor Harry van der Laan shows the model of the ESO La Silla observatory to the Queen. In the background Prince Henrik, Mr. Ebbe Fogh-Hansen (Chairman of the Urania Foundation) and at the right, Mr. Bertil Haarder, Minister of Education.

astronomer had to leave when support to his observatory on the island of Hven was withdrawn by King Christian IV.

Plans for a major planetarium in Copenhagen were made already in the 1960's, but had to be shelved when no agreement could be reached about the site. However, the Tycho Brahe Planetarium is now situated on one of the most beautiful spots in the central city area, next to Sankt Jørgens Lake, and only 5 minutes' walk from the famous Tivoli Gardens. The management expects about 400,000 visitors a year, and facilities for multi-language presentations have been implemented to cater for the many tourists who pass through the Danish capital. It is good to note the heavy involvement of amateur and professional astronomers in the daily life at the planetarium; the first school classes have already been received and the evening courses given under the auspices of "Peoples' University", now held at the planetarium, report the highest number of students of all ages ever recorded.

The planetarium also includes an OM-NIMAX projector; the first films to be shown are "Sacred Site" about Comet Halley, and "The Dream is Alive" about the US Space Shuttle. There is also a much-visited restaurant, "Cassiopeia". No doubt that the public will be attracted!

Judging from the enormous interest of the Danish media in this event there is

every hope that astronomy in Denmark will greatly profit from this new facility. Who knows how many young, potential "Tychos" will be deflected in our direc-

tion after a visit to the Tycho Brahe Planetarium? We at ESO are happy to contribute to this noble cause.

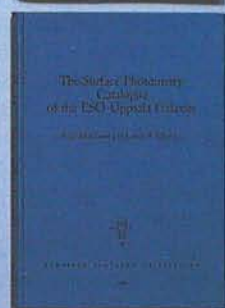
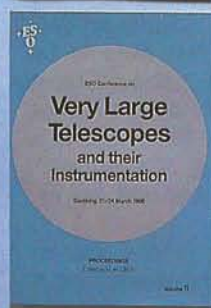
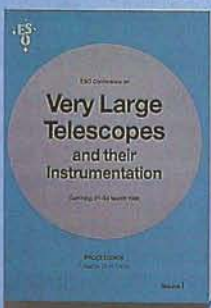
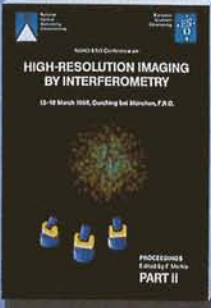
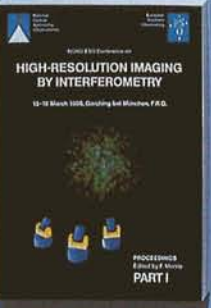
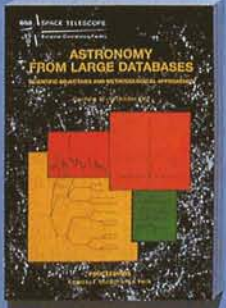
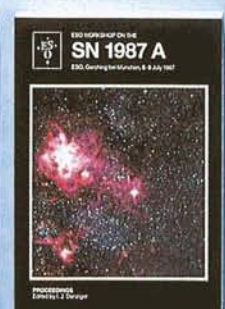
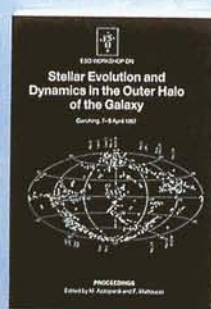
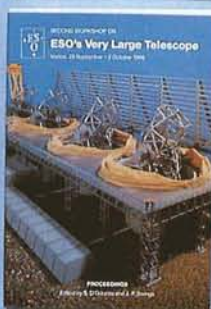
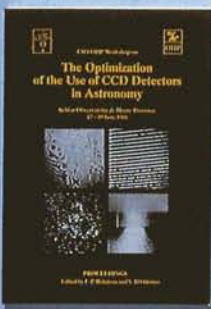
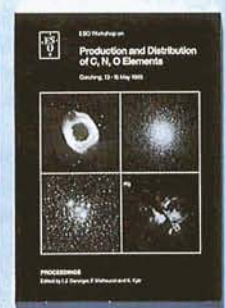
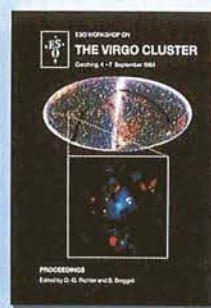
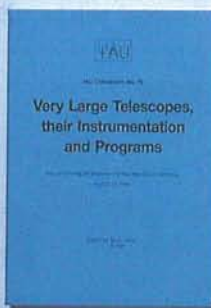
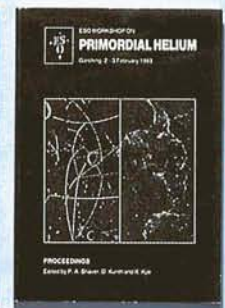
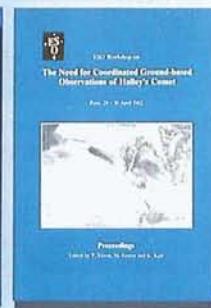
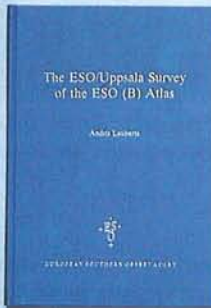
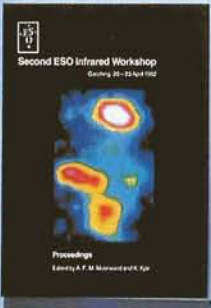
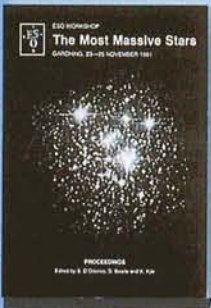
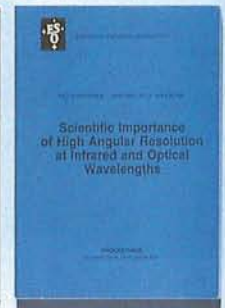
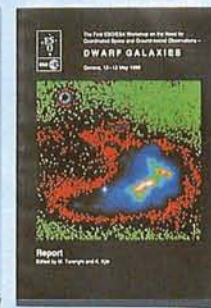
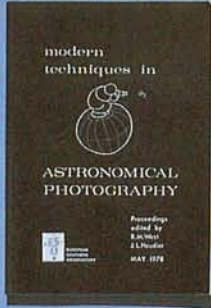
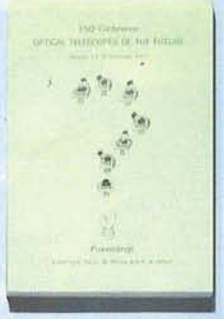
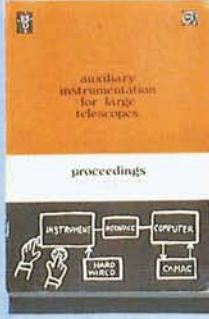
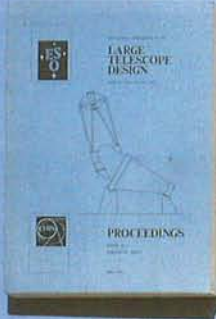
R. M. West

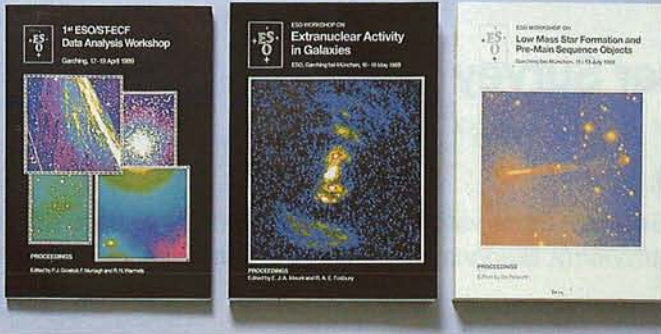


ESA Price Winners Visit ESO

On November 16, seventeen young Europeans visited ESO and the Space Telescope European Coordinating Facility at the invitation of the European Space Agency. They were the winners of an ESA Essay competition based on the theme "Astronomy from Space" – chosen because of the impending launches of the Hipparcos satellite and of the Hubble Space Telescope. The visit, which included practical demonstrations of MIDAS and a tour of the Optical and Photo Labs, was very much appreciated by the young people (all of them high-school students) and was crowned by a warm convivial happening with ESO and ECF staff in a typical Munich downtown restaurant.

P. Benvenuti (ST-ECF)





ESO Publications

Over the years, ESO has published a number of Conference Proceedings and other books. The topics cover most of modern astronomy and reflect current frontlines in astronomical science and technology.

For the benefit of scientists and librarians, all of the volumes are shown here, together with a complete list of titles and quotation of prices (unless out of print). The prices include packing and postage (surface mail). Publications which belong to the ESO Conference and Workshop Proceedings series are numbered.

The books must be prepaid by transfer to the ESO bank account 2102002 with Commerzbank München (BLZ 70040041), or by cheque, addressed to the attention of
European Southern Observatory
Financial Services
Karl-Schwarzschild-Strasse 2
D-8046 Garching bei München
Fed. Rep. Germany

Please make sure to indicate clearly the title and number, and also your full address.

The Magellanic Clouds. Based on the Symposium on the Magellanic Clouds held in Santiago de Chile, March 1969, on the occasion of the dedication of the European Southern Observatory. Ed. by A.B. Muller (out of print).

- No. 1: ESO/CERN Conference on "Large Telescope Design", Geneva, March 1971 (out of print).
 No. 2: Conference on "The Role of Schmidt Telescopes in Astronomy", Hamburg, March 1972 DM 16,—
 No. 3: ESO/CERN Conference on "Auxiliary Instrumentation for Large Telescopes", Geneva, May 1972 (out of print).
 No. 4: ESO/SRC/CERN Conference on "Research Programmes for the New Large Telescopes", Geneva, May 1974 DM 40,—
 No. 5: ESO Conference on "Optical Telescopes of the Future", Geneva, December 1977 DM 40,—
 No. 6: ESO Workshop on "Modern Techniques in Astronomical Photography", Geneva, May 1978 (out of print).
 No. 7: ESA/ESO Workshop on "Astronomical Uses of the Space Telescope", Geneva, February 1979 DM 40,—
 No. 8: ESO/SRC Conference on "Applications of CAMAC to Astronomy", September 1978 (out of print).
 No. 9: ESO Workshop on "Two Dimensional Photometry", Noordwijkerhout, November 1979 DM 40,—
 No. 10: ESO Workshop on "Methods of Abundance Determination for Stars", Geneva, March 1980 (out of print).
 No. 11: The First ESO/ESA Workshop on the Need for Coordinated Space and Ground-based Observations — DWARF GALAXIES, Geneva, May 1980 DM 10,—
 No. 12: ESO Conference on "Scientific Importance of High Angular Resolution at Infrared and Optical Wavelengths", Garching, March 1981 DM 50,—
 Evolution in the Universe. Symposium held on the occasion of the inauguration of the ESO Headquarters building in Garching on 5 May 1981 DM 20,—
 No. 13: ESO Workshop on "The Most Massive Stars", Garching, November 1981 DM 50,—
 No. 14: ESO Workshop on "The Need for Coordinated Ground-based Observations of Halley's Comet", Paris, April 1982 DM 40,—
 No. 15: "Second ESO Infrared Workshop", Garching, April 1982 DM 50,—
 The ESO/Uppsala Survey of the ESO (B) Atlas. Ed. by A. Lauberts. 1982 DM 40,—
 No. 16: ESO Workshop on "Primordial Helium", Garching, February 1983 DM 50,—
 No. 17: Workshop on "ESO's Very Large Telescope", Cargèse, May 1983 DM 40,—
 No. 18: ESO Workshop on "Site Testing for Future Large Telescopes", La Silla, October 1983 DM 25,—
 First ESO-CERN Symposium on "Large-Scale Structure of the Universe, Cosmology and Fundamental Physics", Geneva, Nov. 1983 DM 35,—
 No. 19: IAU Colloquium No. 79: "Very Large

- Telescopes, their Instrumentation and Programmes", Garching, April 1984 DM 80,—
 No. 20: ESO Workshop on "The Virgo Cluster", Garching, September 1984 DM 50,—
 No. 21: ESO Workshop on "Production and Distribution of C, N, O Elements", Garching, May 1985 DM 50,—
 No. 22: ESO-IRAM-Onsala Workshop on "(Sub)Millimetre Astronomy", Aspenäs, Sweden, June 1985 DM 70,—
 No. 23: Second ESO-CERN Symposium on "Cosmology, Astronomy and Fundamental Physics", Garching, March 1986 DM 35,—
 No. 24: Second Workshop on ESO's Very Large Telescope, Venice, September-October 1986 (out of print)
 No. 25: ESO-OHP Workshop on "The Optimization of the Use of CCD Detectors in Astronomy", Observatoire de Haute-Provence, June 1986 DM 45,—
 No. 26: ESO Workshop on the "SN 1987A", Garching, July 1987 DM 50,—
 No. 27: ESO Workshop on "Stellar Evolution and Dynamics in the Outer Halo of the Galaxy", Garching, April 1987 DM 50,—
 No. 28: ESA/ESO Conference on "Astronomy from Large Databases — Scientific Objectives and Methodological Approaches", Garching, October 1987 DM 50,—
 No. 29: NOAO-ESO Conference on "High Resolution Imaging by Interferometry" (2 volumes), Garching, March 1988 DM 90,—
 No. 30: ESO Conference on "Very Large Telescopes and their Instrumentation", (2 volumes), Garching, March 1988 DM 90,—
 The Surface Photometry Catalogue of the ESO-Uppsala Galaxies. Ed. by A. Lauberts and A. Valentijn) 1989 DM 40,—
 No. 31: 1st ESO/ST-ECF Data Analysis Workshop, Garching, April 1989 DM 30,—
 No. 32: ESO/ST-ECF Workshop on "Extranuclear Activities in Galaxies", Garching, May 1989 DM 40,—
 No. 33: ESO Workshop on "Low Mass Star Formation and Pre-Main Sequence Objects", Garching, July 1989 DM 50,—

New ESO Scientific Preprints

(September–November 1989)

671. M. Pierre: Probes for the Large Scale Structure. *Astronomy and Astrophysics*.
 672. G.V. Bicknell et al.: Physical Properties of Jets in Low Luminosity Radio Sources. *The Astrophysical Journal*.
 673. B. Reipurth: Poster Abstracts from ESO Workshop "Low Mass Star Formation and Pre-Main Sequence Objects".
 674. J.-L. Prieur: Status of Shell Galaxies. Invited paper, to be published in the Proceedings of the Heidelberg Conference on "Dynamics and Interactions of Galaxies", Heidelberg, Springer-Verlag.
 675. B. Leibundgut and G.A. Tammann: Supernova Studies III: The Calibration of the Absolute Magnitude of Supernovae of Type Ia. *Astronomy and Astrophysics*.
 676. G.A. Tammann and B. Leibundgut: Supernova Studies IV: The Global Value of H_0 from Supernovae Ia and the Peculiar Motion of Field Galaxies. *Astronomy and Astrophysics*.
 677. G. Contopoulos: Asymptotic Curves and Escapes in Hamiltonian Systems. *Astronomy and Astrophysics*.
 678. A. Renzini: The Evolving Stellar Content of Galaxies and the X-ray Evolution of Elliptical Galaxies. To appear in *Windows on Galaxies*, ed. G. Fabbiano, J.A. Gallagher and A. Renzini (Dordrecht: Kluwer).
 679. G. Setti and L. Woltjer: AGNs and the Spectrum of the X-ray Background. *Astronomy and Astrophysics*, Letters.

A Homogeneous Bright Quasar Survey

C. BARBIERI¹, S. CRISTIANI¹, P. ANDREANI², R. CLOWES³, A. GEMMO¹, C. GOUIFFES²,
A. IOVINO⁴, F. LA FRANCA^{1,5}, A. SAVAGE⁶, R. VIO¹.

¹Department of Astronomy, Padova, Italy; ²European Southern Observatory; ³Royal Observatory, Edinburgh, Great Britain; ⁴Brera Observatory, Italy; ⁵Institute of Radio Astronomy, Bologna, Italy; ⁶UK Schmidt Telescope Unit, AAO, Australia

1. The Dreams

As extremely luminous objects visible to high redshifts, quasars have long offered the promise of directly exploring the distant Universe. Counting quasars, however boring and repetitive it may appear, allows one to address basic issues in Cosmology, such as: when did quasars form and how evolved the gravitational engine providing their extreme energies? How are quasars related to galaxies? When did galaxies form? What structure has the Universe at the largest scales? On what scale does the Cosmological Principle finally apply? Which models can explain plausibly the transition from the smooth Universe of the microwave background to the very inhomogeneous Universe of today?

2. The Reality

A number of quasar surveys, carried out with different techniques and limiting magnitudes, have yielded in the last years a considerable insight, and details of the evolutionary history of the quasar population are slowly emerging as the database increases. Clustering of quasars on small scales has now been confirmed at the 5σ level of significance¹ and there is also evidence for evolution of the QSO correlation function with cosmic time.

With the development of new techniques for automatic detection and analysis of images, a powerful tool has become available to astronomers. However, to obtain useful cosmological information, it is necessary to carry out statistically well-defined surveys, allowing one to quantify selection effects in the first place and to minimize the subsequent investment of telescope time for spectroscopic confirmation of the candidates. The relevance of this point is well illustrated by the chronic issue of isotropy in the extant samples.

In another context, while Wampler and Ponz³ indicated that redshift- and luminosity-dependent biases may superpose to the point of allowing marginal consistency with no evolution, at the other extreme Marshall⁴ claimed that optical samples whose magnitudes are evaluated by means of simple iris

photometry, after only a mean correction for lines, provide bias-free slope and evolution rate of the LF with statistical uncertainties of only a few per cent in all parameters, including the evolutionary time scale. The difficult evaluation of the so-called *Bennett effect*^{5,6} and the “contamination” of the continuum magnitudes by the lines entering the various filter bandpasses give origin to the above-mentioned contradiction. The problems in the evaluation of the QSO evolution rate in the presence of observational biases are explained in detail by Cavaliere, Giallongo and Vagnetti⁷. In order to understand and account for these selection effects, we have been studying the field of SA 94 for many years with complementary techniques².

As a consequence of the unsatisfactory database, the shape of the Luminosity Function and the determination of the form of evolution as $L \propto (1+z)^k$ or $L \propto e^{T/\tau}$ are uncertain. Trends of this form, potentially telling about the mechanism to fuel the central engine (in principle they can reveal if the QSO phenomenon is driven by the surrounding environment or determined by its nuclear conditions only), maybe spuriously favoured by fits that overlook the

observational biases. To probe the real trend, not only the database at faint magnitudes has to be enlarged^{8,9}, but also the incompleteness at bright magnitudes should be bound or removed with better samples allowing an adequately sophisticated analysis.

The PG bright quasar survey¹⁶, at the bright end of the Log N–Log S diagram, is especially affected because of the shape of the luminosity function and of the low ratio (≈ 2.5) F/σ , where F is the flux and σ^2 is the variance of the magnitudes, compared to other existing samples. A true increase of information about LF shape and evolution is obtained only combining rich “homogeneous” samples, i.e. with sensibly matched signal-to-noise ratios: if anything F/σ ought to be larger for the brighter samples with a magnitude limit crossing the steep branch of the LF.

The present situation of quasar counts (for quasars with $z < 2.2$) is summarized in Figure 1.

3. Our Plans

From the above considerations it can be easily seen that a new survey ($F/\sigma > 4$) is required for the bright part of the

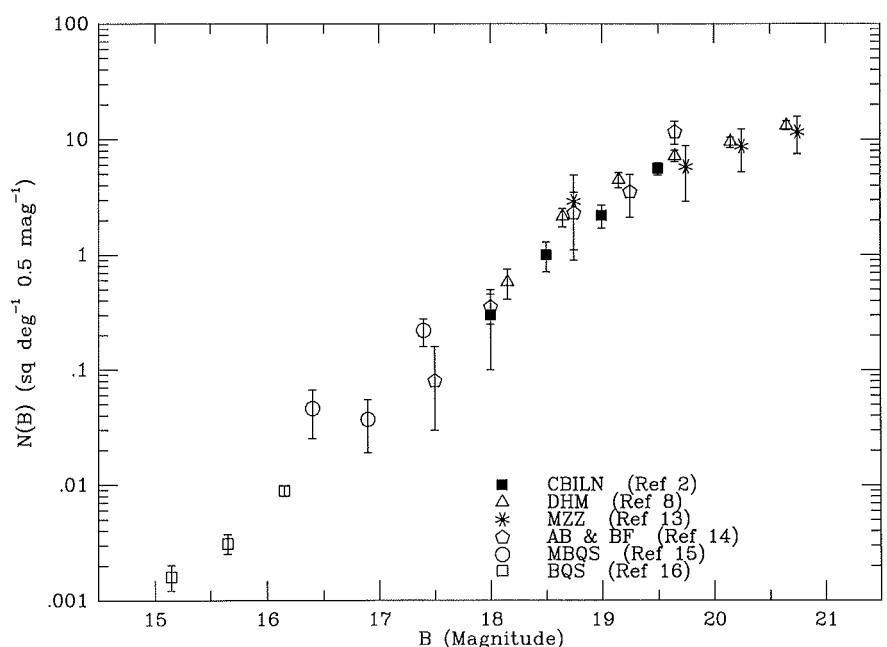


Figure 1: The quasar differential Log N – Log S.

Log N – Log S diagram where the PG sample is incomplete and the information from other surveys is still scanty. This happens at $16 < B < 18.25$, where we expect surface densities of 10^{-2} and 1 quasar ($z < 2.2$) per square degree, respectively.

In order to obtain a number of quasars statistically significant we need to survey an area of the sky of 2000 sq. deg. We have selected the zone around the south galactic pole, extending below $b = -60^\circ$, which has the following advantages:

(a) the galactic absorption is minimized. It may be argued, in fact, that the imperfect knowledge of the galactic extinction prevents a determination of a photometric scale better than a tenth of a magnitude and, ultimately, from a detailed understanding of the fluctuations of the quasar surface density¹⁰. Furthermore, at lower galactic latitudes the reddening would oblige us to loosen the colour-selection criteria, whose even small modification would bring in the quasar locus a number of galactic candidates very expensive in terms of telescope time

(b) the contamination from galactic objects is minimized. We expect to find a large number of quasars and, of course, a much larger number of candidates. Even a small departure from high galactic latitudes would again increase the number of spurious candidates to an unbearable level

(c) a number of other surveys, with complementary techniques, have been carried out on this area of the sky, providing an easy way to calibrate our selection criteria and check the effectiveness and completeness of our search. Other surveys will be carried out in the future: for example ROSAT, which will allow to compare X-ray and optical quasar properties; or galaxy redshift surveys¹¹ which would provide the information about the low-redshift absorbers of the spectra of our higher-redshift bright quasars, etc.

To cover this area of the sky, 77 fields (1925 sq. deg) of Schmidt telescope plates are needed. They will be taken in five (U, B, V, R, I) bandpasses (in place of the 2 or 3 commonly used) not only to select also high redshift candidates (which at those magnitudes will be a small fraction of the quasars), but especially to reduce the locus occupied by stars to a tiny fraction of the multidimensional colour space, thus increasing the success rate and minimizing the time required for follow-up spectroscopy. The plates are taken within a short time in order to reduce the effects of variability and reach objects about one magnitude fainter than the limit of the survey. Quasar counts are obtained indepen-

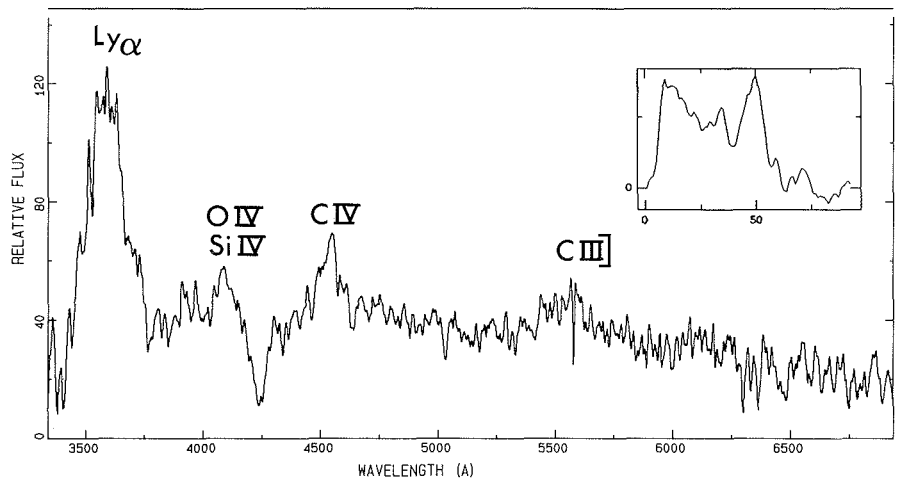


Figure 2: Our first Key-Programme quasar. In the upper right (with the direction of the dispersion inverted) the tracing of the AQD objective prism spectrum.

dently in B, V and R in order to disentangle the K-correction effects. The candidates are selected on the basis of clustering analysis on the multicolour space¹².

To obtain reliable LFs, a good photometric UBVRI calibration is required, and this is accomplished with photoelectric photometry at the 1-m and with CCD photometry at the 2.2-m telescope.

An analogous project in the northern hemisphere will be started with the Asiago Schmidt telescope and will eventually enable us to obtain significant statistics down to $B \approx 15.5$.

4. More Dreams . . .

A better understanding of the quasar luminosity function will not be the only outcome of this programme:

(a) we expect to find a few hundred Seyfert galaxies for which a fine tuning of the multicolour technique will allow us to determine a complete sample

(b) a study of the variability of the objects (by comparison with the plates of the original ESO blue survey) will allow us to study the LF of the BL Lac objects (and to check the completeness of the quasar survey), for which only scanty information is available at present

(c) the large-scale clustering of quasars, for which almost nothing is known, will be studied

(d) precise statistical information will be available for millions of objects, which can be used for stellar counts, galaxy studies, crosscorrelation with catalogues at different wavebands, etc.

5. First Results

The first observations of quasar candidates, selected on plate material previously taken at UKSTU and ESO, started last September. The first one and a half field were completed, objects in five more fields were observed. An improved AQD¹⁷ selection technique,

for UKSTU objective prism data, was successfully tested, with encouraging results both in terms of success rate and completeness, aiming at a sample of QSOs up to $z \approx 3$. After the second run (in November) the first meaningful counts will be produced.

In Figure 2 the spectrum of the first confirmed quasar of our Key-Programme is shown. It is nothing special (apart from the probable Broad Absorption Lines) but it has already more than one hundred comrades. And when a thousand of them will gather, some revolution may burst.

In this way, counting, counting, we hope to fulfil our dreams . . .

References

1. Iovino, A., Shaver, P.A., 1988, *Ap. J.* **330**, L13.
2. Cristiani, S., Barbieri, C., Iovino, A., La Franca, F., Nota, A., 1989, *Astr. Ap. Suppl.* **77**, 161.
3. Wampler, J., Ponz, D., 1985, *Ap. J.* **298**, 448.
4. Marshall, H.L., 1985, *Ap. J.* **289**, 457.
5. Bennett, A.S., 1962, *M.N.R.A.S.* **125**, 75.
6. Murdoch, H.S., Crawford, D.F., Jauncey, D.L., 1973, *Ap. J.* **183**, 1.
7. Cavaliere, A., Giallongo, E., Vagnetti, F., 1989, *Astron. J.* **97**, 336.
8. Boyle, B.J., Fong, R., Shanks, T., Peterson, B.A., 1987, *M.N.R.A.S.* **227**, 717.
9. Koo, D., Kron, R., 1988, *Ap. J.* **325**, 92.
10. Weedman, D., 1986, *Quasar Astronomy*, Cambridge Univ. press, p. 22.
11. De Lapparent et al., 1989, *The Messenger* **55**, 5.
12. Warren, S.J., Hewett, P.C., Irwin, M.J., 1987, *I.A.U. Symp.* **124**, 661.
13. Marano, B., Zamorani, G., Zitelli, V., 1988, *M.N.R.A.S.* **232**, 11.
14. Marshall, H.L., et al., 1984, *Ap. J.* **283**, 50.
15. Mitchell, K.J., Warnock, A., Usher, P.D., 1984, *Ap. J.* **287**, L3.
16. Schmidt, M., Green, R.F., 1983, *Ap. J.* **269**, 352.
17. Clowes, R., et al., 1984, *M.N.R.A.S.* **207**, 99.

ESO's Early History, 1953–1975

V. Earliest Developments in Chile; 24 March 1966: The Road on La Silla Dedicated*

A. BLAAUW, Kapteyn Laboratory, Groningen, the Netherlands

"If we look around here, we see what has been achieved in the short period of a little more than one year. — — — an oasis in the desert."
From the speech by the President of the ESO Council, delivered at the dedication of the road on La Silla.

Introduction

While – as described in the previous article – in Europe Directorate and Council established ESO's administrative basis, and the first telescopes were built or acquired under the guidance of the Instrumentation Committee, work in Chile proceeded equally energetically. Under the leadership of André Muller, since January 1, 1964 Superintendent for Chile, a great variety of tasks had to be taken up: building up staff for administration and construction, organizing office facilities, setting up temporary camps as basis for the activities on and around La Silla, learning to know the Chilean world of government and provincial authorities and of contractors, etc. A challenging but demanding assignment! For it is one thing to build up an organization in one's own country with its well-known legal structure and social traditions – but another one to do so in a foreign country with unfamiliar language, different customs and different rules.

Two important "happenings" in Chile offer themselves as reference points for the historical account. One, in March 1966, is the dedication of the road to the summit area of La Silla, the completion of which was a natural inducement for Council to have its meeting in Chile. The second one, three years later, in March 1969, is the dedication and celebration of the completion of the first stage of the constructions on La Silla, when the middle-size telescopes had become operational: these celebrations coincided with Council's second meeting in Chile. In the present article I shall follow developments leading up to the first one of these events: the period 1964–1966.

Early in 1964, when there still was the prospect of a combined AURA-ESO settlement, Muller was engaged in work on the mountain Cinchado within the AURA territory, south-west of Tololo. However, these activities were rather abruptly terminated after the working group of Heckmann, Fehrenbach, Rösch and Muller as described in article III, had explored possible sites outside the AURA domain and found La Silla. This

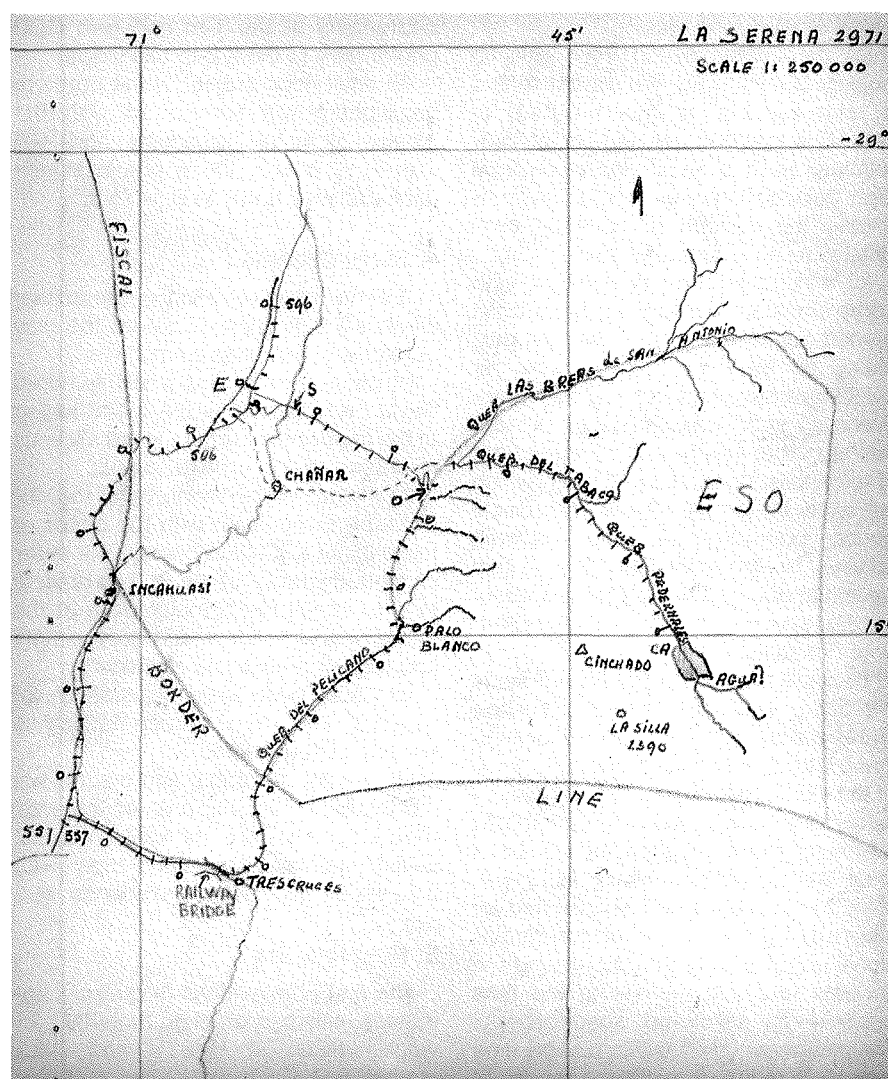
switch had been no small matter: as mentioned in the ESO Annual Report for 1964 (p. 13), the work on Cinchado had implied road construction and erection of temporary housing requiring 500 mule loads of building material to be transported to the top of Cinchado, much of which had to be brought down again . . . From then on, all effort had to be concentrated on La Silla.

Main sources for the present account are: (a) a series of three reports by Muller to the ESO Directorate, covering the period up to the middle of 1965, copies of which were sent by Muller to J.H. Oort as President of the ESO Council

[1]; (b) reports presented by the Director, Heckmann, to the Council and his letters to Oort in which he reports on his visits to Chile in March–April 1964, August and October 1964, March–April 1965, and September–October 1965 [2]; (c) the minutes of Council and FC meetings in the FHA; and (d) the Annual Reports for the years 1964 to 1966.

The Acquisition of the La Silla Territory

On October 30, 1964, a contract was signed in Santiago between ESO and the Government of Chile for the pur-



Map A: Reproduction – at about half the original size – of a map drawn by A.B. Muller and accompanying his report to the ESO Directorate of June 29, 1964, describing explorations to find the best access road to La Silla.

* Previous articles in this series appeared in *Messengers* No. 54–57.

chase of an area of 627 square kilometres including the mountain La Silla [3]. It formed part of more extended Government property within which the ESO domain had been staked out as proposed by ESO with most of the boundaries following dry riverbeds (called *quebradas*); see map B. The site is situated in the border region of the provinces Coquimbo and Atacama, pertaining to the communities of Vallenar and La Higuera, respectively. The contract defines the contours of the property by means of the geographic longitude and latitude of the five points A to E marked on map B. The relatively low price ESO paid for the territory, 8000 dollar [4], reflects the interest on the part of the Chilean Government in having the Observatory established in their Country.

Preceding the transfer, such questions as the accessibility of the mountain, the possible amount of water supply, the fate of the few settlers on the territory, and the elimination of existing and potential claims for mining rights

had to be cleared. Therefore, already in the intervening months between the choice of La Silla and the conclusion of the contract, much activity took place in the area, to some of which we shall return below. Also, an unexpected obstacle was encountered when, notwithstanding the property rights of which the Government was convinced, it turned out that ownership in the southern part of ESO's area, forming part of the Estancia Chingoles, could be claimed by a private owner, the Urrizar family. In order to avoid time-consuming legal procedures, ESO came to an agreement with the Urrizar owners, buying for 6000 dollars this part of the territory once more [5] – still at a quite reasonable price. Moreover, the Urrizar family granted ESO the use of 50% of the yield of a neighbouring water source on their territory if the need might be. More particulars on this episode are given in Heckmann's account [6].

Parallel to the acquisition of the La Silla territory progressed that of the site

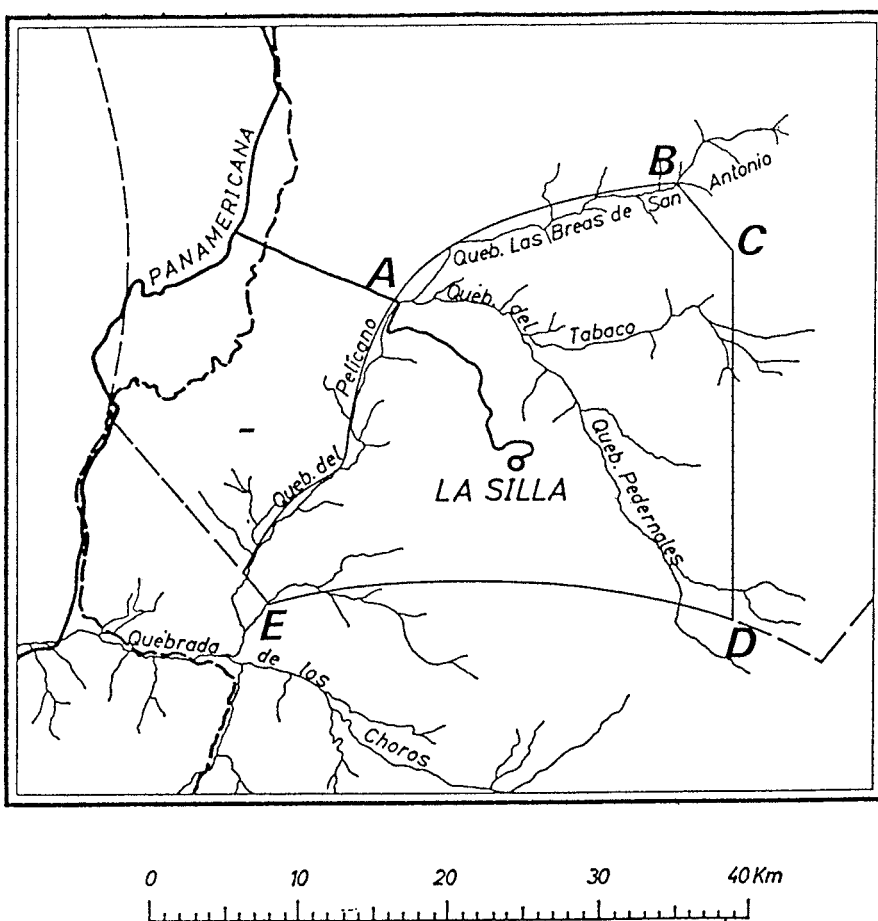
in the city of Santiago on which ESO planned to build its Headquarters, and the purchase of the Guesthouse. We shall return to the History of the Headquarters in the next article, and first follow developments around the Observatory.

Building up the Observatory; First Step: Road and Camps

As a home base for the work on the Observatory site, ESO – like AURA – established an Office in La Serena, capital of the Province of Coquimbo, where the necessary contacts could be entertained with government services and contractors; it also was the nearest town with schooling facilities for young children of ESO staff. These latter included the Muller family who moved from Holland to La Serena in March 1964. At a distance of 480 km from Santiago, the capital of Chile, La Serena became the natural centre from where all work had to be co-ordinated. Yet, with La Serena still being 150 km distant from the summit of La Silla, construction programmes as well as the first operation of the Observatory would also require extensive provisional facilities for living quarters, construction work, storage and administration in the La Silla area itself. Therefore, camps had to be erected at its base as well as on the summit. But the very first question was, of course, how to get there!

The first one of Muller's reports, of June 29, 1964, contains a hand-drawn map of the La Silla area which we reproduce here at about half the original size (map A). It must have been based on the Government map No. 2971, copy of a relevant section of which is in EHA-I.C.3.1. which also contains contour maps of this area. Muller's map serves well to illustrate the earliest moves.

When Heckmann, in his letter to Oort of April 21, 1964 quoted in article III, wrote about Cinchado-Nord (the official name of La Silla in the mapping of the Instituto Geográfico Militar) as being the most interesting of the mountains surveyed and accessible from the Panamericana via about 35 km primitive road, he referred to a different track than what would become the present road between the Panamericana and Camp Pelicano. [N.B. André Muller informs me that the name La Silla, meaning The Saddle, was at that time already used by the carboneros (charcoal burners) in the valleys around the mountain.] The track mentioned by Heckmann branched off from the Panamericana at point 557 indicated in map A and entered Quebrada Pelicano via Tres Cruces, passing over a railway bridge as marked in the map. This bridge would have been a difficult



Map B: The ESO property as defined in the purchase contract between ESO and the Chilean Government of October 30, 1964. The boundaries are fixed by the geographic co-ordinates of the points A, B, C, D, E and the centrelines of the quebradas Pelicano and Las Breas de San Antonio.

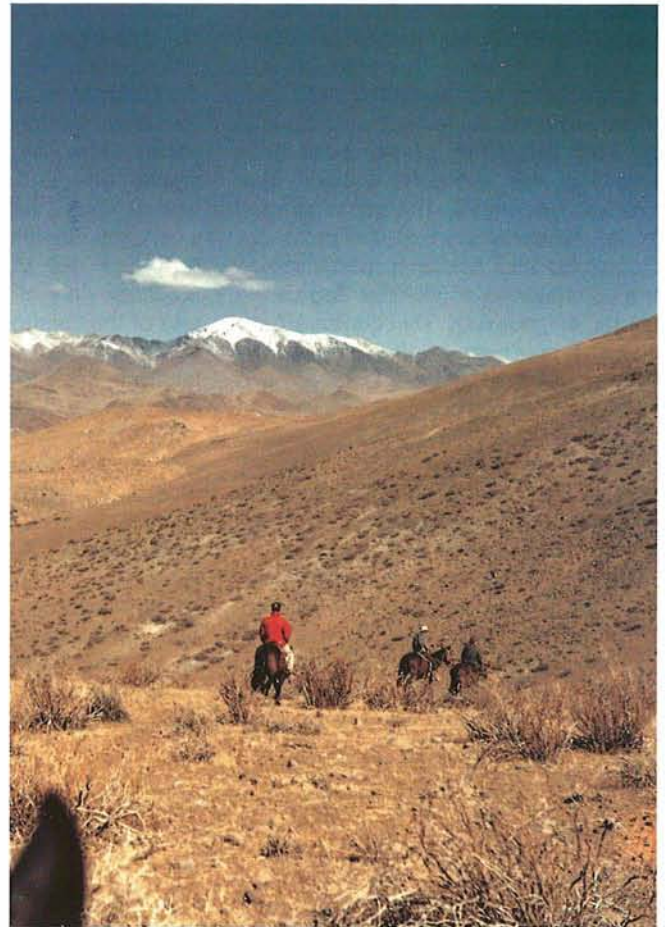
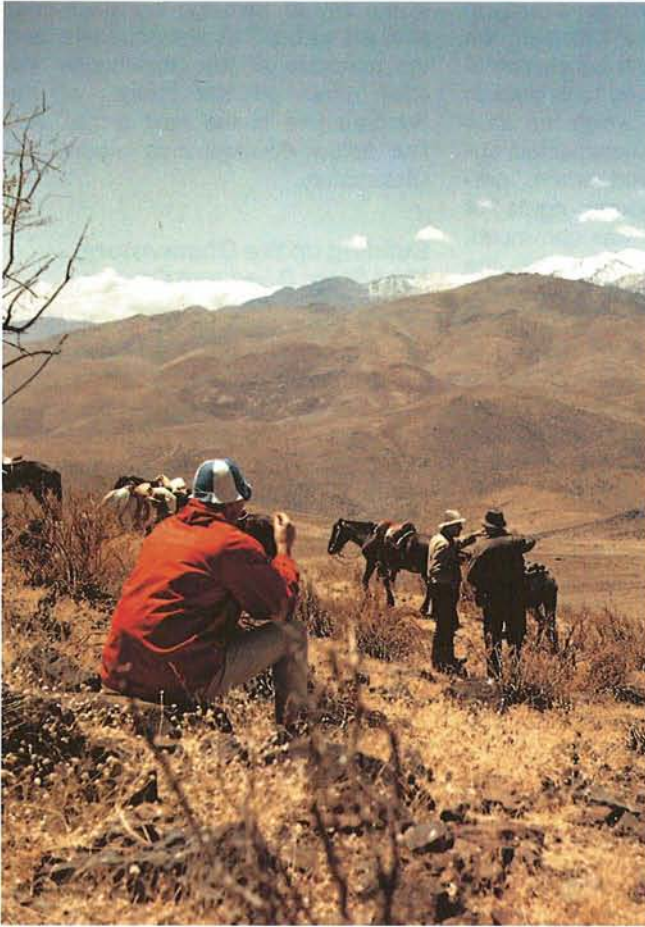
Thin drawn line: boundary of ESO property.

Thin dashed line: boundary of Government property of which the ESO territory formed part.

Heavy lines: Panamerican Highway and access road to La Silla.

Heavy dashed line: Railroad track.

Adapted from Figure 2 in ESO Annual Report 1964.



In October 1964, Ch. Fehrenbach as Chairman of the Instrumentation Committee, the architect F.W. de Vlaming and the author, together with ESO Staff, explored – still on horse-back – La Silla for planning of the location of the telescope buildings and the associated facilities. In both photographs, from left to right, de Vlaming, André Muller and Otto Heckmann. Photographs by the author.

obstacle for future transport. However, Muller's first report states: "There does exist a much better possibility. A reasonably good track was found by Muller during his investigation of the area Chañar on the 18th and 25th of June. On the 18th the road to Chañar was found, but the track indicated on the map from Chañar to O does not exist. On airphotographs a road was found from the Panamerican Highway to O and this track was recognized by him while flying on the 24th from Copiapo to La Serena. On the 25th a successful attempt was made to get to point O and also to CA in the Quebrada Pedernales. --- the first time it was a bit difficult to get from the new road to the track EO, but later three different tracks were found from the new road to the access road to O. --- It is clear that the road to Pedernales and later to La Silla will run over the points E to O. To get from O to the top of La Silla, ESO will have to construct a road of more or less 40 km length. ---" As visitors of La Silla arriving from the Panamerican Highway nowadays will note, their path to Camp Pelicano leads along the, formerly very primitive, track EO.

Whereas Muller's last remark refers to the definitive road to the top, a provisional one was a first requirement for the construction work. Also immediately required was a source of water, even if it were to be used only temporarily. One source was located with the help of the geologist O. Castello of the Instituto de Investigaciones Geológicas in the area marked CA on the map. Simultaneously, exploration in the La Silla area for finding the most suitable track for approaching the top was carried out by F. Unz, the collaborator of Siedentopf who had carried out atmospheric turbulence measures at Zeekoegat and subsequently did similar work on Cerro Tololo; he recommended to approach the top from the same area, i.e. from CA. Thus, originally it was planned to reach the summit area from point O along a primitive road through Quebrada del Tabaco and Quebrada Pedernalis to the area CA and from there along about 5 km of new, provisional road to the top.

This project was not carried out, however. Muller erected at the foot of the mountain, near the junction of Quebrada Pelicano and Quebrada Las Breas de San Antonio, at altitude about 1000 m,

the principal base camp for the operations: Camp Pelicano, close to the position where it still is today. From here he chose a new track that led straight into the slopes of the mountain, not using the tracks in the Quebradas at all. The definitive road, as we know it now, deviates little from this provisional one. Construction of the road in provisional form started in March 1965 and around the middle of that year it was good enough to allow heavy construction vehicles to reach the summit area. Also, the sites for the telescopes and other buildings were then levelled.

This early stage did not yet include the road to the top reserved for the 3.6-m telescope, neither the levelling of this top; the road went as far as the area around the site for the Schmidt telescope. Putting this road in definitive shape, including asphalt surfacing and widening it here and there would be a matter for the future, when no heavy traffic would spoil the surface any more. Construction works for the 3.6-m telescope were still a matter for the future... Thus, late 1965 ESO was ready for the dedication of its road, to be combined with Council's first meeting in

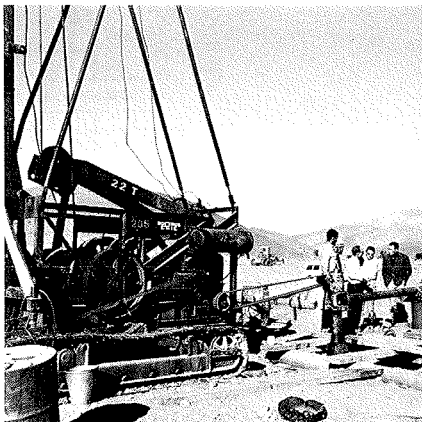
Chile. A report on the road construction on La Silla has been published by H. O. Voigt in ESO Bulletin No. 3 of February 1968. The engineer Voigt had been appointed per October 1, 1964 as Assistant Director for the construction activities. But before arriving at the dedication festivities, we must turn to other aspects of the early work.

The Problem of the Mining Rights

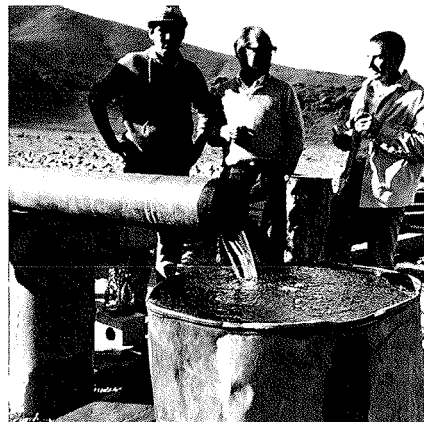
When Council decided on May 26, 1964 to choose La Silla for the Observatory, and consent on the part of the Chilean Government could be taken for granted, this did not yet imply that Muller and his collaborators could freely move and get to work on the mountain. Their work was still hampered by legal aspects connected with the elimination of existing or potential claims for mining rights. A few explanatory remarks on this subject are in order here.

In Chile, where much of the economy depends on the production of its mines, special laws protect their exploration to the effect that the owner of land like that around La Silla is not automatically also the owner of the minerals occurring below the surface: other parties may claim the right to explore mines on such territory, a right to be granted by the Government. This paramount importance of mining explains why, for example, the very first paragraph of the first article of the contract for the purchase of the La Silla territory reads: *"No mining operations shall be conducted without the authorization of the Head of State of Chile -- --."* For ESO it was – and still is – necessary to avoid mining on its territory because of the resulting disturbance of the atmosphere by dust and illumination. ESO therefore had to claim itself the right for exploration whenever it was demonstrated by another party that minerals could be found in critical parts of its domain. Claiming mining rights involves payments to the Government, and the rights thus guaranteed are of temporary nature only and must be re-obtained at repeated costs. As mining rights can be sold – for instance by prospective explorers to ESO – it is obvious that there is a strong speculative aspect against which ESO had to defend itself continually.

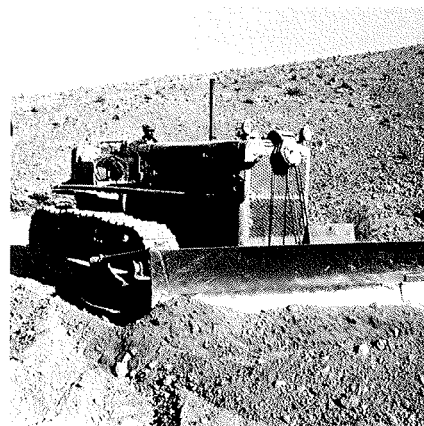
This defense has been one of the tasks of ESO's legal advisors in Chile and it was, from the outset, one of the Directorate's main worries as is evident from Heckmann's reports to Council, for instance those after his trips to Chile in August and October 1964 and March – April 1965. Early in 1964, the clearance of mining claims slowed down the activities of Muller's group on the mountain [7] because preparations for road



June 1965: First successful water drilling near Camp Pelicano.



June 1965: Road construction on La Silla.



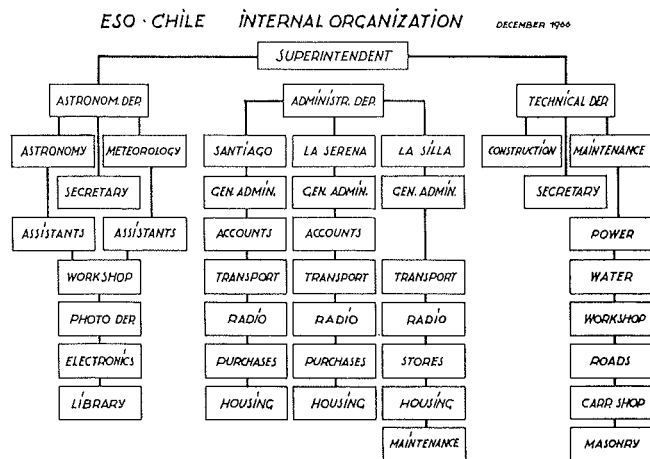
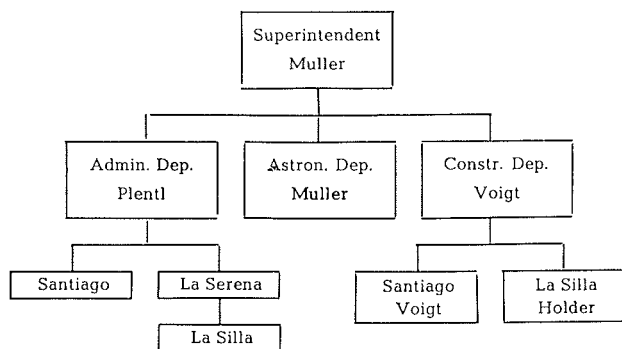
All four photographs from negatives in the ESO Historical Photographs Archives.

construction might awaken the interest of outside parties in searching for minerals in those particular areas. Characteristic is the following section of a letter by Heckmann to Oort of April 3, 1965 [8]: *"6. Wir haben mit den Minenrechten mancherlei Mühen. Das gefährlichste lag unmittelbar auf dem Gipfel von La Silla. Es war vor uns da, wurde aber, als wir kamen, in seiner Lage und Orientierung so fixiert, daß es uns sehr störte. Ich war für ein paar Tage sehr verzweifelt. Unser Minen-Advokat Urrutia hat aber vor Gericht in La Serena dieses Minenrecht mit Erfolg angefochten. -- --"*

The Building Programme; Early Architectural Planning

Anticipating developments after the ratification of the ESO Convention (of early 1964), the ESO Committee in its meeting of February 1963 installed a Working Group for Buildings under the Chairmanship of the ESO Director. It was to draft a programme for the erection of the Observatory (domes, offices, hostels, workshops, etc. and time schedule) in accordance with the wishes of the astronomers in the ESO countries. This led to a Memorandum of

November 8, 1963 which was accepted by the ESO Committee in its meeting of November 15, 1963 and endorsed after the ratifications. At the same time, the Directorate prepared a "Short Memorandum on the ESO Building Activity" [9] dated October 7, 1963. (Note that at that time the choice of the Observatory site had not yet been made.) The memorandum was also meant for information of potential construction firms. It was proposed to realize the Observatory in two steps. The first of these, to be finished "about 1966", should cover everything associated with the installation and operation of the middle-sized telescopes described in my previous article together with the Schmidt telescope, and the second, to be finished "about 1970", should cover the realization and operation of the 3.6-m telescope and the associated facilities. The first stage was to include on La Silla such elements as the Boarding House, Workshop and technical facilities and a few residences, and the second stage, apart from the building for the large telescope, extensions required for the use of this telescope. Also included in this planning was the Headquarters Building in Santiago, correspondingly subdivided in a first and second stage.



Building up ESO in Chile: The structure of the Organization as shown in the ESO Annual Reports for 1965 (left) and 1966 (right).

As part of this planning, it was necessary to obtain architectural designs and cost estimates. ESO therefore contracted the firm of the Dutch architects F.W. de Vlaming and H. Salm who, a.o. projects, had been associated with the radioastronomical establishments in the Netherlands [10]. De Vlaming visited the building sites in October 1964 in the company of ESO staff and astronomers including Fehrenbach as President of the Instrumentation Committee and the present author, the latter particularly in connection with the housing of the 1-m telescope which was expected to soon be operational. The preliminary designs of de Vlaming have provided a first basis for the planning and the general lay-out of the Observatory, but the rather ambitious, "representative" nature of his designs have ultimately in some cases been replaced by more sober implementations.

A rather detailed description of the planning by the Working Group for Buildings and the Directorate has been published in *ESO Bulletin* No. 2 of August 1967 by J. Ramberg, at that time Assistant Director of ESO. This article also describes the status of execution by the end of 1966: the design work by the architect and his associates had been completed, consulting engineers of the construction firms had been associated with the project, and offers from construction firms were being negotiated. In many respects, the execution of the project was to become a joint European-Chilean undertaking, including a Chilean architect and Chilean firms for the constructions.

Progress over the Years 1964–1966

The situation in the La Silla area at the end of 1964 is – too modestly! – summed up as follows in the Annual Report for 1964:

"a) Office in La Serena, functioning with five persons active.

b) Camp Pelicano, with two old houses and four new ones installed, a carpenter's workshop in use, fifteen persons active, animals' camp installed and functioning with five horses and six mules, two wells ready with one pump installed.

c) Road project [i. e. planning and layout of the road], ready from camp Pelicano to the top of La Silla."

At that moment the small group of ESO employees in Chile consisted of André Muller as Superintendent, with Hans-Emil Schuster, a former pupil of Heckmann, appointed per October 1, 1964 as Assistant-Astronomer; furthermore, there were the Camp Supervisor Hernan Carrasco and five more technical and administrative staff [11]. We also reproduce here from the ESO Annual Reports for the years 1965 and 1966 the schematic representations of the structure of the organization, exhibiting its rapid expansion after 1964.

The year 1965 saw progress of work in the La Silla area on many fronts. Apart from the major accomplishment, the road construction, Camp Pelicano began to take its more definitive shape after having served initially in provisional form. For the power supply, which had been obtained provisionally from a small portable generator brought from South Africa, a power house was erected at Camp Pelicano with a battery of generators whose output was to grow as the demand would increase. On the summit area of La Silla a small temporary camp was constructed, including storage room, some living quarters, a power house and a temporary workshop. A beginning was made with the building for the GPO telescope which would soon be transferred from South Africa to La Silla. Also, a radio connection between Camp Pelicano and the summit Camp was installed. Meteorolo-

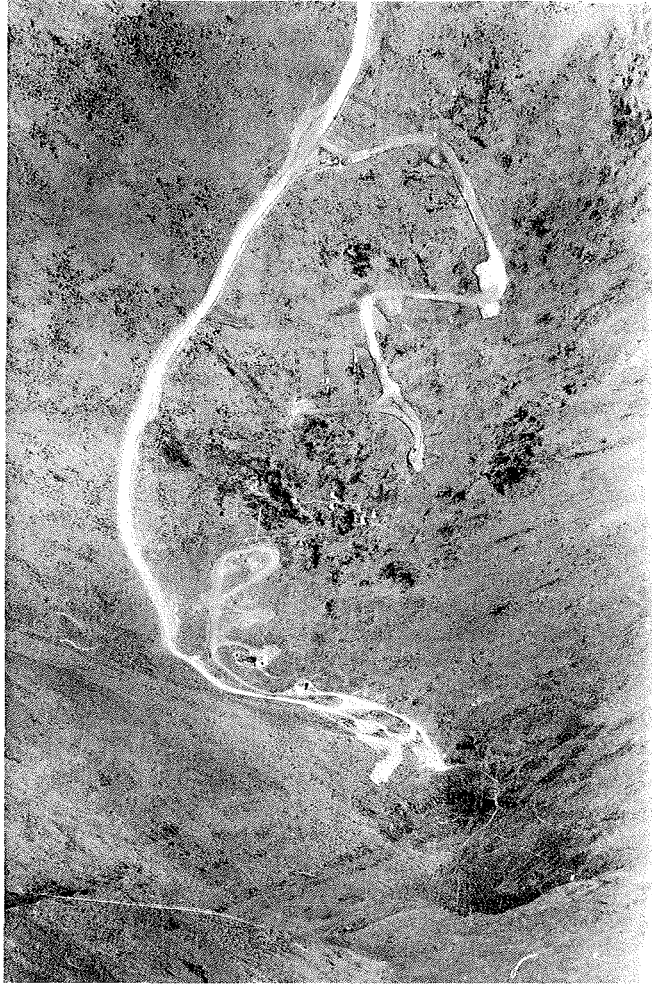
gical observations were conducted throughout the year. They included measures of cloudiness, wind velocity, wind direction, temperature and humidity and were reported by Muller in the first issue of the *ESO Bulletin*, of November 1966. (Meteorological reports by Muller for subsequent years have been published in Bulletins Nos. 3, 4 and 7 for the years 1966, 1967 and 1968.)

For supplying the Observatory with water, a number of boreholes were drilled near Camp Pelicano in 1965 and their output was promising, but the really important question was, of course, whether the yield would remain sufficient under the continual use by the Observatory in operation. Checks in 1966 and thereafter showed that the use would not be exhaustive. As the visitor of La Silla notices, the water is transported from the level of Camp Pelicano (at about 1000 m) to the summit at about 2400 m in three steps, with two high-pressure pumps in between (at altitudes 1500 and 1950 m). The construction of the water and power supply have been described by S. Klingenberg in *ESO Bulletin* No. 3 of February 1968.

Organizational Structure and Employees

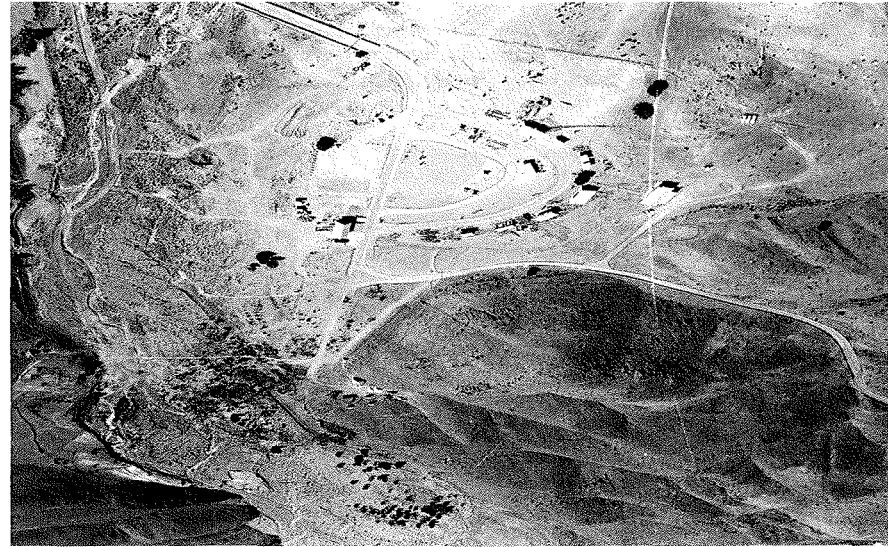
By the time Muller and his collaborators were ready for the dedication of March 1966, the activities in Chile were grouped in three departments: an administrative one, one for constructions, and one dealing with miscellaneous tasks including meteorological observations; this latter under Muller himself together with Schuster. Much of the activity centred on La Silla and around Camp Pelicano. Engaged in Camp Pelicano had become also Albert Bosker whom we encountered earlier as one of the assistants of Muller during the site tests in South Africa. Bosker

January 1966: Aerial photographs of first stage of road construction on the summit of La Silla. South is at the top, north at the bottom. Note that the road did not yet extend to the main and secondary tops in the southern background of the left-hand photograph, now occupied by the 3.6-m telescope and the NTT. The more detailed right-hand photograph shows that the only telescope building under construction was the one for the GPO.



joined ESO this time on more permanent basis, from February 1965, first as assistant Camp Boss, and from November 1965 as Storekeeper (Chief Bodega) at Pelicano. Under the Camp boss fell matters of board and lodging for the workers at La Silla, transport, storage, radio links, stable boys, and the animal population of horses and mules still used for patrolling the property. In the course of 1966 a second, now more definitive Camp was erected near the top of La Silla under the same supervision, for the housing and board of part of the construction workers.

The administrative department had an office in La Serena, with Arturo Cuthbert as bookkeeper, but it became more and more centred on Santiago where it was supervised per January 1, 1965 by the Assistant Administrator H. J. Straatman. From the middle of 1965 all administration was headed by R. Pleintl under Muller's supervision. The department of constructions fell under the supervision of H. O. Voigt mentioned before and the engineer R. H. G. Holder who joined ESO per May 16, 1965. Of the many other



Camp Pelicano, January 1966. At lower right, the access road from the Panamerican Highway. At left, the road leading to the summit area of La Silla. At 1/3 from top, to the right of the middle of the photograph, the earliest, provisional Camp settlement.

Photograph from negative by R. Holder in the ESO Historical Photographs Archives.

Laboratory, and from January 1, 1965 in La Serena, and Mrs. Christa Euler who became a secretary at the Santiago Office per January 1, 1966 [12]. Naturally, there were many organizational links between La Serena and Santiago and with the corresponding divisions within the Office of the Director in Hamburg-Bergedorf.

The ESO Guesthouse

In the course of 1964, with more and more activity developing in Santiago, the need was felt for a *pied à terre* in this city, rather than always having to use hotel accommodation. A quite satisfactory solution was found by the acquisition of what has become the ESO Guesthouse, formerly belonging to the Spaarwater family. Situated in the Vitacura district, not far from the future Headquarters, with many rooms and surrounded by an attractive garden on a lot of 0.44 ha, it could easily be transformed into both offices for administration and temporary lodgings. In its meeting of December 1964 Council approved the purchase, and the transaction was concluded in March 1965. In May the Director could report that the house was being adapted to ESO's needs, and was run by the housekeeper Mrs. Carmen ("Hilde") Fritsch under the supervision of Mr. J.A. Briggs, Assistant Administrator in the Santiago office [13]. The hospitality and good care of the late Mrs. Fritsch until her retirement in the late 1970's will be gratefully remembered by many of ESO's staff members and visiting astronomers of those early years.

Council Meeting and Dedication, March 1966

The activities described before reached a milestone with the dedication of the road on La Silla and Council's first meeting in Chile. (Also the FC met there these days.) ESO's road was an excellent achievement and worthy of a celebration indeed. Over its total length of 20 km from Camp Pelicano to the summit it has no inclination exceeding 12%, no sharp curves, and the average width at the time of completion was 5 m. Never were serious obstacles encountered by transport of heavy and large parts of equipment in the later stages of building up the Observatory. In addition to the 20 km mentioned, about 5 km of access road had been paved to the various buildings on the summit. For the connection of Camp Pelicano with the Panamerican Highway, 17 km of the existing but quite primitive road had been improved as a joint project of ESO and the Chilean Public Works Department.

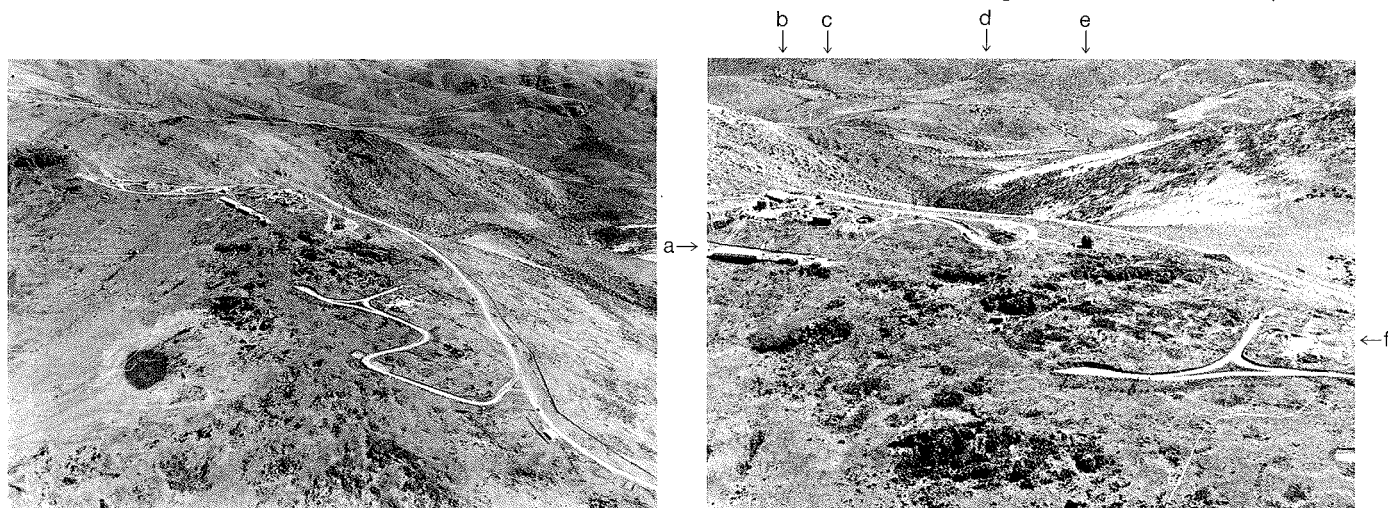
Council members arrived in Santiago on March 21 and left in the beginning of April. On March 23 they went to La Serena by bus and the next day arrived at Camp Pelicano. Here, in the morning of the 24th, the dedication ceremonies took place in the presence of many authorities and guests. They started with the benediction by the Archbishop of La Serena, after which ESO's President G.W. Funke delivered the inauguration speech in which he stressed the growing importance of Chile as a centre of astronomical activity. Funke's speech, with translation into Spanish, has been published in *ESO Bulletin* No. 3 in February 1968. Let me quote a few of Funke's words:

ruary 1968. Let me quote a few of Funke's words:

"If we look around here, we see what has been achieved in the short period of a little more than one year. Under the able leadership of Dr. A.B. Muller, Europeans and Chileans have created an oasis in the desert. --- We have to express our gratitude to every astronomer, technician and workman who cooperated in the joint effort. In particular the Chilean obrero has to be mentioned, because his readiness to work under the exceptional conditions of this area, his untired willingness to undergo the hardship --- made our work possible."

The ceremonies were concluded with a speech by the Intendente (Governor) of the Province of Coquimbo. Subsequently, Council and visitors drove by bus and car on the newly opened road to the summit area of La Silla. Council stayed overnight in Camp Pelicano and the next day visited places on the ESO domain. They made once more the trip to the summit, but this time in the now old fashioned but more romantic way – on horse-back.

During the next days Council visited the AURA site on Cerro Tololo and a copper mine in the vicinity of La Serena, before returning by bus to Santiago on the 29th. March 30 scheduled a visit to the University of Chile's Cerro Calan Observatory and a general reception, and on March 31 and April 1 Council held in Santiago its 6th meeting. For most of the Council members it must have been their first visit to South America. Neither the minutes of the Council meeting nor the ESO Annual Report tell



October 1966, first constructions on La Silla.

Left: Overview. Right: Close-up of the central part of the construction site.

- (a) Camp for the construction workers.
- (b) The lower part of the building for the GPO with next to it the provisional mechanical workshop.
- (c) Foundation for the 1-m telescope building.
- (d) Foundation for the 1.5-m telescope building.
- (e) The temporary dome of the 1-m telescope.
- (f) Site preparation for the Hostel.

Photographs from negatives by R. Holder in the ESO Historical Photographs Archives.



Second Extension of ESO Headquarters

Regular visitors to the ESO Headquarters in Garching will have noticed – also in the audio domain – that a major construction has been going on since mid-August this year. The second extension to the Headquarters building was decided in order to provide much-needed room for new staff members and more visitors, in particular because of the increased influx in connection with the VLT project, now shifting into very high gear.

The architect's solution to the problem consisted in adding a fifth floor to the southernmost part of the building, executed in light steel elements. This will provide 25 additional offices with space for about 50 more desks, within a total floor area of 450 square metres. It is expected that this space will be allocated to Science Division staff members who will liberate their old habitats below, making room for staff from other Divisions.

It is planned that the construction phase will last until mid-February 1990. The picture shows the view from south-east, on November 6, 1989.

much about these events, but the relevant documents are found in the section of the ESO Historical Archives originating from Oort [14], one of the participants.

Visits to Chile of Council, of FC and of other ESO Committees always have been extremely useful for a proper evaluation of the planning and the operation of the Observatory. The minutes of this first Council meeting in Chile reveal considerable, unforeseen rediscussion of the geographic structure of the establishment in Chile, although no fresh points of view were presented. An understandable development, because the complexity of the geographic structure of the organization and the enormous effort of the ESO staff required for its realization could only now, *in situ*, be fully appreciated by Council.

References and Notes

Note: For lists of the meetings of ESO Committee and Council see the tables in articles I and IV.

Abbreviations used:

EHA = ESO Historical Archives (see *The Messenger* of December 1988).

FHA = Files Head of Administration at ESO Headquarters.

Heckmann Sterne = O. Heckmann, *Sterne, Kosmos, Weltmodelle*, Verlag Piper and Co., München-Zürich, 1976.

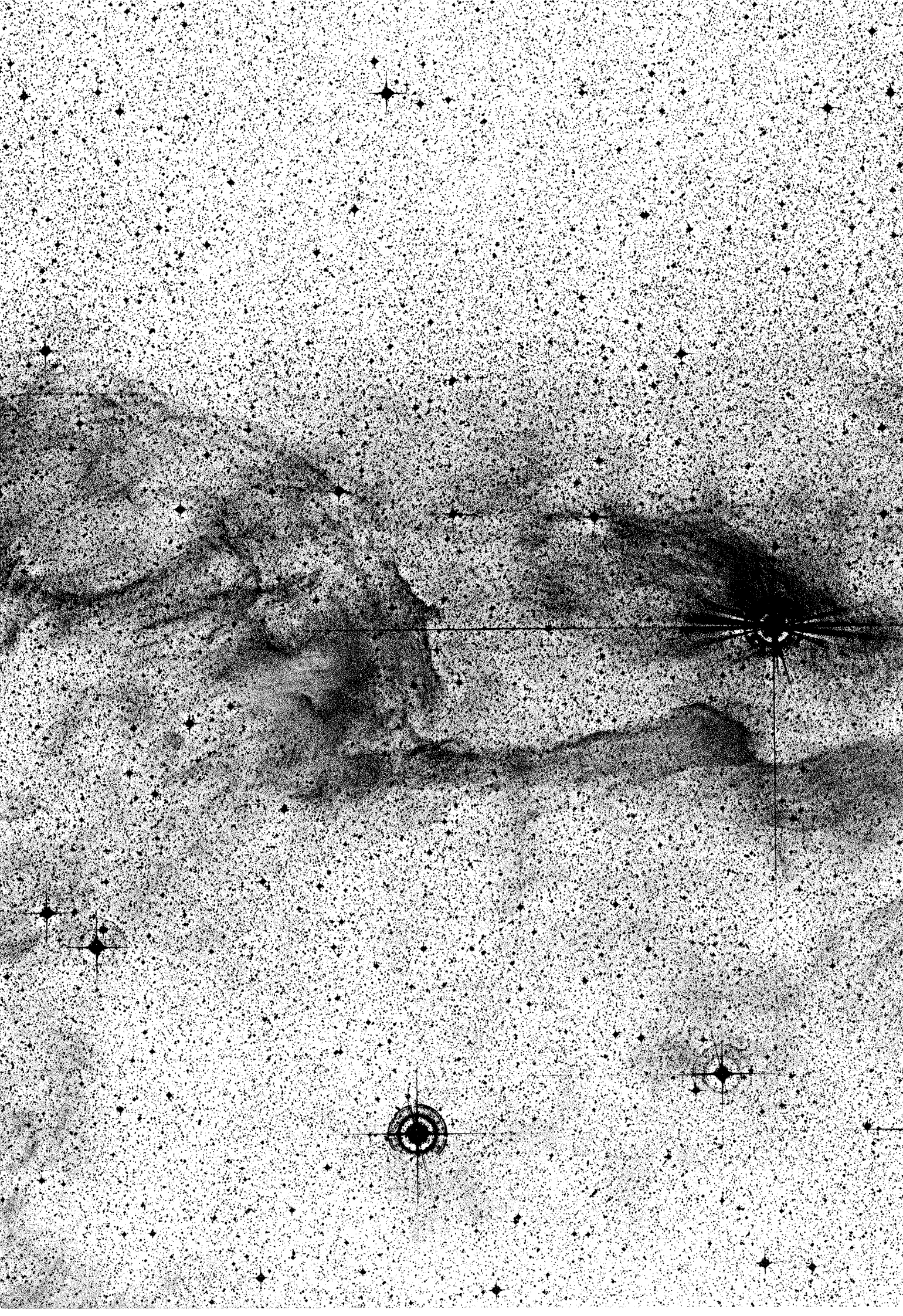
- [1] EHA-I.A. 2.13.
- [2] Council Documents Chile-8, 12, 15, 16 in EHA-I.A. 2.14. and letters in EHA-I.A. 2.10.
- [3] Minutes Council Meeting 2–3 Dec. 1964 and *ESO Basic Texts* Section B.3.
- [4] Cou. Doc. Chi-12 in EHA-I.A. 2.14.
- [5] See ref. 4.
- [6] Heckmann Sterne p. 298ff.
- [7] See Muller's reports mentioned before.
- [8] In EHA-I.A. 2.10.
- [9] EHA-I.C. 3.2.
- [10] EHA-I.C. 3.8.
- [11] Annual Report 1964.
- [12] Lists of employees were at regular intervals drawn up by the Administration in Bergedorf for the FC. For instance, they are found in doc. FC 32a and 32b for the situation per April 1, 1965 and in doc. FC 92 per Oct. 1, 1966; these documents are part of the FHA.

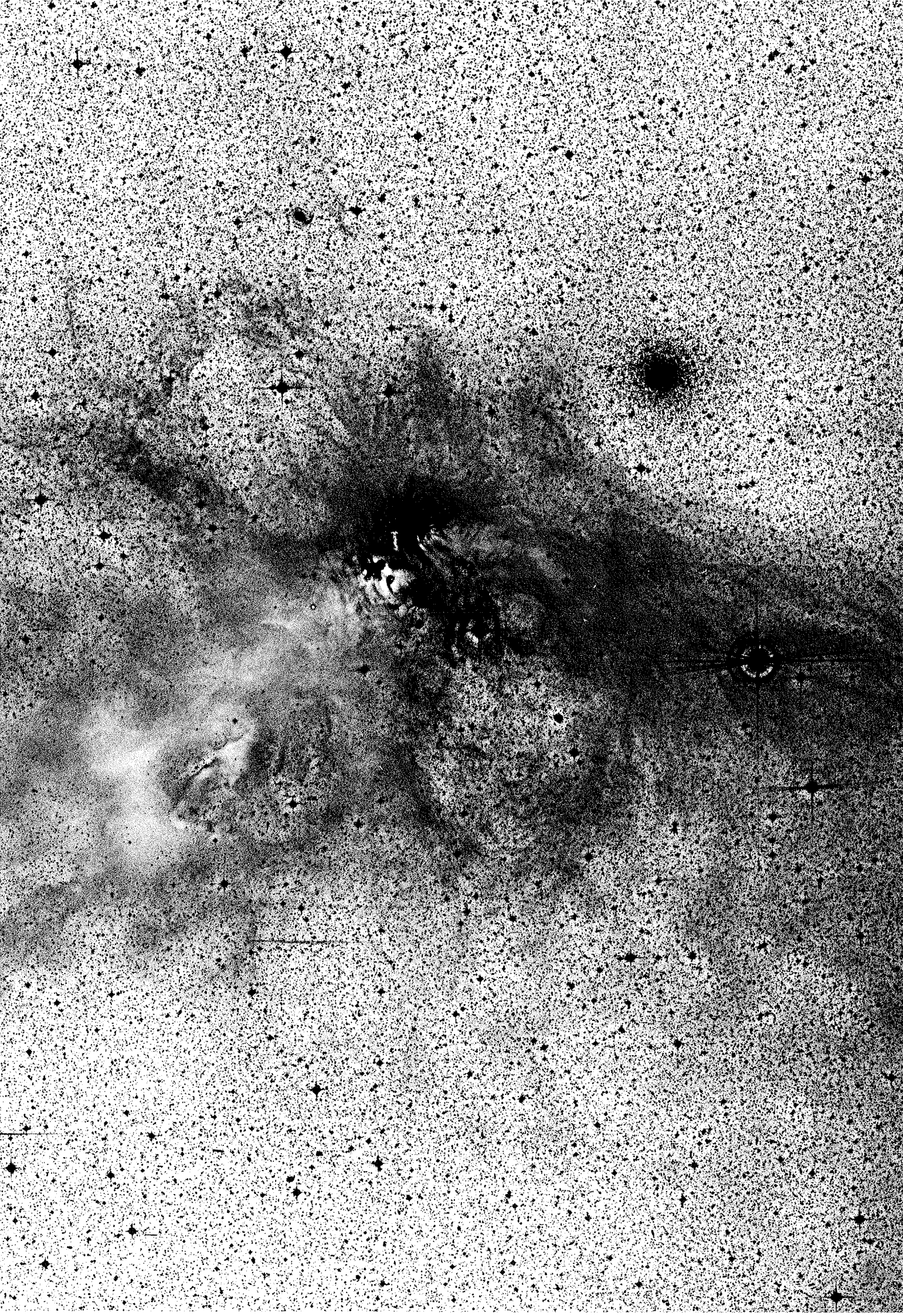
[13] Cou. Doc. Chi-15 in EHA-I.A. 2.14; for preparatory work also Cou. Doc. Chi-9, 10 and 11.

[14] EHA-I.A. 2.15.

The R Corona Australis Cloud

The southern constellation Corona Australis contains this fine molecular cloud, known as the R CrA cloud after a young variable star, which is surrounded by a reflection nebula in the northern part of the cloud. It appears that the cloud has been perturbed by an outside event from the north-west, perhaps a supernova explosion. Low mass star formation is actually taking place in the cloud: many T Tauri stars and several Herbig-Haro objects are found there and a cluster of embedded infrared sources is located in the north-western front of the cloud. The globular cluster to the right is NGC 6723. There are also several minor planet trails in the field. From a 150-min ESO Schmidt plate (IIIa-F + RG630), obtained by G. Pizarro and H.-E. Schuster; text by B. Reipurth, photographic work by C. Madsen. ▶





V745 Sco – a New Member of the Elusive Group of Recurrent Novae

H. W. DUERBECK, ESO and Astronomisches Institut der Universität Münster, F. R. Germany

Up to late July, 1989, the six novae which have shown repeated outbursts in the last 130 years, are: V394 CrA, T CrB, RS Oph, T Pyx, U Sco and (likely) V1017 Sgr. On July 30, William Liller, a regular visitor to La Silla and owner of a private observatory in Viña del Mar (a sea resort on the coast of Chile), discovered on a sky patrol film a 10th-magnitude star that was not there the night before. Its position coincided, as was found after some re-examination of old photographic plates, within an arcsecond of the position of a nova that had flared up on May 10, 1937. This poorly known nova, V745 Sco, thus became the seventh known recurrent nova.

The writer, who has a continuous interest in novae, had just begun a three-month stay on La Silla as the first astronomer of ESO's newly instituted Senior Visitor Programme. While recent outbursts of U Sco and V394 CrA were studied by astronomers at the South African Astronomical Observatory, joint efforts made this nova an ESO nova: There was Thomas Augusteijn, who informed me in time of the discovery, Hugo Schwarz, who offered some joint observing time at the 1.4-m Coudé Auxiliary Telescope/Coudé Echelle Spectrometer, and the TRS people, who were so kind to postpone the aluminization of the CAT mirror for a few weeks to rearrange some test nights. Finally, there was the possibility to make fairly regular observations with EFOSC2 at the 3.5-m New Technology Telescope which was undergoing a series of astronomical tests in August/September. While the observations and reductions of the CES spectra were relatively straightforward, those of EFOSC2 were improvised: there was no guiding possibility, no calibration lamps, but much enthusiasm and expertise from the other users. Finally, using the lines of a planetary nebula for establishing the dispersion curve, and some spectral standards and the cool component of the recurrent nova itself for calibration, a series of composite spectra of V745 Sco were obtained, covering the range 3620–8270 Å. It was fortunate that the evolution of the outburst proceeded very rapidly, so that, when the engineering staff took over again, the most interesting phases had been covered.

So much for the observations. What about the results? As already mentioned, the group of recurrent novae is not only small, but also inhomogeneous,

and poorly understood. It is still unclear whether the outbursts are caused by thermonuclear runaways in degenerate hydrogen-rich matter accreted on the surface of a massive white dwarf (some authors evoke accretion events on main-sequence stars to explain the outbursts of T CrB and RS Oph). Both these objects have, as well as V1017 Sgr, late giants as mass-donating components, while the cool components of V394 CrA, T Pyx and U Sco appear to be dwarf stars, whose absorption lines can hardly be detected against the continuous background of light produced in the accretion disk.

As can be clearly seen in the later spectra obtained with EFOSC2 (Fig. 1), V745 Sco has a giant companion as mass-donor: the strong TiO bands indicate a spectral type of M6 III. This object has a strong wind (and likely the white dwarf accretes its fuel from it). Indications for this wind are, first, the

narrow emission lines observed in the early outburst phases. They clearly showed up in the CES spectra taken in the first days after outburst, and obviously are emitted by the wind material, which was photoionized by the flash of the nova explosion. Especially interesting is the region around the line [OIII] 5007: At this early phase, no forbidden oxygen emission is expected from the expanding shell, while it clearly is present in V745 Sco (Fig. 2). Near to it is an FeII line at 5018 Å: it has a weak narrow component originating in the slowly moving wind material, and also a broad component formed in the rapidly moving nova shell. In the third night following the outburst, the broad component is only noticeable as a slight bending in the stellar continuum, while in the fifth night, when a deceleration had taken place, it is clearly visible. Such narrow emission lines were discovered before in only one other recurrent nova, in RS

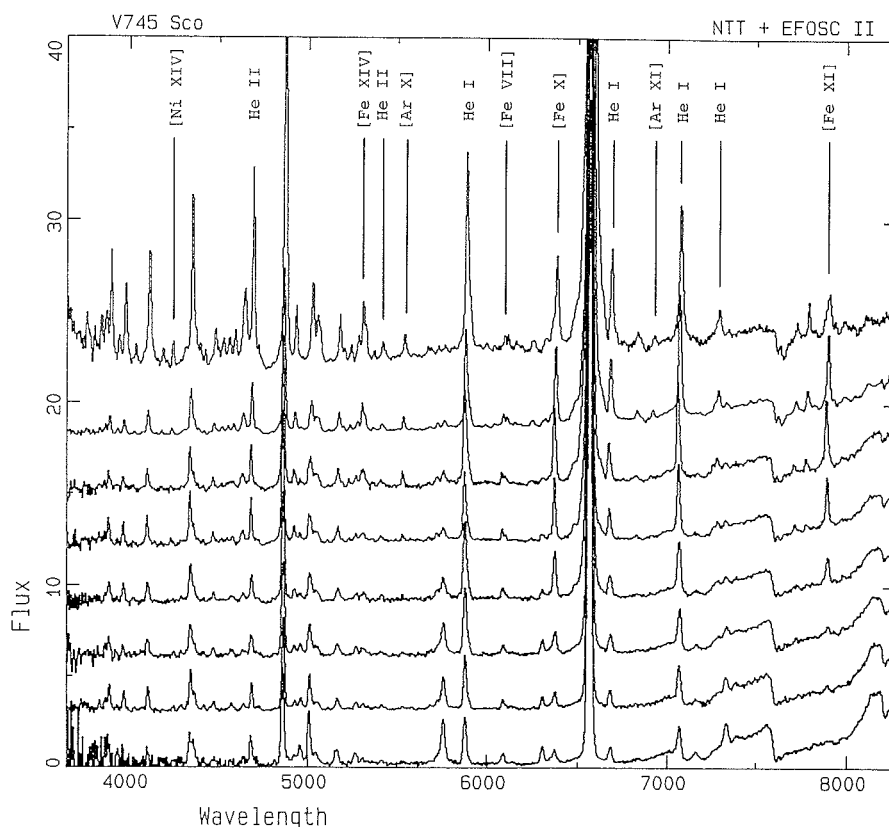


Figure 1: The later phases of the outburst of V745 Sco, shown in spectra taken by T. Augusteijn, J. Melnick, H.E. Schwarz and the writer with EFOSC2 attached to the 3.5-m New Technology Telescope. The spectra were taken (from top to bottom) on August 9, 11, 13, 15, 17, 24, 28 and September 9, and are separated by 3 (arbitrary) flux units to avoid overlapping. While the first spectrum still shows emission lines typically found in classical novae, the coronal lines reach maximum strength in the following days and decline afterwards. In the later phases, medium and low-excitation lines of [NII], [OI], [OII] and [OIII] increase in strength. Note also the TiO bands of the giant M6 companion in the infrared.

Oph during its 1958 outburst (and subsequent ones).

A few days later, when the rapidly expanding shell ejected from the white dwarf had time to strongly interact with this slowly moving material, its kinetic energy became thermalized by collisions: “coronal” lines of high excitation potential are formed in the surrounding shell: lines of [FeVII], [FeX], [FeXI] and [FeXIV], as well as those of [NiXII], [AX] and [AXI] rapidly increased in strength and reached maximum intensity around August 12. Again, there is a similarity with RS Oph, however, while the coronal spectrum in RS Oph took six weeks to acquire maximum strength, this process took hardly two weeks in V745 Sco. Three weeks later, when the last spectrum was taken, hardly a trace of them remained.

What else was found? V745 Sco is quite faint, even at maximum, and obviously very distant. The interstellar sodium lines show 11 components, produced by distinct interstellar clouds of different radial velocity, as do the calcium lines (the strong interstellar extinction, however, makes the latter ones difficult to observe). We estimate that the interstellar visual extinction is 3^m , and that the distance to V745 Sco is of the order of 10 kpc; it likely belongs to the galactic bulge.

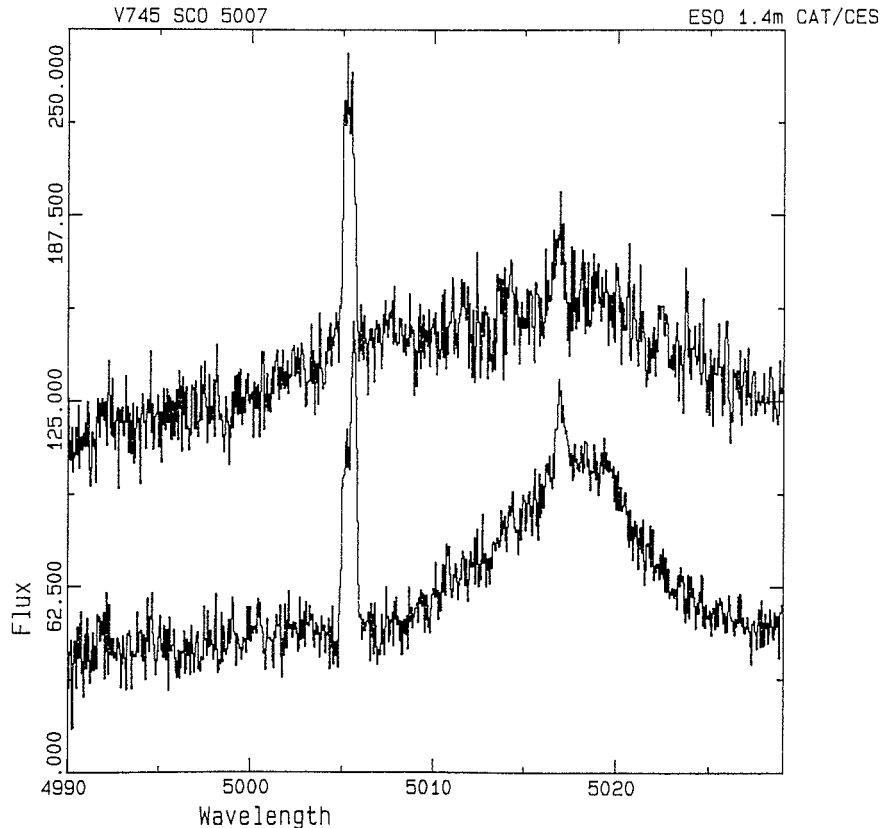


Figure 2: The region of the [O III] line at 5007 Å in V745 Sco, observed on August 2 and 4, three and five days after outburst, with the Coudé Echelle spectrometer at the 1.4-m Coudé Auxiliary Telescope by H.E. Schwarz and the writer. Note the different appearance and temporal development of the [O III] line at 5007 Å and the Fe II line at 5018 Å. While the first formed in the wind of the companion, the second arises mainly in the expanding nova shell.

Photometry and High Resolution Spectroscopy of Two Southern T Tauri Stars

C. CHAVARRIA^{1,2}, E. COVINO³, M. FRANCHINI⁴, R. STALIO⁵ and L. TERRANEGRA¹

¹ Instituto de Astrofísica, Óptica y Electrónica, Puebla, México

² Instituto de Astronomía, UNAM, México, D. F., México

³ Osservatorio Astronomico di Capodimonte, Napoli, Italy

⁴ Osservatorio Astronomico di Trieste, Trieste, Italy

⁵ Dipartimento di Astronomia, Università di Trieste, Trieste, Italy

Introduction

In an attempt to determine rotational velocities, photometric rotational periods and possible correlations with chromospheric activity, a sample of southern T Tauri or suspected T Tauri stars was monitored in May 1989 with the CAT+CES 1.5-m and the 50-cm ESO telescopes at La Silla. Unfavourable weather conditions limited our original goals. Nevertheless, some interesting results were obtained. Here we report some preliminary results for two stars from our sample: T Cha and CoD -33° 10685.

T Cha: According to the catalogue of Herbig and Bell (1988), no spectro-

scopic observations of T Cha exist; its T Tauri nature is suggested only by the RW Aurigae-Type variability, and by its location in a dark cloud. The star has a probable photometric period of 3.2 days (Mauder and Sosna 1975). There is also a discrepancy of about $2^m.5$ in the data for the apparent visual brightness of the star given by Mauder and Sosna (1975), and by Mundt and Bastian (1980 and references therein).

CoD -33° 10685: This is a fairly well-studied T Tauri star of spectral type K2 (Herbig, 1967), with a rotational velocity $v \cdot \sin i = 48$ km/s and a visual magnitude of 10.3. It is also a suspected linear polarization variable (Drissen et

al., 1989). All these properties make CoD -33° 10685 a good candidate for BY Draconis-type variability.

The Observations

Owing to the prevailing weather conditions, we decided to limit our observations to the spectral range of the Na I D lines in order to study the outer and colder parts of the stellar atmosphere. Three spectra of each star were taken on three different nights, and the spectra of a number of reference stars were obtained as well. The latter were convolved with different synthetic rotational profiles in steps of 5 km/s over the ve-

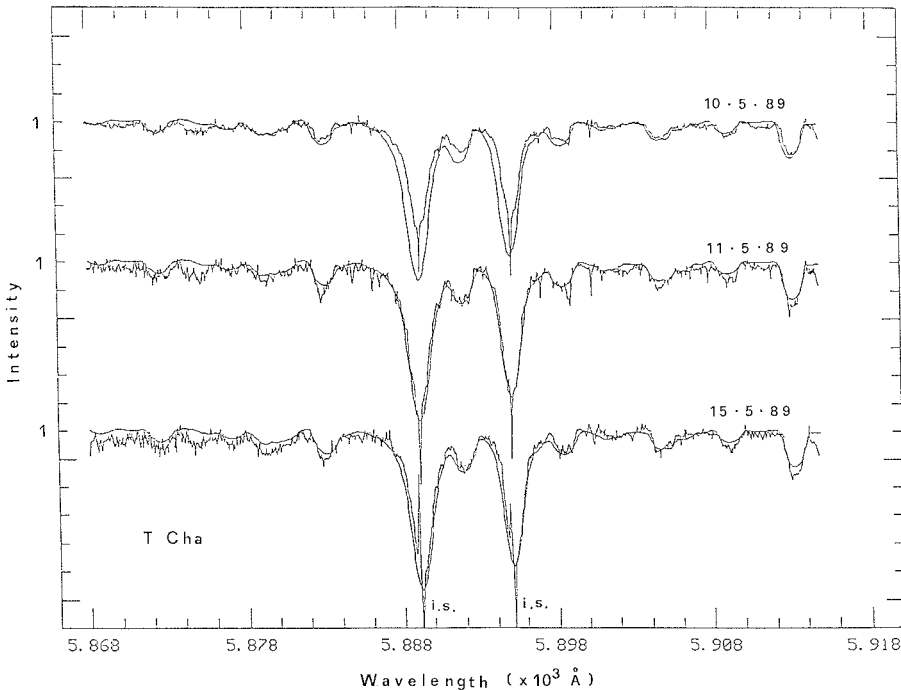


Figure 1: The spectrum of T Cha observed during the nights of May 10, 11 and 15, 1989 compared with the convolved spectrum of the standard star HD 190248 (G8 V).

locity range $30 \leq v \cdot \sin i \leq 50$ km/s, in order to obtain spectral types and projected rotational velocities of T Cha and CoD -33° 10685. This procedure was repeated for each available spectrum of T Cha and CoD -33° 10685. The best fits of the convolved spectra with the programme stars are shown in Figures 1 and 2. The estimated spectral types and $v \cdot \sin i$ are reported in Table 1.

Our photometric observations show

that the brightness of CoD -33° 10685 was quite stable, with a mean visual magnitude of $V = 10.46 \pm 0.03$. This value is consistent with previous photoelectric observations of the star obtained in the 1977–1979 period by Bastian and Mundt (1979) and Mundt and Bastian (1980).

Mauder and Sosna (1975) report that, during the period between December 1971 and April 1972, T Cha showed

Table 1:

| Star | V | Sp.Ty. | $v \cdot \sin i$ [km s ⁻¹] |
|-----------------------|-------|--------|---|
| CoD -33° 10685 | 10.46 | K2 | 48 ± 10 |
| T Cha | 10.5 | G8 | 48 ± 10 |

day-to-day visual brightness variations in the interval $15.2 < V < 11.5$, with typical daily changes higher than 1^m and a mean visual magnitude of 13.3. The same authors also found a quasi-periodic modulation in the brightness of T Cha, with a period of about 3.2 days. We now find that T Cha has a visual magnitude $V = 10.5 \pm 0.1$, in extremely good agreement with the photometric determinations by Bastian and Mundt (1979) and Mundt and Bastian (1980), but we did not observe any night-to-night changes in the brightness higher than $0^m.1$. If the object observed by Mauder and Sosna and by us is really the same, this means that now T Cha is considerably brighter ($\Delta V = 2.8$) and in a more quiescent phase than in the past.

Our estimates of spectral type and $v \cdot \sin i$ for CoD -33° 10685 are in excellent agreement with those given by Bouvier et al. (1986), and very similar to those found by Finkenzeller and Basri (1987). An inspection of our fits for both stars (see Figs. 1 and 2) suggests that variability might be present in the Na I D lines. To detect any possible night-to-night changes in the line profile, a more reliable comparison was made following the procedure outlined by Finkenzeller and Basri (1985). We simply divided the spectra of the target stars by the processed spectrum of the reference star.

The resulting “profiles” are shown in Figures 3 and 4 for CoD -33° 10685 and T Cha respectively. It can be clearly seen that the spectra of both stars are variable in the Na I D lines on a time scale of one day or less. In the case of T Cha, based on its spectral type, projected rotational velocity, photometric variability, IR excess (Glass and Penston, 1974) and association with a dark cloud, we conclude that it is a low-mass PMS star. In the case of CoD -33° 10685, multiple narrow blue shifted absorptions are superimposed on the emission profile. The most blue-shifted component has variable intensity (by about a factor 2), and a radial velocity of about -92 km/s relative to the star. On the red side, a broad variable absorption is present, with a minimum at $+125$ km/s relative to the star (see Fig. 3). All these features can be explained by the simultaneous presence of a complex mass outflow and of infalling matter onto the star. The time scales of

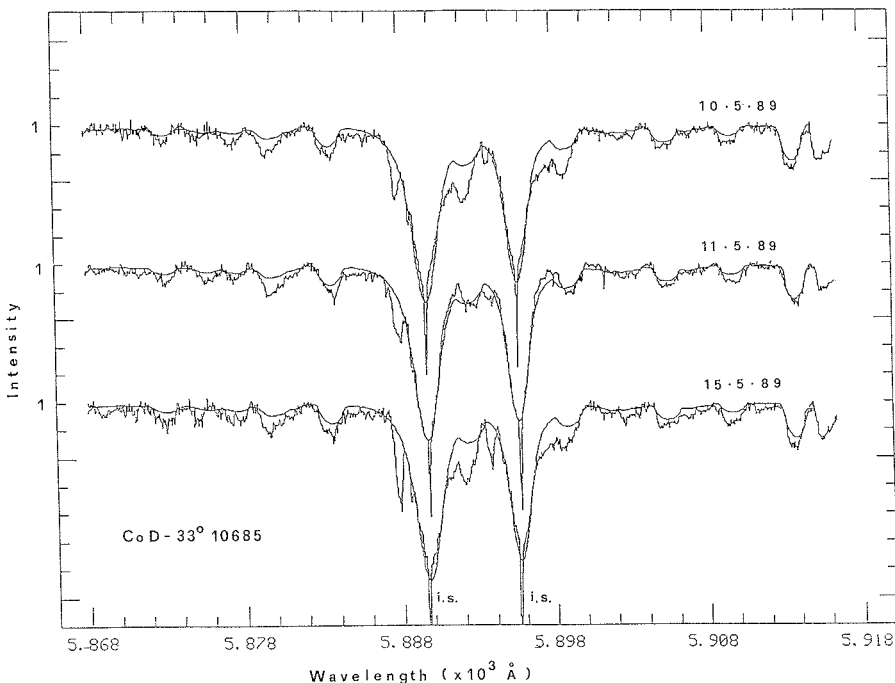


Figure 2: The spectrum of CoD -33° 10685 observed during the nights of May 10, 11 and 15, 1989 compared with the convolved spectrum of the standard star HD 191408 (K2 V).

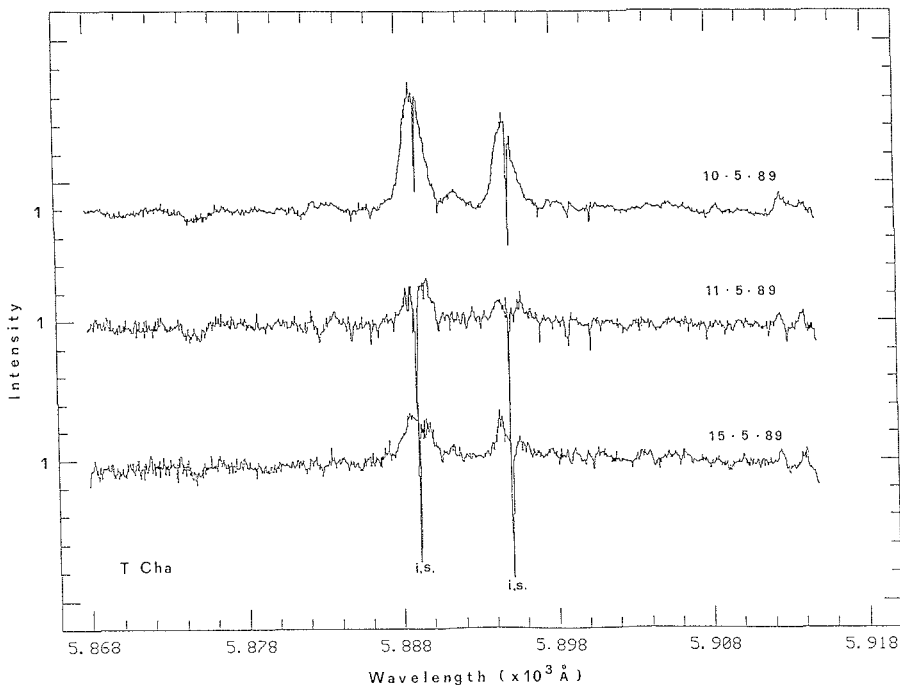


Figure 3: The ratio between T Cha observed during the nights of May 10, 11 and 15, 1989 and the convolved spectrum of the standard star HD 190248 (G8 V). Radial velocities of blue-shifted and red-shifted components are indicated.

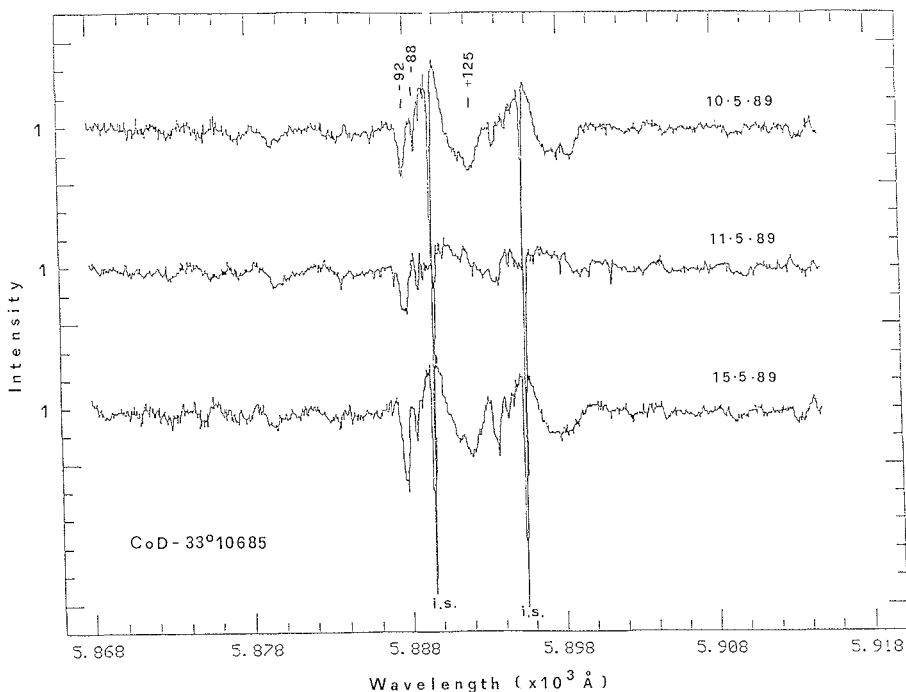


Figure 4: The ratio between CoD $-33^{\circ} 10685$ observed during the nights of May 10, 11 and 15, 1989 and the convolved spectrum of the standard star HD 191408 (K2 V).

the variations suggest that this occurs near the star surface.

References

- Bastian, U., Mundt, R.: 1979, *Astron. Astrophys. Suppl.*, **36**, 57.
 Bouvier, J., Bertout, C., Benz, W., and Mayor, M.: 1986, *Astron. Astrophys.*, **165**, 110.
 Finkenzeller, U., Basri, G.: 1985, *The Messenger*, **42**, 20.
 Glass, I.S., Penston, M.V.: 1974, *Mon. Not. Roy. Astron. Soc.*, **167**, 237.
 Herbig, G.H.: 1977, *Ap. J.*, **214**, 747.
 Herbig, G.H., Bell, K.R.: 1988, *Lick Obs. Bull.* No. 1111.
 Mauder, H., Sosna, F.M.: 1975, *I.B.V.S.*, 1049.
 Mundt, R.: 1980, *Ap. J.*, **280**, 749.
 Mundt, R., Bastian, U.: 1980, *Astron. Astrophys. Suppl.* **39**, 245.

STAFF MOVEMENTS

Arrivals

Europe:

- DIERCKX, Peter (B), System Manager
 KRAUS, Maximilian (D), Mechanical Design Engineer
 LIU, X. (RC), Associate
 PRAT, Serge (F), Mechanical-Project Engineer
 SCHLÖTELBURG, M. (D), Fellow
 STIAVELLI, M. (I), Fellow
 WANG, L. (RC), Associate
 ZUFFANELLI, E. (I), Secretary

Chile:

- CARTON, Ph. (F), Optical Technician
 GIRAUD, E. (F), Associate
 HAINAUT, O. (B), Coopérant

Departures

Europe:

- AZIAKOU, P. (F), Administrative Clerk Purchasing
 FANG, Y. (RC), Associate
 GROENEN, E. (B), Assistant Head of Administration
 PONZ, D. (E), Science Applications Programmer

Chile:

- BAUERSACHS, W. (D), Senior Mechanical Engineer

Discovery of a Low Mass B[e] Supergiant in the SMC

M. HEYDARI-MALAYERI, ESO

1. Introduction

Peculiar emission-line B supergiants are a group of early-type stars with the following typical characteristics: (a)

strong Balmer emission lines frequently with P Cygni profiles, (b) permitted and forbidden lines of FeII, [FeII], [OII], etc. and (c) strong infrared excess possibly

due to thermal radiation from circumstellar dust. They represent one of the two main groups of early-type emission line stars in the Magellanic Clouds

(MCs). The other group consists of the classical P Cygni stars and their hotter counterparts, Of-like objects. The S Dor variables, also called Hubble-Sandage variables, are the most extreme variables of the P Cygni and Of-like objects (Stahl et al., 1985). The B[e] supergiants are located in the HR diagram in the same region as S Dor variables and represent evolved evolutionary stages of the most luminous and presumably the most massive O stars (Zickgraf et al., 1986).

The B[e] supergiants are very rare objects: only nine stars of this type have been detected in the MCs among which three belong to the SMC: R4, R50 and S18 (Zickgraf et al., 1986; Zickgraf et al., 1989, and references therein). Here we report the discovery of a new B[e] supergiant in the SMC. This star, lying in a relatively isolated region of the wing, roughly 30 minutes south of the HII regions N81 and N83, was originally catalogued as an H α emission line nebula by Henize (1956) – hence its designation N82. In Lindsay’s (1961) catalogue of emission-line stars and planetary nebulae N82 is listed as number 495. No detailed observational data have been reported for N82. We came across this star serendipitously in the course of a study of low-excitation compact HII regions in the SMC (Heydari-Malayeri, 1989).

The present investigation is important for several problems concerning the evolutionary stages of massive stars, in particular the interpretation of S Dor or Hubble-Sandage variables, the upper mass cut-off of massive stars, stellar stability, mass loss and circumstellar envelopes. Furthermore, in view of the very small number of B[e] stars in the MCs, especially in the SMC, search for new members is very important in order to improve our knowledge of the physical properties of these stars.

2. Observations

2.1 High dispersion spectroscopy

N82 was observed with the CASPEC spectrograph attached to the ESO 3.6-m telescope on June 16 and 17, 1989. The 31.6 lines mm⁻¹ grating was used with a 300 lines mm⁻¹ cross dispersion grating and an f/1.5 camera. The detector was a high resolution CCD chip of type RCA SID 503, 1025 × 640 pixels, each pixel 15 μ m. We used two central wavelengths at 4500 Å and H α with exposure times from 30 minutes to 2 hours. The effective spectral ranges were 4000–5020 Å and 6140–7240 Å respectively. The resulting resolution was \sim 0.3 Å in the 2 × 2 binned mode.

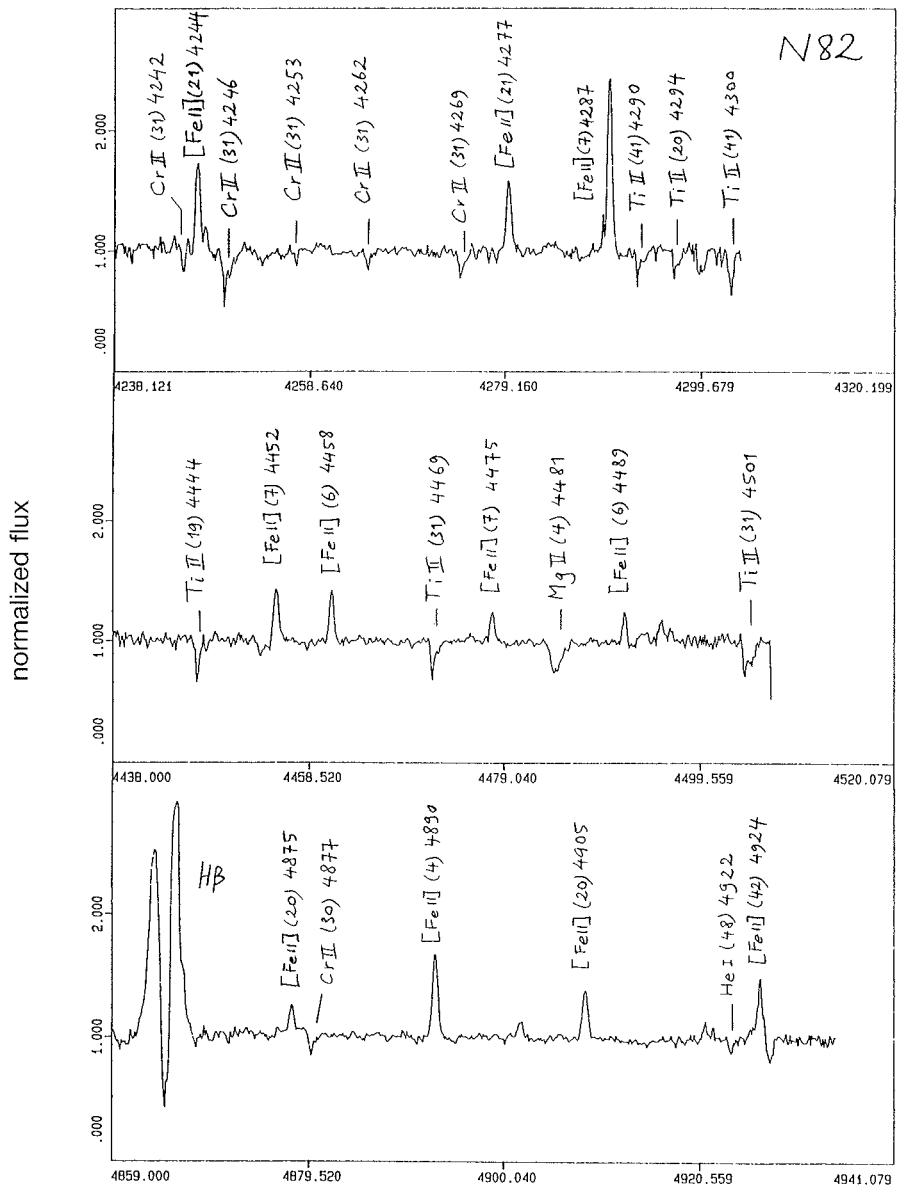


Figure 1: Three sections of the high dispersion spectrum of N82 obtained using the CASPEC in the blue.

Thorium-Argon lamp spectra were used for the wavelength calibrations. Flat-field exposures were also taken. Initially, low dispersion spectra of N82 had been obtained on June 4, 1988, using EFOSC at the 3.6-m telescope (3600–7000 Å).

2.2 Photometry

The single-channel photometer was used at the Cassegrain focus of the ESO 1-m telescope on June 5, 7 and 8 and July 10, 1989 to obtain UBVRI photometry of N82. The magnitudes are as follows: V = 14.25, U-B = -0.13, B-V = 0.12, V-R = 0.21, V-I = 0.20, accurate within $\sim \pm 0.02$ mag. The V magnitude agrees well with the photographic magnitude (14.24) derived by Lindsay (1961). The near IR photometry was obtained on August 12, 1989 using the ESO 2.2-m telescope with its standard IR

photometer. The results are: J = 13.42, H = 12.58, K = 12.38 with errors ± 0.04 and L > 10.

3. Spectral Characteristics

Using the derived colours, a colour factor of Q = -0.22 was obtained for N82. This corresponds to spectral types B7–B8 (Henden and Kaitchuk, 1982). The presence of strong Balmer emission lines, especially very strong H α , implies a spectral type earlier than A0 (Slettebak, 1986; Jaschek et al., 1988; see below Sect. 5). The spectrum of N82 is typical of B[e] stars. It is very rich in emission lines of singly ionized iron, both forbidden and permitted. Apart from the Balmer hydrogen lines, the [Fe II] lines are the strongest emission lines of the spectrum. The [Fe II] lines (typical FWHMs \sim 40 km s⁻¹) are much

more numerous than FeII lines. There are also a large number of absorption lines of CrII and TiII. Neutral oxygen around N82 is evidenced by the [OI] emission line at 6300 Å. Three sections of the spectrum are displayed in Figure 1. Note the striking similarities with the other SMC B[e] star R50 (Zickgraf et al., 1986, Fig. 8). However, unlike R50, N82 shows no central absorption on FeII lines.

P Cygni profiles of Beals (1950) type III stand out for H γ , H β and H α Balmer lines. The central absorption dip in all cases is well pronounced. The separation of the longward and shortward components of all the P Cygni profiles for H γ , H β and H α are 152.6, 146.2 and 104.6 km $^{-1}$ respectively. H δ does not display a P Cygni profile; it appears as a strong absorption line inside a broad absorption feature.

The radial velocities of the different species were measured with respect to the Sun. The mean radial velocity derived from the [FeII] lines is 204.8 \pm 5.6 km s $^{-1}$. The FeII lines show a similar mean velocity, but the scatter is much larger. These values compare well with the radial velocities of the central absorption dips in H γ , H β and H α , i.e. 200.7, 207.3 and 201.5 km s $^{-1}$ respectively. The mean radial velocities derived from the absorption lines of CrII and TiII seem to be somewhat higher, 217.5 and 210.2 km s $^{-1}$ respectively.

An interesting feature of N82 is that the absorption lines mostly show an asymmetric two-component profile. The blue component is usually stronger than the red one which shows broad wings (Fig. 1). Some of the absorption lines were deconvolved into their components. For instance, the components of CrII 4246.4 have heliocentric velocities of 237 and 273 km s $^{-1}$, while those of TiII 4468.5 show velocities of 207 and 250 km s $^{-1}$ respectively.

The spectral type of N82 is quite uncertain since, as for the other MC B[e] supergiants, it is difficult to derive a spectral type from the photospheric lines. The only photospheric lines detected are MgII 4481.1 and HeI 4921.9 Å.

No [NII] lines at 6548,84 are detected in the red CASPEC spectra. Likewise, there is no sign of emission from [OII] λ 3727 or [OIII] λ 5007 in our long slit spectra. This probably means that N82 is not associated with nebulosity as confirmed by images obtained through R and H α filters.

4. Mass

From a distance modulus of 19.1 we derive an absolute magnitude of $-4.85 + A_v$ for N82 which corresponds

to supergiants (Humphreys and McElroy, 1984). Assuming two extreme cases, i.e. supergiants of type B0 and B9, we derive colour excesses E(B-V) of 0.35 and 0.12 respectively (Schmidt-Kaler, 1982). From the corresponding bolometric corrections (Humphreys and McElroy, 1984) we obtain two limiting bolometric magnitudes of -8.6 and -5.6 . Using the grids of evolutionary models of massive stars with mass loss and overshooting (Maeder and Meynet, 1988), initial masses of $\sim 35 M_{\odot}$ and $15 M_{\odot}$ are derived for N82. Similarly, when a black body is fitted to the dereddened UBVR data (Fig. 2) bolometric magnitudes of -6.5 and -5.5 are obtained for B0 and B9 stars respectively, corresponding to masses of ~ 20 and $10 M_{\odot}$. These values should be compared with the masses of the three SMC stars R4, R50 and S18 which have been estimated to be 30–50 M_{\odot} (Zickgraf et al., 1986; 1989). Consequently, N82 seems to be the lowest mass B[e] star in the SMC. Note that all the B[e] stars of the MCs are classified as B0–B3 supergiants, except R66 which is B8Ia. The lower visual magnitude of N82 with respect to those of R4, R50 and S18 (13.09, 11.56 and 13.31 respectively) is unlikely due to extinction, as N82 lies in the SMC wing; moreover its extinction is comparable with those of the above-mentioned stars.

5. Discussion and Conclusions

Many properties of the B[e] supergiants can be understood in terms of a two-component wind model first put forward by Zickgraf et al. (1985) to interpret the characteristics of R126 ($M_b = -10.5$), considered to be the prototype of B[e] stars in the MCs. The model consists of a cool, dense and slowly expanding disk-like wind component and a hot-line-driven fast polar wind. Accordingly, the emission lines come from the pole-on viewed disk produced by a Be type mass loss from equatorial regions of the stellar atmosphere. The difference between the velocities of FeII and [FeII] is attributed to the differential rotation of the slowly expanding disk. The broad absorption lines of highly ionized species (FeIII, AlIII, SiIV, CIV and NV), detected in the ultraviolet range, originate in the high-velocity polar wind. It will be interesting to observe N82 in the UV to check for the presence of a “hybrid spectrum”. However, note that Waters et al. (1987) using the IRAS far-IR observations to study the characteristics and mass loss ratios of Be stars conclude that very luminous stars with $M_b > -7.8$ to -8.5 cannot form disks due to the high radiation pressure that dominates the winds, and

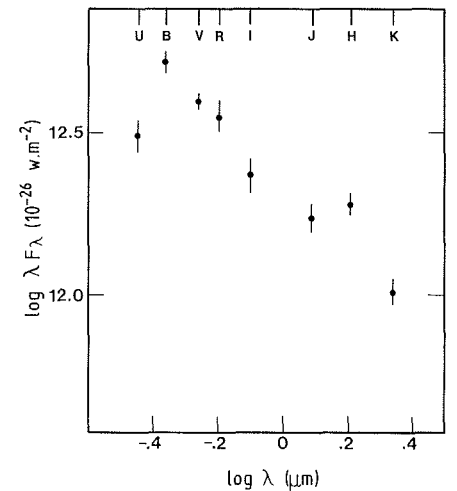


Figure 2: Continuum energy distribution of N82 deduced from broad band photometry.

that mass loss due to the Be mechanism is negligible. At lower luminosities, the Be mechanism dominates the mass loss, resulting in enhanced equatorial mass loss.

The strong IR excess detected towards the B[e] supergiants in the MCs is interpreted to be due to thermal radiation from circumstellar dust. The B[e] supergiants form a clearly distinct group on the right-hand side of the (J-H)–(H-K) diagram due to their large (H-K) excess (Zickgraf et al., 1986). As far as N82 is concerned, no inference can be drawn on the presence of dust around it, since the object was not detected in the L band. A special feature of N82 is that an important IR excess is detected particularly in the H band (Fig. 3). If this feature is due to dust emission, the dust must have an unlikely extraordinary colour temperature of ~ 200 K! Therefore, the feature should have another origin, for example emission lines due to Brackett series or a late-type companion. The second hypothesis seems more plausible because the J-H and H-K colours of N82 correspond to late-type stars, especially since no ionized gas is detected towards N82. More observations in the future are needed in order to clear up the IR properties of N82. If the late-type companion is confirmed, N82 would represent the prototype of a new class of B[e] supergiants. Note that R84, an Of-like object and one of the most spectacular emission line stars in the LMC, is known to have a late-type companion classified as an M2 supergiant by Cowley and Hutchings (1978).

Now we argue that N82 is not an Ae or A-type shell star. According to Jaschek et al. (1988), there are very few A-type stars with emission in the Balmer lines. These cases belong to Ae/Be stars and to close binaries. As a rule, emission features in Balmer lines de-

crease towards later B types. Usually, at B9 only H α is in emission and H β is only seen up to B8. Before A0 the emissions are much stronger than the level of the continuum (see also Slettebak, 1986) whereas for A-type stars no case is known with emission exceeding this level. This is so striking that one may discriminate the Be from Ae stars. P Cygni type profiles are only seen in two very peculiar objects HD31648 and 41511. Moreover no [FeII] emission lines are reported for Ae stars.

Similarly, N82 is probably not a pre-main sequence Herbig Ae/Be star, as it does not meet two of the three membership criteria (Strom et al., 1972): (1) it does not lie in an obscured region, and (2) it does not illuminate fairly bright nebulosity in its immediate vicinity. Moreover, N82 is too bright to be a Herbig Ae/Be star. Strom et al. (1972) give a list of 12 Galactic stars of this type with known distances. If we place these stars in the SMC, their V magnitudes will range from 17 to 22. The brightest one, HD 200775, assumed to lie at 440 pc from the Sun (Whitcomb et al., 1981), may be fainter than 17 if its distance is overestimated.

The two-component absorption feature is probably due to the shell phenomenon. It would probably suggest that non-radial pulsations can enhance the mass flux from the equatorial regions of rapidly rotating Be stars (Waters et al., 1987). This is the first time such a feature is detected in a Magellanic B[e] star.

Zickgraf et al. (1986) concluded that the MC B[e] stars are massive post-main sequence objects of mass $30 \leq M \leq 80 M_{\odot}$. The present result hints that

these stars may originate from lower initial masses. This raises the question: how small can the mass of a B[e] star in the MCs be? If future surveys confirm the presence of low mass B[e] stars in the MCs, this will have important implications for current models of massive star evolution in the Clouds.

In particular, it would support the binary hypothesis for the B[e] supergiants. It should be underlined that two of the three already known B[e] stars in the SMC, R4 and S18, are interpreted to be double systems (Zickgraf et al., 1987; Shore et al., 1987, Zickgraf et al., 1989). It is interesting to consider the case of the LMC P Cygni star R81. Wolf et al. (1981) had estimated a mass of higher than $50 M_{\odot}$ for this star. Recently, Stahl et al. (1987), owing to several years of almost continuous monitoring with high photometric precision, discovered that R81 is an eclipsing close binary system. The new data reduce the mass of R81 to $\sim 33 M_{\odot}$.

Acknowledgements

I am indebted to Dr. C. Gouiffes who kindly provided the UBVRI photometry of N82. I would like to thank Dr. T. Le Bertre for the near IR observations and discussions. I am grateful to Prof. I. Appenzeller for very important comments and suggestions. I would like also to thank Drs. O. Stahl and D. Hutseméckers for helpful discussions.

References

- Beals, C.S.: 1950, *Publ. Dominion Astrophys. Obs.* **9**, 1.
 Cowley, A.P., Hutchings, J.B.: 1978, *Publ. Astron. Soc. Pacific* **90**, 636.
 Henden, A.A., Kaitchuk, R.H.: 1982, *Astronomical Photometry*, New York, Van Nostrand Reinhold.

- Henize, K.G.: 1956, *Astrophys. J. Suppl.* **2**, 315.
 Heydari-Malayeri, M.: 1989, *Astron. Astrophys.* submitted.
 Humphreys, R.M., McElroy, D.B.: 1984, *Astrophys. J.* **284**, 565.
 Jaschek, M., Jaschek, C., Andriolat, Y.: 1988, *Astron. Astrophys. Suppl. Ser.* **72**, 505.
 Lindsay, E.M.: 1961, *Astrophys. J.* **66**, 169.
 Maeder, A., Meynet, G.: 1987, *Astron. Astrophys. Suppl. Ser.* **76**, 411.
 Schmidt-Kaler, T.H.: 1982, in Landolt-Börnstein, New Series Group IV, Vol. 2b, eds. K. Schaifers and H.H. Voigt, Springer, Berlin.
 Shore, S.N., Sanduleak, N., Allen, D.A.: 1987, *Astron. Astrophys.* **176**, 59.
 Slettebak, A.: 1986, *Publ. Astron. Soc. Pac.* **98**, 867.
 Stahl, O., Wolf, B., de Groot, M., Leitherer, C.: 1985, *Astron. Astrophys. Suppl. Ser.* **61**, 237.
 Stahl, O., Wolf, B., Zickgraf, F.-J.: 1987, *Astron. Astrophys.* **184**, 193.
 Strom, S.E., Strom, K.M., Yost, J.: 1972, *Astrophys. J.* **173**, 353.
 Waters, L.B.F.M., Coté, J., Lamers, H.J.G.L.M.: 1987, *Astron. Astrophys.* **185**, 206.
 Whitcomb, S.E., Gatley, I., Hildebrand, R.H., Keene, J., Sellgren, K., Werner, M.W.: *Astrophys. J.* **246**, 416.
 Wolf, B., Stahl, O., de Groot, M.J.H., Strecken, C.: 1981, *Astron. Astrophys.* **99**, 351.
 Zickgraf, F.-J., Wolf, B., Stahl, O., Leitherer, C., Klare, G.: 1985, *Astron. Astrophys.* **143**, 421.
 Zickgraf, F.-J., Wolf, B., Stahl, O., Leitherer, C., Appenzeller, I.: 1986, *Astron. Astrophys.* **163**, 119.
 Zickgraf, F.J., Wolf, B.: 1987, in *Circumstellar Matter* (eds.) I. Appenzeller, C. Jordan, p. 439.
 Zickgraf, F.-J., Wolf, B., Stahl, O., Humphreys, R.M.: 1989, *Astron. Astrophys.* **220**, 206.

CASPEC Observations of the Most Metal-Deficient Main-Sequence Star Currently Known

P. E. NISSEN, *Institute of Astronomy, University of Aarhus, Denmark*

The apparent absence of first generation stars with zero or negligible amounts of heavy elements is a long-standing problem in connection with theories of nucleosynthesis in stars and models of galactic chemical evolution. Despite extensive search on objective-prism plates, only two stars are known to have a metal abundance less than 1/1000 of the solar metal abundance, i.e. $[Fe/H] < -3.0$. The first one is G64-12, a main-sequence turnoff star, with $[Fe/H] = -3.5$ (Carney and Peterson

1981). The other one is CD $-38^{\circ}245$, a red giant with $[Fe/H] = -4.5$ (Bessell and Norris 1984). Here I briefly report on some CASPEC observations of a main-sequence turnoff star having a similar low metal abundance as CD $-38^{\circ}245$. Surprisingly, this new ultra-metal-deficient star is a double-lined spectroscopic binary.

The observations with the Cassegrain Echelle Spectrograph (CASPEC) at the ESO 3.6-m telescope were carried out October 13–17, 1989, under excellent

conditions. The sky was clear and the seeing was extremely good. At Cerro Vizcachas the monitor displayed an average FWHM of the seeing profile of 0".66, 0".49, 0".61 and 0".66 on the four nights. At the 3.6-m the seeing was around one arcsec. This gave a high throughput of CASPEC even if the entrance slit was set to a width of 1".2 only in order to obtain the maximum (two pixel) resolution, $R = 35.000$, of the instrument.

The aim of the observing programme

(carried out in collaboration with W.J. Schuster, UNAM, Mexico) is to determine abundance ratios of various elements in a large sample of very metal-deficient stars. Most of the stars were selected from a catalogue of 220 halo stars with metallicities determined from uvby- β photometry (Schuster and Nissen 1989). Spectra with $S/N \geq 100$ in the wavelength range 5150–6150 Å were obtained for 55 stars of which the majority have $[Fe/H]$ in the range -3.0 to -2.0 . When the spectra have been reduced and analyzed by model atmosphere techniques the trends of abundances of α -elements, odd-Z elements, iron-peak elements, and s-process elements can be studied as a function of $[Fe/H]$. The results are expected to give new information about the formation of the first heavy elements in the universe and the early evolution of the Galaxy.

One star immediately turned out to be much more metal deficient than the other stars. It had been selected from Beers, Preston and Shtetman (1985), who on the basis of objective-prism plates and medium-resolution spectroscopy of the CaII K line suggested star No. CS 22876-32 to be very deficient in metals.

From UVB photometry ($V = 12.82$, $B-V = 0.40$ and $U-B = -0.27$) the star is estimated to be at the main-sequence turnoff for old halo stars. In Figure 1 the spectral region around the MgI triplet is shown for this star and a sequence of stars with decreasing values of $[Mg/H]$. The stars are main-sequence turnoff stars and have about the same effective temperature as CS 22876-32 ($T_{\text{eff}} \approx 6000$ K) according to the Strömberg uvby- β photometry. The remarkable line weakness of CS 22876-32 is obvious and there is no doubt that the star is a binary.

From the equivalent widths measured, the magnesium abundance of CS 22876-32 is estimated to be 1/10000 of the solar magnesium abundance i.e. $[Mg/H] = -4.0$. This is an order of magnitude lower than the abundance of G64-12, the other ultra-metal-deficient main-sequence star known, and it is comparable to the magnesium abundance of the red giant CD $-38^{\circ}245$. Other metals in CS 22876-32 may be even more deficient. Thus, it is striking that the NaI doublet at 5890 Å is not seen in CS 22876-32.

In the last few years there has been an increased interest in the chemical composition of very metal-deficient stars. The reason is that non-standard, inhomogeneous Big Bang models produce a significant fraction of heavy elements (Applegate, Hogan and Scherer 1987). The inhomogeneities are

supposed to arise in connection with the transition from the QCD phase of the early universe to the hadron phase and lead to neutron-rich and neutron-poor regions. The chemical compositions of stars like CS 22876-32 set upper limits to the amount of heavy elements produced in the Big Bang, and may therefore be used as a discriminatory test between homogeneous (standard) and inhomogeneous models. In particular it would be very interesting to measure the beryllium abundance in very metal-deficient stars. Thus, Malaney and Fowler (1989) conclude that if a primordial Be/H ratio of 10^{-13} or higher is detected in metal-deficient stars then it would be a dramatic confirmation of inhomogeneities in the early universe and would also leave open the possibility of $\Omega_{\text{Baryon}} = 1$. The Be abundance can be determined from the Bell resonance doublet at 3130 Å. The blending by metal lines is very severe in normal stars but would be much less of a problem in an ultra-metal-deficient star like CS 22876-32.

However, the high atmospheric absorption at 3100 Å ($\sim 1^{\text{m}}.5$ at La Silla) and the relative low CCD sensitivity in the UV may prohibit high resolution, high S/N spectra to be taken at this wavelength at least with present-day telescopes.

The binary nature of CS 22876-32 makes it an even more interesting star. Spectra obtained on three consecutive nights show about the same separation between the two sets of Mg lines suggesting that the orbital period is rather long. Further high resolution observations with the aim of determining the orbital parameters of CS 22876-32 would be very useful. This and other metal-deficient, double-lined spectroscopic binaries should also be checked for eclipses. If we are lucky to find a metal-deficient, spectroscopic and eclipsing binary then masses and luminosities of the components can be determined with high precision. This would allow us to make a unique test of models of metal-deficient stars and thereby the age determination of the Galaxy would be much more reliable.

References

- Applegate, J.H., Hogan, C.J., Scherrer, R.J.: 1987, *Phys. Rev. D* **35**, 1151.
 Beers, T.C., Preston, G.W., Shtetman, S.A.: 1985, *Astron. J.* **90**, 2089.
 Bessell, M.S., Norris, J.: 1984, *Astrophys. J.* **285**, 622.
 Carney, B.W., Peterson, R.C.: 1981, *Astrophys. J.* **245**, 238.
 Malaney, R.A., Fowler, W.A.: 1989, *Astrophys. J.* **345**, L5.
 Schuster, W.J., Nissen, P.E.: 1989, *Astron. Astrophys.* **222**, 69.

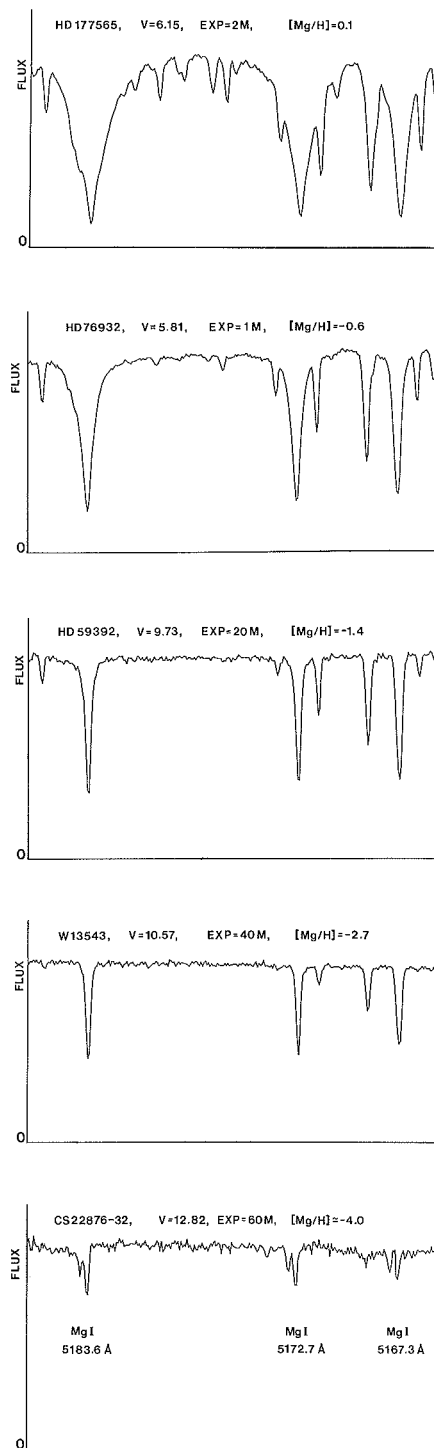


Figure 1: Spectra of the MgI triplet for main-sequence turnoff stars having about the same effective temperature ($T_{\text{eff}} \approx 6000$ K) but widely different values of the Mg/H abundance ratio. Note that CS 22876-32 is a binary star and has extremely weak lines.

The spectra were obtained with the ESO 3.6-m CASPEC instrument during a recent observing run, October 13–17. Exposure times (EXP) are given on the figure. The spectra were reduced on-line using the IHAP system available at the telescope. Bias, dark and scattered light have been subtracted, and the spectra are flat-fielded but not rectified and normalized. However, the zero-point for the flux is marked on each spectrum. Note that wavelength is increasing towards the left.

The Peculiar Colour-Magnitude Diagrams of the Metal-Rich Globular Cluster NGC 6553

B. BARBUY, Universidade de São Paulo, Brazil

E. BICA, Universidade Federal do Rio Grande do Sul, Brazil

S. ORTOLANI, Osservatorio Astronomico, Padova, Italy

1. Introduction

NGC 6553 = GLC 88 (R.A. = $18^{\text{h}} 05^{\text{m}} 11^{\text{s}}$, DEC. = $-25^{\circ} 55' 1''$; 1950.0) is a metal-rich globular cluster of low Galactic latitude ($l = 5^{\circ} 253$, $b = -3^{\circ} 029$) at a heliocentric distance of about 5.7 kpc (Webbink, 1985), in the direction of the Galactic centre.

It shows the following interesting properties: (1) it is one of the most metal-rich galactic globular clusters (Morgan, 1959; van den Bergh, 1967; Bica and Pastoriza, 1983; Zinn and West, 1984); (2) it is a good example of an inner bulge globular cluster; (3) it shows a core with relatively dispersed, and therefore resolvable stars.

For these reasons, we decided to investigate NGC 6553 in detail: in a first important step, we obtained colour-magnitude diagrams (CMD) from B, V, R and I images, and then we identified members suitable for a detailed spectroscopic study in order to determine the cluster metallicity for a second step.

In this work, we present some of the resulting CMDs, and discuss the impact of these observations for studies of super-metallic populations.

2. Observations

BVRI frames were obtained at the 1.5-m Danish Telescope, equipped with the high resolution CCD ESO # 8. The frames used were taken with a seeing of about 0.8 arcsec.

The reductions were done at the ESO Garching computer centre using the Daophot and Romafot packages, in Midas environment.

3. Colour-Magnitude Diagrams

Due to its high metallicity, NGC 6553 presents a peculiar CMD morphology, as it can be seen in the V vs. (B-V) diagram for the whole field (Fig. 1 a) and for giant stars only (Fig. 1 b); as well as in the V vs. (V-I) for the whole field (Fig. 2 a) and for giants only (Fig. 2 b). The giant stars in this diagram, as well as in the other diagrams where we present the same selection for different colour combinations, are divided in two groups with different symbols according to their V-I colour (higher or lower than 3.2, roughly corresponding to the giant turnover in the V vs. (V-I) diagram).

3a. Morphology of the Red Giant Branch (RGB)

Figure 2a shows that the RGB forms an arc, and that the stars at the RGB tip are as faint as the horizontal branch (HB) stars. This is due to a strong molecular opacity of TiO bands in the B, V and R filters, whereas in the I filter only the weak FeH Wing-Ford band is present in these spectral types. This is clearly seen in Figure 2b where only stars from the upper RGB arc are selected. The curvature of the RGB arc might be used as a metallicity indicator.

The amplitude of the distortions that the RGB undergoes depends on the relative strength of the opacity in the different filters. The effect is so strong in the V vs. (B-V) diagram (Fig. 1) that it might be misleadingly interpreted as a wide giant branch arising from a metallicity dispersion. We thus leave a cautionary remark for CMD observations of composite metal-rich populations in galaxy nuclei, which become available with large telescopes and the Hubble Space Telescope.

On the other hand CMDs using I magnitudes as luminosity indicator do not

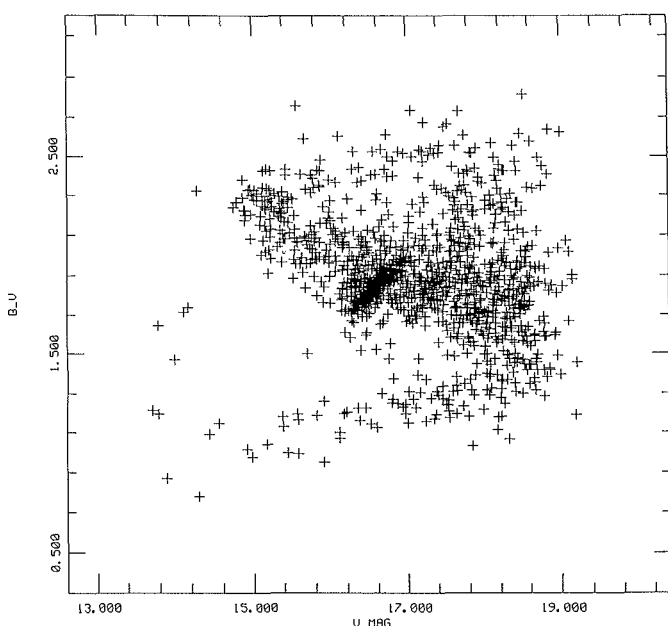


Figure 1a: V vs. (B-V) diagram.

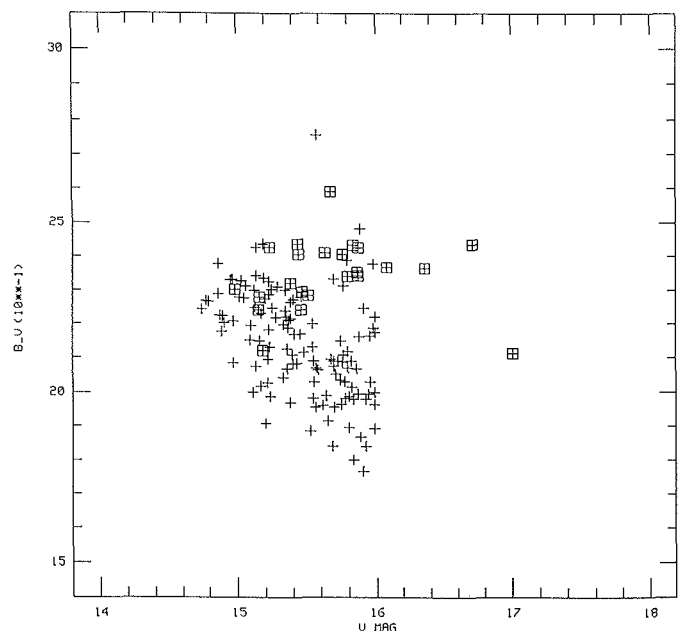


Figure 1b: Same as (1a) but for bright member giants. Crosses and squares represent respectively hotter and cooler giants. Notice that in this colour combination their loci partly overlap.

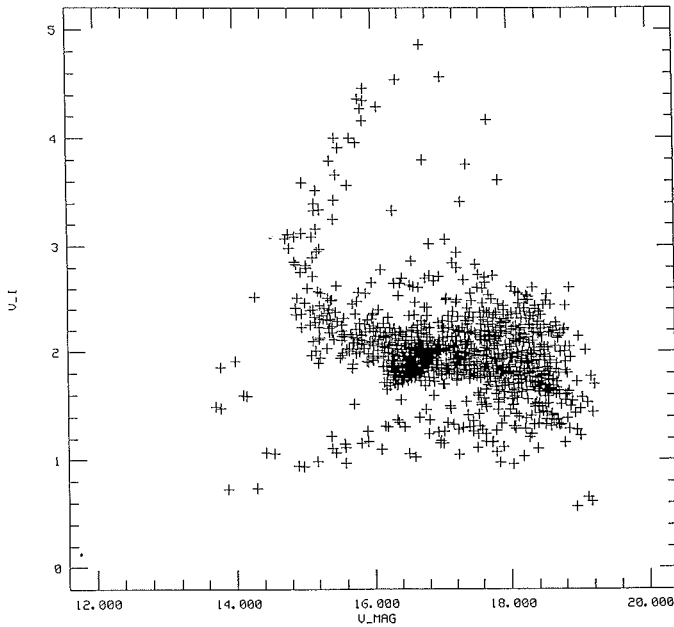


Figure 2a: V vs. $(V-I)$ diagram.

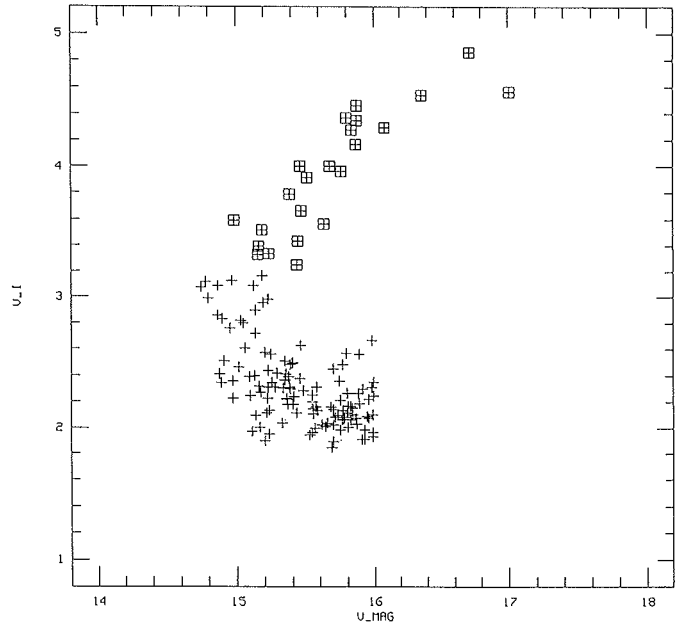


Figure 2b: Same as (2a) but for bright member giants. Notice the pronounced arc.

show a prominent turnover (e.g. Fig. 3), because of the weak opacity in it as discussed above. Consequently the CMD I vs $(V-I)$ appears to be particularly suitable for metallicity dispersion studies in galaxies.

3b. Morphology of the Horizontal Branch

NGC 6553 shows a very red HB, which in some diagrams does even cross the RGB. The HB is otherwise tilted, which can be attributed to three effects:

(i) At about the same magnitude as the HB, there might be a clump of ascending RGB stars, in a phase where the H-burning shell crosses the chemical discontinuity left by the convective envelope. The tilting might be partly due to the presence of this clump (see Fusi Pecci, 1989).

(ii) Differential blanketing, which affects the magnitudes along the HB depending on the stellar temperatures, can produce a tilting in the same direction as observed.

(iii) A differential reddening across the cluster field could also produce similar tiltings (Armandroff, 1988).

4. Reddening and Age

The reddening and the age of NGC 6553 were estimated by comparing its CMDs with those of 47 Tuc, of an age typical of old globular clusters, and Pal 12, an exceptionally young globular cluster of the outer halo. They were all observed with the same instrumentation and reduced in the same way (Ortolani, 1988; Aurière and Ortolani, 1988; Gratton and Ortolani, 1988).

The reddening is estimated to be about $E(B-V) = 1.0$, from a comparison of loci in the turn-off and SGB regions with respect to 47 Tuc. Since NGC 6553

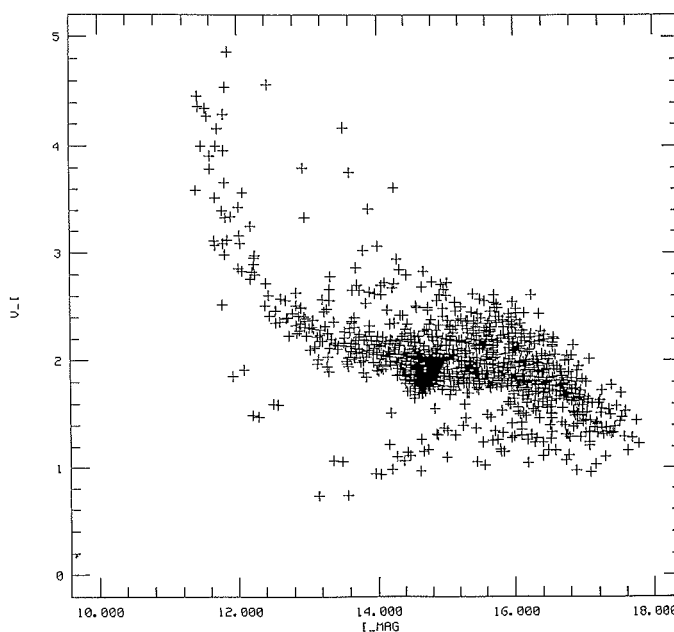


Figure 3a: I vs. $(V-I)$ diagram.

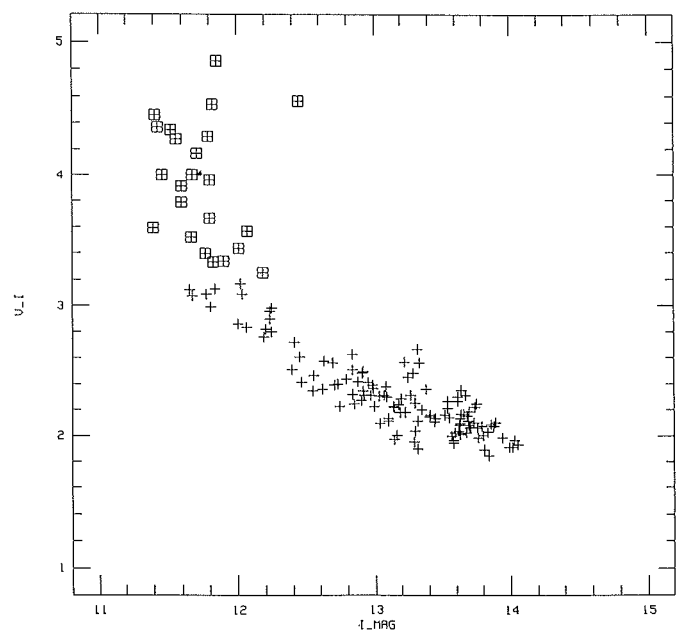


Figure 3b: Same as (3a) but for bright member giants. This colour combination appears to be suitable for metallicity dispersion studies in composite populations like galaxy nuclei.

is considerably more metal-rich than 47 Tuc, part of this “reddening” should be due to an opacity difference: adopting the usual value of $E(B-V) = 0.8$ for NGC 6553 (Webbink, 1985), an opacity difference of 0.2 magnitudes is found.

For estimating the age, the magnitude difference between the turn-off and the HB is used (see Buonnano et al., 1989). NGC 6553 seems to be slightly younger than the classical globular clusters (see Ortolani et al., 1989), which would have important implications for the epoch of the inner bulge formation.

5. Impact of the CMDs of NGC 6553

The colour-magnitude diagrams of NGC 6553 are very important for the

study of super-metallic populations: in particular those present in bulges of elliptical galaxies. Indeed a major difficulty of population syntheses using stellar libraries is the adoption of isochrones for a super-metal-rich population; theoretical computations of such isochrones are not available, and the CMDs of NGC 6553 provide, for the first time, information on the CMD morphology for such systems.

References

- Armandroff, T.E. 1988, *Astron. J.* **96**, 588.
 Aurière, M., Ortolani, S. 1988, *Astron. Astrophys.* **204**, 106.
 Bica, E., Pastoriza, M. 1983, *Astrophys. Spa. Sci.* **91**, 99.

- Buonnano, R., Corsi, C.E., Fusi Pecci, F. 1989, *Astron. Astrophys.*, in press.
 Fusi Pecci, F. 1989, in “Astrophysical Ages and Dating Methods”, 5th IAP Workshop, eds. E. Vangioni-Flam, M. Casse, J. Audouze, Ed. Frontières, to appear.
 Gratton, R., Ortolani, S. 1988, *Astron. Astrophys. Suppl.* **73**, 137.
 Morgan, W.W. 1959, *Astron. J.* **64**, 432.
 Ortolani, S. 1988, Space Telescope Technical Report, ST-ECF-ESO, Garching.
 Ortolani, S., Barbuy, B., Bica, E. 1989, in “Astrophysical Ages and Dating Methods”, 5th IAP Workshop, eds. E. Vangioni-Flam, M. Casse, J. Audouze, Ed. Frontières, to appear.
 van den Bergh, S. 1967, *Astron. J.* **72**, 70.
 Webbink, R.F. 1985, in “Dynamics of Star Clusters”, eds. J. Good, P. Hut, Reidel, p. 541.
 Zinn, R., West, M.J. 1984, *Astrophys. J. Suppl.* **55**, 45.

On the Theoretical Ratio of Some Nebular Lines

A. ACKER, “Equipe Populations Stellaires”, Observatoire de Strasbourg, France

J. KÖPPEN, M. SAMLAND, Institut für Theoretische Astrophysik, Heidelberg, F. R. Germany, and

B. STENHOLM, Lund Observatory, Sweden

1. Introduction

As pointed out by Rosa (1985) and Wampler (1985), the response of the IDS system seems to show a dependence on the value of the input intensity. Peimbert and Torrès-Peimbert (1987) give a review of different determinations of the factor K in the relation between the flux F and the instrumental signal $S = F^{(1+K)}$. The value of K seems to be small (0.03) if the emission lines appear over a strong continuum – which is rare for planetary nebulae –, and K is higher (0.08) for lines over a weak continuum. The value adopted by Peimbert and Torrès-Peimbert is 0.07.

These corrections must be taken into account, as systematic errors will affect the determination of physical parameters. In particular, if line intensities are uncorrected, then:

- the extinction factor c ($H\beta$) is too high, by about 0.15;
- the electron temperature is too low;
- the He/H abundance is underestimated and the heavy element abundance is too high, if the determination is based on collisionally excited emission lines.

2. ESO Observations of Planetary Nebulae

Since 1984, two of us (A.A. and B.S.) have conducted a spectroscopic survey

of the planetary nebulae of our Galaxy, in the spectral range 400 to 740 nm and with a low resolution of about 1 nm (see Acker and Stenholm, 1987). We have used first the IDS system, and since July 1987, a CCD detector, both mounted on the Boller & Chivens Cassegrain Spectrograph at the 1.5-m telescope at La Silla. We have obtained spectra of more than 1000 planetary nebulae: about 400 spectra taken with the IDS and 120 with the CCD are measured.

2.1 The [OIII] doublet

Here we compare theoretical predictions with observed values for the emission lines ratio [OIII] r 500.7 nm versus [OIII] at 495.9 nm, taking into account the interstellar extinction c .

Figure 1a presents the raw data for IDS spectra. For the 342 spectra measured, we found:

$$I(500.7)/I(495.9) = 3.01 \pm 0.23.$$

On Figure 1a we see that, for faint lines ($I(495.9) < 10^3$), the ratio of the [OIII] doublet shows highly dispersed values. For very strong lines ($I(495.9) > 10^5$), the ratio becomes too faint, due to saturation effects. The central part of the relation shows clearly that the observed ratio is higher than the theoretical one. Figure 2a shows that the relation $I(500.7)/I(495.9)$ versus $I(495.9)$

has the same appearance for the CCD data as for the IDS data.

The coefficient β' is calculated as follows, assuming a theoretical value of 2.88 for the [OIII] doublet as proposed by Mendoza (1983), and the value of the extinction c derived from our data through the Balmer decrement (see Acker et al., 1989) using the “HOPPLA” code written by J. Köppen:

$$(I(500.7)/I(495.9))_{\text{obs}} = (2.88 \times 10^{0.013c})\beta'$$

By selecting the lines with intensities in the range $10^3 - 10^5$ we found:

$$\beta' = 1.0316 \pm 0.0478 \text{ (CCD)}$$

$$\beta' = 1.0317 \pm 0.0403 \text{ (IDS)}$$

These values lead to the following values of the “Rosa-coefficient” $\beta = 1/\beta'$:

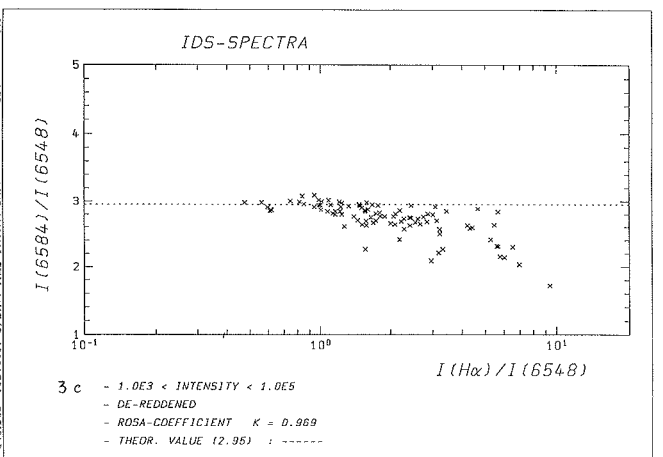
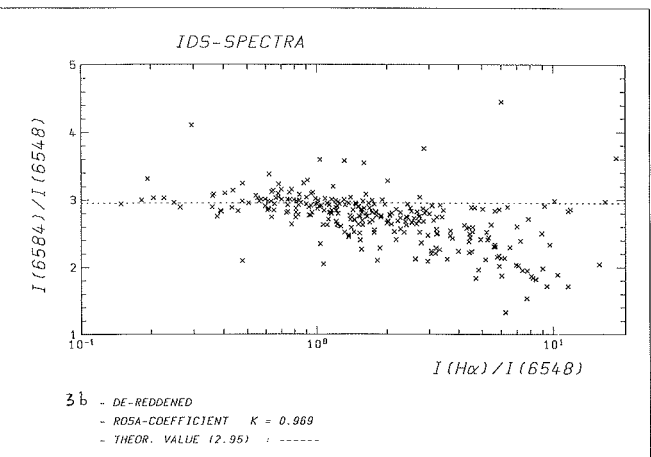
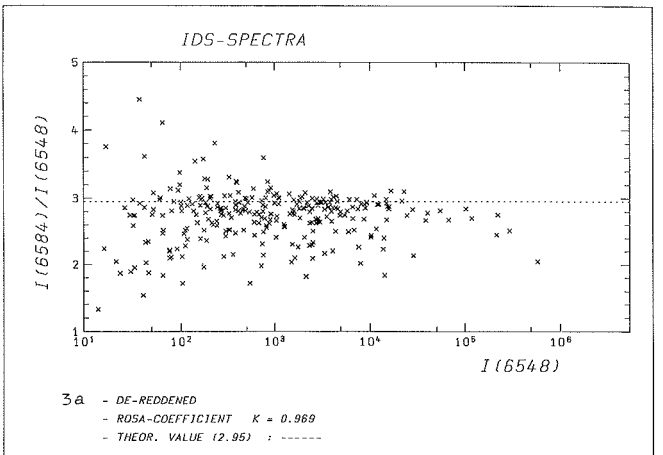
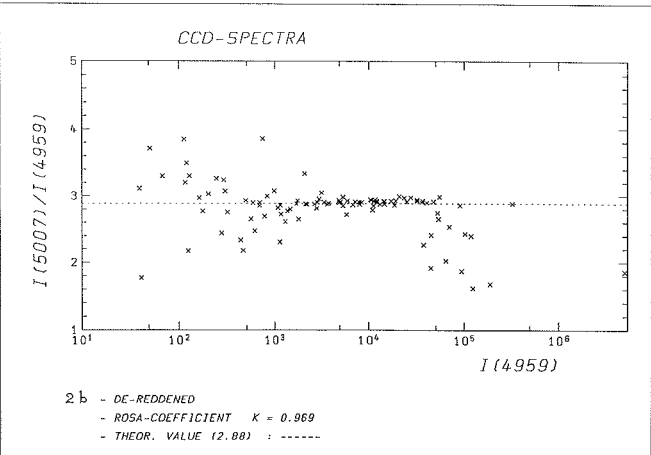
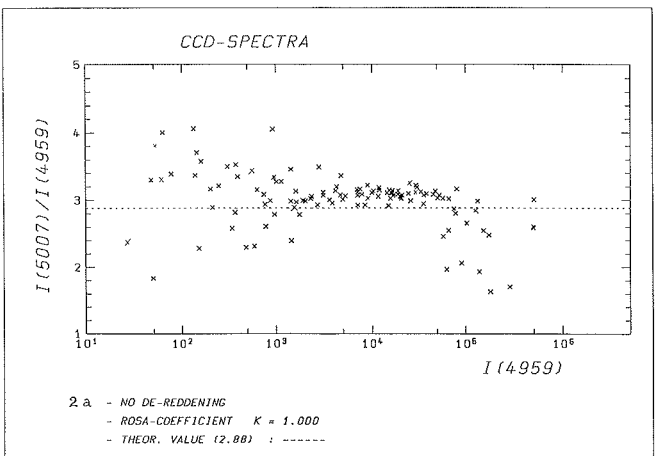
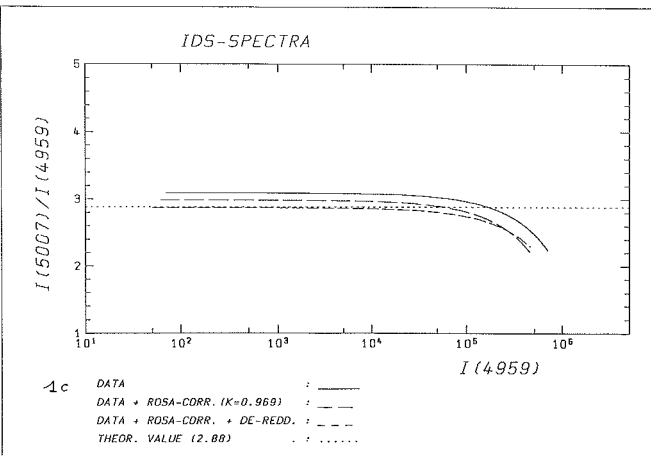
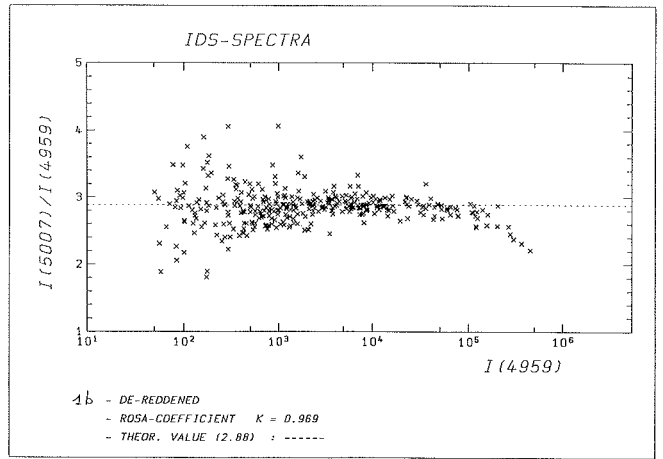
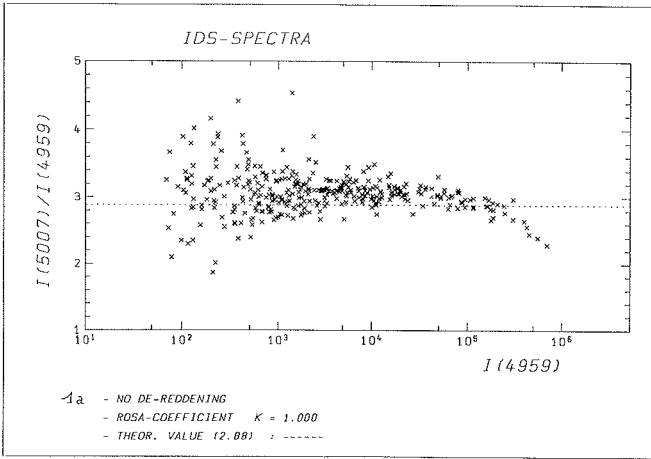
$$\beta = 0.969 \pm 0.047 \text{ (CCD)}$$

$$\beta = 0.969 \pm 0.038 \text{ (IDS)}$$

These values are similar to the value given by Rosa (1985): $\beta = 0.96 \pm 0.02$.

On Figures 1b and 2b, we report the corrected IDS (1b) and CCD (2b) intensities, using the “Rosa-coefficient” $\beta = 0.969$. Figure 1c gives the mean relations calculated for the IDS data.

The excellent agreement we found between the IDS and the CCD data suggests that the discordance with the theoretical predictions cannot be due to instrumental effects only. To check this assumption, we study now the possible non-linearity shown by the [NII] red lines.



045152 2003081 6/23/04 TIME 10:10:08 DATE 03.04.04 ARES: 00321.045

2.2 The [NII] doublet

On our IDS spectra, we could measure the [NII] doublet for 267 nebulae. We found: $I(658.3)/I(654.8) = 2.92 \pm 0.32$, comparable to the theoretical value of 2.95. On figure 3a, we show the observed intensities corrected of the interstellar reddening and of the "Rosa effect". The average behaviour of the $I(658)/I(655)$ line ratio versus the $I(655)$ value is comparable to the correlation found for the [OIII] lines shown on Figure 1a, but it appears that the "Rosa-correction" has perhaps not to be applied here.

The measure of the [NII] doublet is affected by the proximity of the $H\alpha$ line, implying for all [NII] doublets the use of the "Multiple-Gaussian-Fit" procedure of the IHAP programme. The deconvolution of the ($H\alpha$, [NII]) blend becomes

measurable if $I(H\alpha)/I(655) > 0.2$, as shown by the Figure 3b. On this figure, the value of the [NII] lines ratio decreases with an increasing ratio $R = I(H\alpha)/I(655)$: if $R < 1$, the intensity of the 655 line seems underestimated. If $1 < R < 4$, the $I(658)/I(655)$ ratio is near to the theoretical value of 2.95. For higher values of the [NII] lines, saturation would decrease the observed line ratio. This effect is clearly visible for the strongest lines (Figure 3c).

The number of CCD spectra measured up to now is not sufficient to allow any conclusion concerning the [NII] lines ratio.

3. Conclusions

From the analysis of our IDS and CCD spectra of planetary nebulae, we have shown that a nonlinearity proposed for

the IDS receptors cannot be made responsible for the apparent discrepancy between the observed [OIII] line ratio and the predicted one expected to lie around 2.9. It seems possible that the true intensity ratio of these forbidden lines is likely to be around 3.0 – as proposed by Rosa (1985). Further observational and theoretical work is needed.

References

- Acker, A., Köppen, J., Stenholm, B., Jasniewicz, G.: 1989, *Astron. Astrophys. Suppl.* in press.
Acker, A., Stenholm, B.: 1987, *The Messenger* **48**, p. 16.
Peimbert, M., Torrès-Peimbert, S.: 1987, *Rev. Mex. Astron.* **14**, 540.
Rosa, M.: 1985, *The Messenger*, **38**, p. 15.
Wampler, E.J.: 1985, *The Messenger*, **41**, p. 11.

EFOSC Observations of the Inner Echo Around SN 1987A

*F. PARESCE, W.B. SPARKS and F. MACCHETTO,
Space Telescope Science Institute, Baltimore, Maryland, USA, and
Astrophysics Division, Space Science Department of ESA*

Time varying light echoes around bright supernovae have been known since their first detailed observation in 1901–1902 by Ritchey, Kapteyn and Perrine around Nova Persei 1901 (GK Per) and the first comprehensive theoretical model put forth by Couderc in 1939.

In this framework, they are understood as due to the delayed reflection (echo) of the supernova light pulse from nearby interstellar or circumstellar dust clouds. The temporal variability, of course, is a consequence of the sweeping action of the pulse through an anisotropic and inhomogeneous reflecting medium.

The recent SN 1987A has not disappointed observers of this phenomenon due to its relative vicinity and complexity of the surrounding material. The overriding scientific importance of the detailed study of the SN light echoes resides in their ability to shed light on its past evolutionary history (the SN in search of its past as it has been aptly put recently) by progressively illuminating the circumstellar region into which objects as massive as the SN 1987A progenitor are expected to deposit a very significant fraction (up to 1/2) of its mass. The two key observational as-

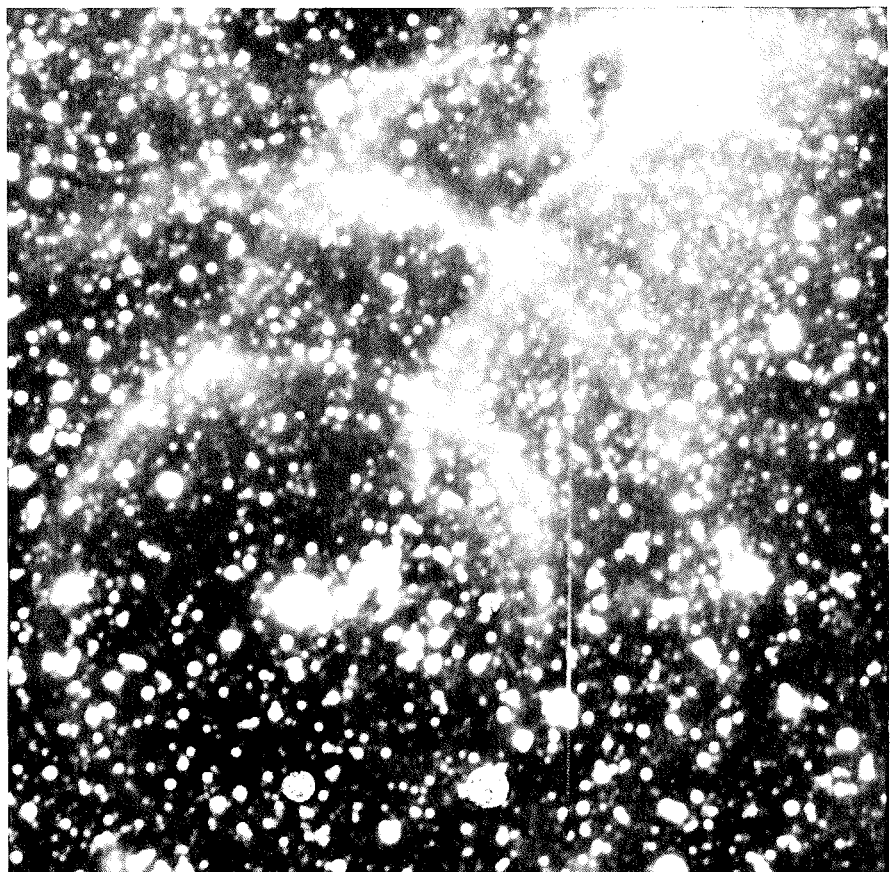


Figure 1.

pects of this endeavour are the ability to image very faint features next to relatively bright objects and continuous monitoring to capture the complex temporal variations of the phenomenon.

The most dramatic echoes around SN 1987A are those first announced by Crotts in 1988 and now located at approximately 500 and 1250 light-years from the SN (see *The Messenger*, **52**, p. 13, and **54**, p. 28) these are understood to be due to sheets of intervening interstellar gas and dust completely unrelated to the SN itself and, thus, of limited significance to the issue of SN evolution. As the SN fades, however, it becomes easier to discern faint features located in the immediate vicinity of the SN, but until September 1988 nothing within $10''$ – $20''$ of the star could be measured even under intense and very sensitive scrutiny (see *The Messenger*, **55**, p. 49).

This situation changed suddenly when Crotts and Kunkel and Bond, Panagia, Gilmozzi and Meakes both reported evidence of the appearance of an inner echo at $8''$ – $10''$ from SN 1987A in October 1988 and January 1989. Because of the inherent faintness of the ring against the glare of the SN and the clutter of the crowded star field nearby, its reality had to be tempered with some caution.

To better establish not merely its existence but, more importantly, its physical association with the SN, we used a slightly different approach to the problem. On February 10, 1989 we used the EFOSC operating in the coronagraphic mode on the 3.6-m telescope with a broad-band V filter and four linear polarizers oriented at position angles 0° , 45° , 90° and 135° to measure not only the total but also the polarized flux of radiation scattered from circumstellar material around SN 1987A. We clearly detected a faint arc of V-band emission with a sharp inner and outer boundary centred on the supernova and of radius $8''.3$ and width $\approx 2''.5$ most prominent in the Eastern quadrant between 45° and 135° position angle. Its azimuthally averaged surface brightness in this position angle range is 21.8 ± 0.2 V mag arcsec $^{-2}$. In this particular region, the detected radiation is found to be partially linearly polarized with a degree of polarization 0.15 ± 0.04 and an electric vector orientation of $\approx 0^\circ$ position angle.

The accompanying image (Fig. 1) taken with our set-up at La Silla shows the direct 1-minute V band exposure taken during our February run. The field of view is $2'.9 \times 2'.9$; North up and East to the left with a linear intensity scale from 250 adu (black) to 450 adu (white). The SN is the bright source at the centre of

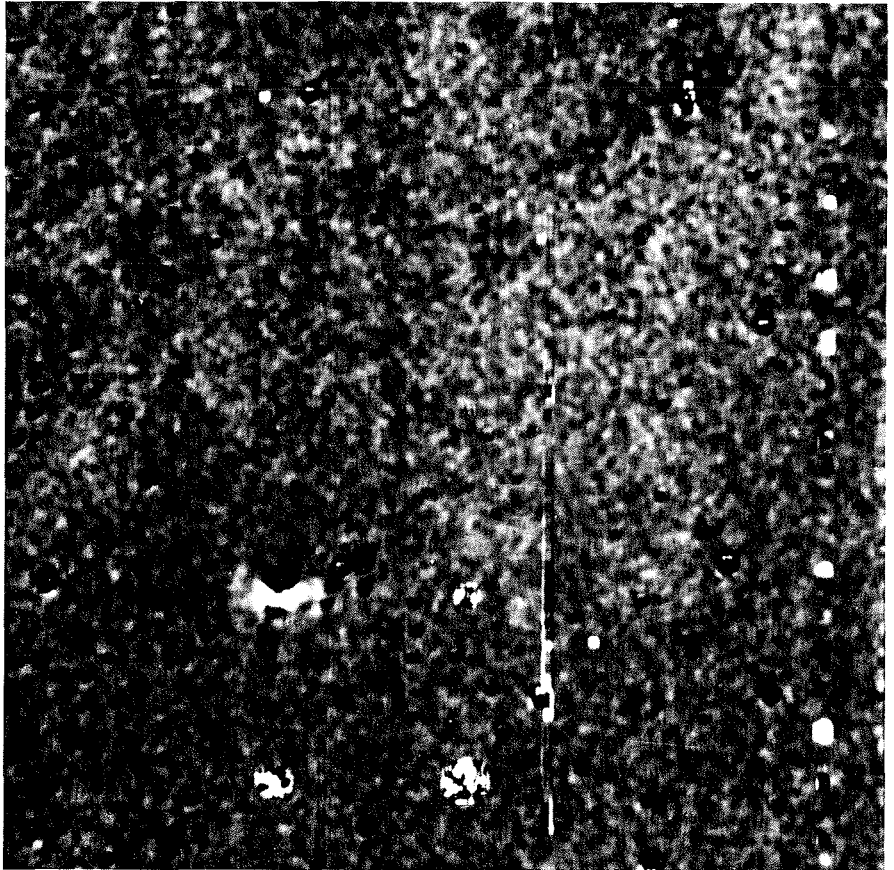


Figure 2.

the well-known outer two interstellar ring echoes. The SN lies behind the $3''$ diameter coronagraphic spot (the other spots in the field are barely visible as noisy circular regions forming a square pattern with the SN). The inner echo can be seen as the faint circular feature surrounding the SN with a sharp outer rim in the East at $\approx 10''$ radius. For a distance of 52.5 kpc, 1 arcsec in this image corresponds to ≈ 0.8 light-year.

A peculiarity of this inner echo in contrast to the outer ones is its marked spatial asymmetry. This characteristic is quite obvious in the polarized flux and especially in the Q Stokes parameter image shown in the accompanying Figure 2 obtained with EFOSC. In this latter figure, we show an image of the difference between the 0° polarizer intensity and the 90° polarizer intensity of the same field as shown in Figure 1. Notice how effectively all the stars seen in Figure 1 have dropped out from Figure 2 leaving only the SN and its echo. This last image reveals the ring to actually consist of two bright $\approx 90^\circ$ long arcs centred on the East and West directions. It is not too clear yet whether there is any emission at all in the N and S quadrants. The light immediately inside the areas in the butterfly pattern is also polarized but

we cannot determine yet whether this is instrumental in origin. Incidentally, the disappearance of the two outer echoes from Figure 2 shows that they are not linearly polarized, as expected.

The linear polarization figure of 15% unambiguously establishes the feature to be due to scattered light from dust grains located at ≈ 15 light-years in front of the SN such that the scattering angle is $\approx 30^\circ$. These grains most plausibly reside in a fragment of a circumstellar shell formed by the deceleration of a red giant wind by the bubble of gas formed by the fast wind of the main sequence supergiant progenitor. Thus, these measurements can be taken as clear indications of the reality of the postulated red giant phase of the SN. Continued investigations of this type should prove very beneficial in unraveling the nature of the SN through the detailed study of the structure and composition of its immediate surroundings. No other technique we know of at this point will allow such an investigation.

We hope ESO will continue to carefully monitor the immediate surroundings of this fascinating object especially now that the SN is rapidly fading and the reflected radiation begins to probe the inner regions behind the SN.

“Deep” Rotation Curves of Edge-on S0 Galaxies

E. CAPPELLARO¹, M. CAPACCIOLI¹, and E. V. HELD²

¹Osservatorio Astronomico, Padova, Italy; ²Osservatorio Astronomico, Bologna, Italy

We present a sample of “deep” rotation and velocity dispersion curves from stellar (absorption) spectra obtained at La Silla in February 1989. These record observations are part of a long-term project conceived to investigate how the dynamical behaviour of galactic disks depends on the bulge-to-disk light ratio, and to unravel the three-dimensional shapes of dark haloes in early-type disk galaxies (for a review of this matter, see Bender et al., 1989, Capaccioli and Caon, 1989, and Capaccioli and Longo, 1989). The targets: NGC 2310, NGC 3115, and NGC 4179, are edge-on S0 galaxies, chosen among the few such objects with fairly large angular sizes (distances ≤ 25 Mpc) in order to minimize the resolution problems (see Fig. 1).

The spectra of the programme galaxies were secured with the ESO Faint Object Spectrograph and Camera (EFOSC), attached to the Cassegrain focus of the 3.6-m telescope, and equipped with the high resolution RCA CCD No. 8. In binned mode, this detector gives 320×512 pixels of $30 \mu\text{m}$, equivalent to $0''.675$ on the sky. We chose the grism coded as “Orange 150” in the ESO *Users Manual*, which provided us with a dispersion of 3.9 \AA px^{-1} over the wavelength interval from 5000 to 7000 \AA .

Several spectra along the major axis of each galaxy were obtained with exposure times ranging from 1500 to 3600 s. To best exploit the full length of the slit (3'6), each galaxy was centred alternatively at one or the other end of the slit. This procedure was conceived to achieve both the wanted spatial coverage of the source and the simultaneous recording of a “clean” enough night sky spectrum; the latter must be extremely well sampled, since it is usually the dominant signal in the absorption spectra taken anywhere outside the effective isophotes of early-type galaxies. In our least favourable case – that of the most extended object NGC 3115 – the edge of the slit opposite to the nucleus viewed a region of the galaxy as faint as $\mu_B \approx 24.5$, i.e. ~ 7 times fainter than the average night sky surface brightness. As further precaution, offsetting the telescope by $\sim 20'$ we obtained also several long exposure spectra of the blank night sky, as close as possible in time to the astrophysical exposures; during the reduction phase, they turned out to be fundamental for

the successful reduction of the material of two of the three objects. Comparison spectra of a He- Ar lamp were secured before and after each exposure. Finally, spectra of some template stars in the range of spectral classes from G8 to K1 were also taken on the same nights.

The raw CCD data were processed with MIDAS. Standard recipes were applied for the bias and dark subtraction, and for the careful flat-fielding based on both dome and down-sky exposures at different count levels. The complex distortion pattern was mapped using the

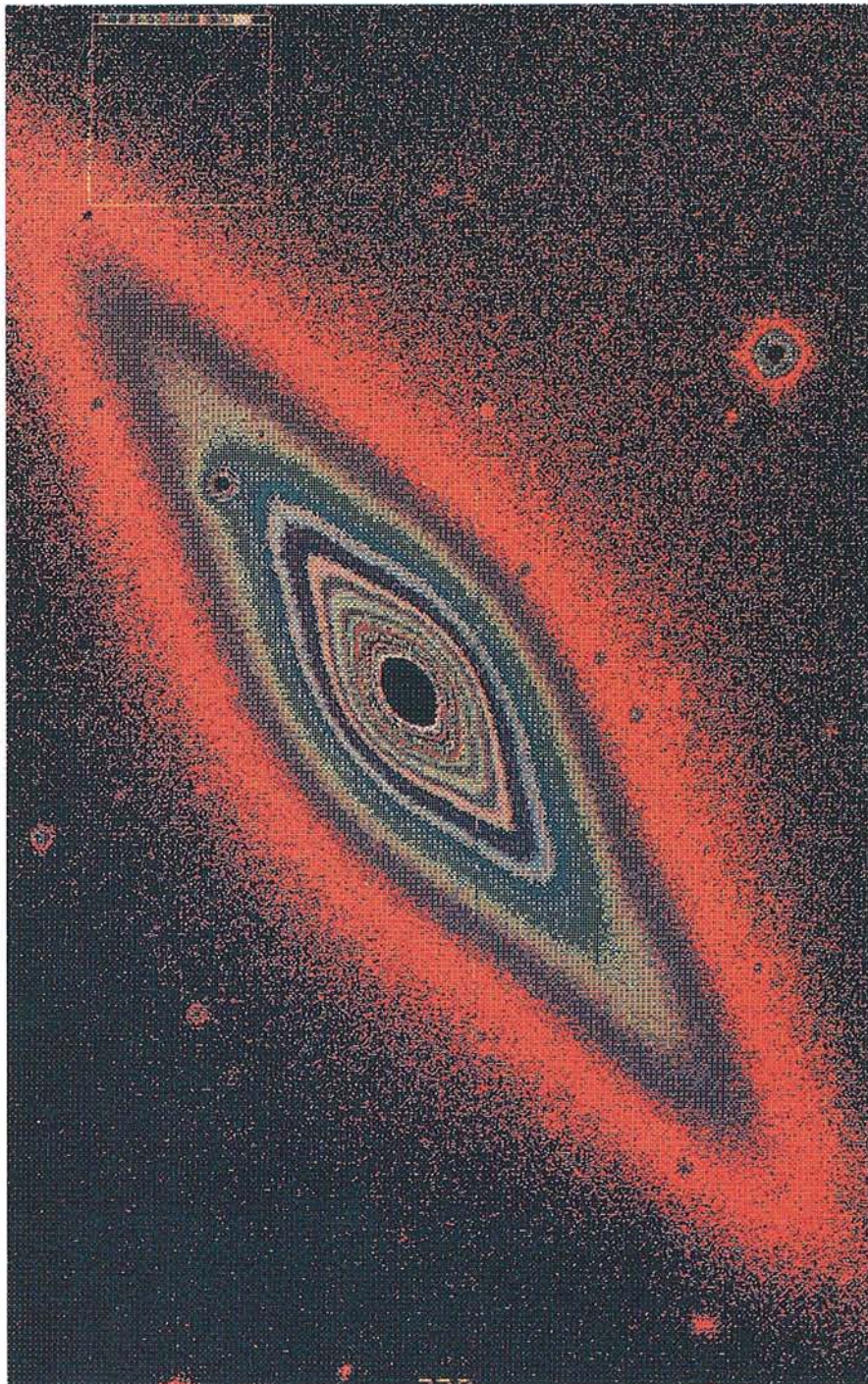


Figure 1: R-band CCD image of the edge-on S0 galaxy NGC 4179, secured with the ESO-MPI 2.2-m telescope (courtesy of Dr. G.P. Piotto). Our kinematical measurements cover the full length of the major axis of the galaxy shown in this $2' \times 3'$ picture.

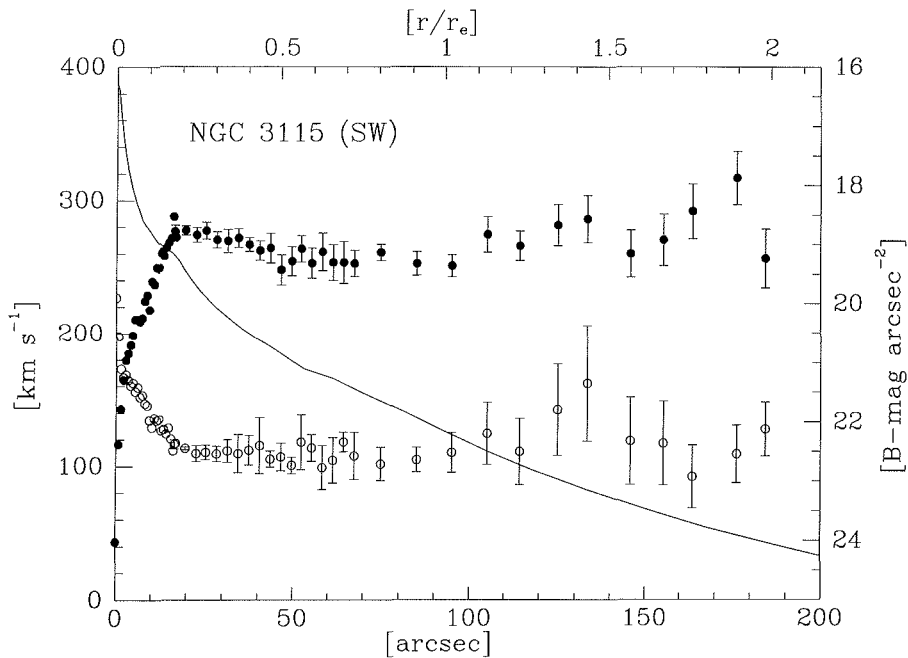


Figure 2: Radial velocity $V(r)$ (full dots) and velocity dispersion $\sigma(r)$ (open circles) measurements as a function of the galactocentric distance (in arcseconds and in units of the effective radius) along the SW semimajor axis of the bright edge-on S0 galaxy NGC 3115. $V(r)$ is corrected for the systemic velocity, and $\sigma(r)$ is re-scaled by a factor 0.75 (see text). The error bars represent the dispersion of the actual data averaged within each bin. The solid line is the major axis B-band light profile taken from the photometric study by Capaccioli et al. (1987). Note that the kinematical data extend to $r = 2r_e$, where $\mu_b = 24$, a record for absorption line spectroscopy.

comparison spectra to derive a line-by-line wavelength calibration. In the material of this run, we find that the position of the comparison lines drifts over the detector during the night, the maximum displacement being of the order of 1 pixel. This is of consequence for the absolute velocity scale only, in that it leaves a zero-point uncertainty of $\pm 50 \text{ km s}^{-1}$. In fact, the shift between two astrophysical exposures can be corrected by the match of the night sky emissions.

The crucial step in the reduction pipeline has been the subtraction, from the galaxy spectra, of the contribution by the night sky light. In the case of NGC 2310 – the smallest galaxy of the sample – the sky spectrum was extracted directly from the “free” side of the galaxy exposure, i.e. from that side of the slit opposite to the nucleus of the object. Instead, the spectra of NGC 3115 and NGC 4179 extend so much that no part of the slit is really free from the galaxy signal; thus, also the offset sky exposures had to be used for the sky subtraction. In both cases, the galaxy frames corresponding to the same semiaxis were individually sky subtracted, and then averaged by means of an algorithm allowing to correct for cosmic ray events.

The kinematical data were extracted by the package of programmes de-

veloped by Bender (1989). The core of the procedure is the cross-correlation, at each radial bin, of the continuum-subtracted galaxy spectrum with that of a template. No significant dependence of the results on the different template stars has been found.

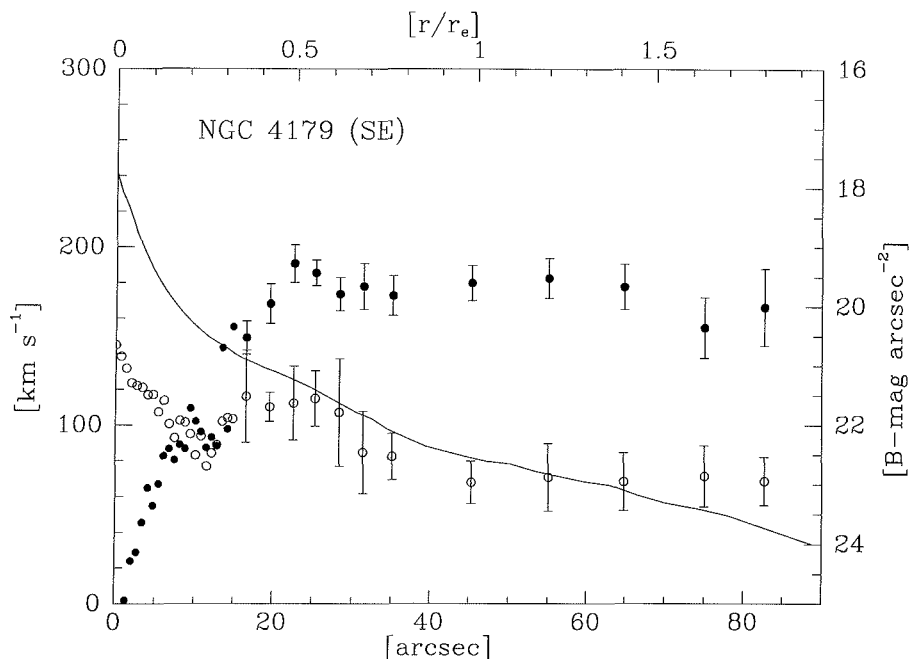


Figure 3: Same as Figure 2, for SE semimajor axis of the edge-on S0 galaxy NGC 4179 shown in Figure 1. The photometric information is taken from a study by Capaccioli, Fasano, and Held (in preparation).

Rotation and velocity dispersion curves for two of our three galaxies, together with the B-band light profiles along the major axes, are presented in Figures 2 and 3. The original data have been averaged within intervals whose sizes increase with the galactocentric distance; the scatter internal to each interval (r.m.s. of the mean) is shown by error bars in the figures. The kinematical centre (and the associated systemic velocity) of each galaxy was assumed to coincide with the peak in the velocity dispersion profile. Symmetry arguments relative to the two sides of the major axis rotation curves are not effectively applicable to our material, given the small overlap between opposite side spectra.

We want to warn explicitly the potential users of the preliminary data presented here that, contrary to the rotational velocities $V(r)$, the values of the velocity dispersion, $\sigma(r)$, produced by the plain application of our reduction procedure are 50–70% larger than previous literature measurements. Inspection of Figure 4 shows that the problem is in our scale since, after re-scaling by a constant factor, our data match very well the other measurements (which include some still unpublished photographic spectra obtained with the Boller & Chivens spectrograph at the ESO 1.5-m telescope). The reasons why the broadening functions of the long exposure galaxy spectra are significantly larger than the short exposures on the template stars are probably understood, but we still lack a procedure to compute the correction factors.

Figures 2 and 3 show that our kinematical measurements reach the record distance, for absorption spectra, of $\sim 2 r_e$; this is twice the size of the effective isophote (the one which encircles half of the total light of the galaxy), and corresponds of a surface brightness $\mu_B \approx 24$.

In order to appreciate the improvement of these over the literature data on absorption line kinematics, one can see for example the “Atlas of velocity dispersion profiles and rotation curves for elliptical and lenticular galaxies” by Di Martino, Busarello and Longo (1989, preprint).

In all cases, our rotation curves exhibit the standard signatures of S0 galaxies, i.e. the bumps characteristic of systems where the “conspiracy” between the disk and the bulge is not finely tuned (cf. Capaccioli, 1979). More importantly, they confirm that the flat trend noted at small galactocentric distances – where disks may be still prominent – is maintained at larger distances, well in the range where the bulge is dominant; for instance, according to Capaccioli et al. (1987), the major axis light profile of NGC 3115 is dominated by the bulge at all galactocentric distances $> 0.45 r_e$. In spite of the fact that, thanks to the unique performances of EFOSC, our measurements have almost doubled the range of radial distances covered by previous kinematical mapping, these deep data do not provide us with any strong evidence for dark matter in early-type disk galaxies, say comparable to the HI rotation curves in late-type disk galaxies. The reasons are the still “short” radial range, and the uncertainties introduced by the non-negligible velocity dispersion and by the modelling. All this matter is under investigation. A full account of the observations described here, and the relative astrophysical discussion, will be presented elsewhere.

References

- Bender, R., 1989, *Astron. Astrophys.*, in press.
 Bender, R., Capaccioli, M., Macchetto, F., and Nieto, J.-L., 1989, *The Messenger*, **55**, 6.
 Capaccioli, M., 1979, in *Photometry, Kinematics, and Dynamics of Galaxies* (Austin, Texas), ed. D.S. Evans, Texas Univ. Press: Austin, p. 165.
 Capaccioli, M., and Caon, N., 1989, in *1st ESO/ST-ECF Data Analysis Workshop* (Garching, FRG), eds. P.J. Grosbøl, F. Murtagh and R.H. Warmels, p. 107.
 Capaccioli, M., and Longo, G., 1989, in *Windows on Galaxies* (Erice, Italy), eds. J. Gallagher and G. Fabbiano, Kluwer Acad. Publ.: Dordrecht, in press.

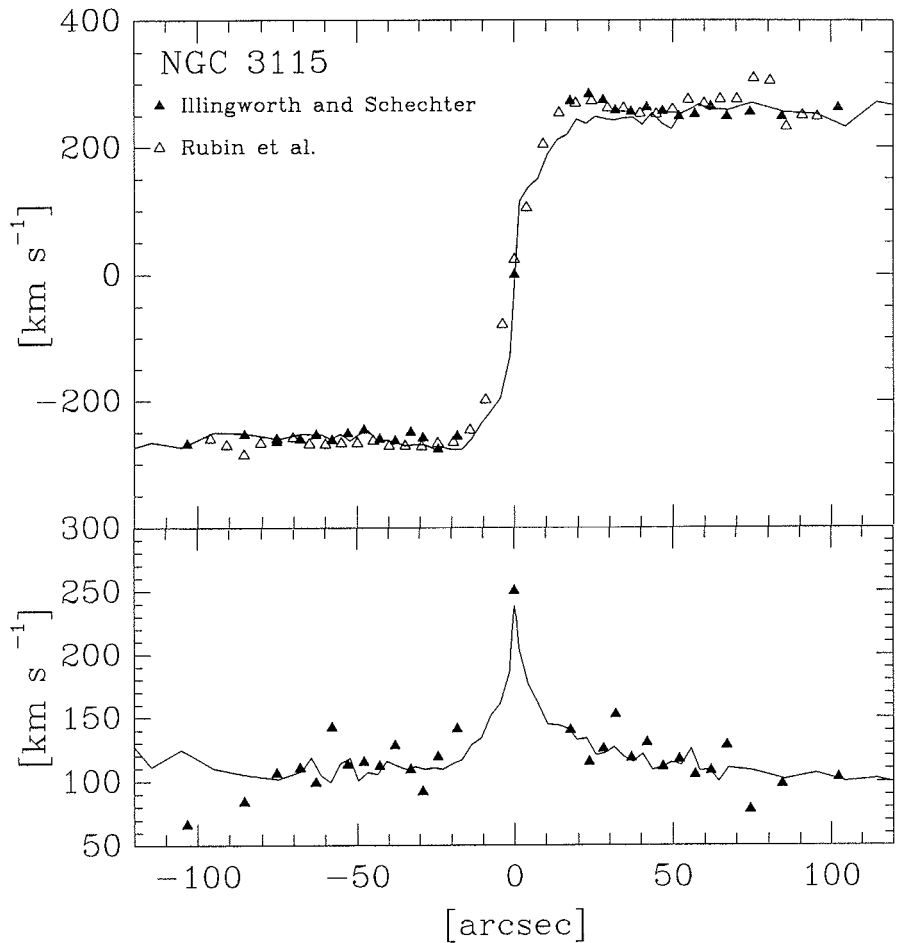


Figure 4: Comparisons between the rotation and velocity dispersion curves of NGC 3115 from this study (solid line) and the kinematical data published by Rubin et al. (1980) and Illingworth and Schechter (1982).

- Capaccioli, M., Held, E.V., and Nieto, J.-L., 1987, *Astron. J.*, **94**, 1519.
 Illingworth, G., and Schechter, P.L., 1982,

- Astron. J.*, **256**, 481.
 Rubin, V.C., Peterson, C.J., and Ford Jr., W.K.I., 1980, *Astron. J.*, **239**, 50.

International Portrait Catalogue

One of the last days in September this year, I went to Berlin (West) to give a talk at the Wilhelm Foerster Volkssternwarte (People’s observatory), on the occasion of the 100th anniversary of its “Bamberg” refractor.

Among the speakers was also Dieter B. Herrmann, Director of the Archenhold-Sternwarte in Berlin-Treptow, GDR, and noted astronomical historian, who had come over to celebrate this jubilee of one of the oldest, still functioning large telescopes, in this case exclusively installed for public education purposes.

Quite apart from the happy event which brought us together, I learned about Professor Herrmann’s efforts to establish the world’s most comprehensive collection of portraits of astronom-

ers, in particular for the benefit of (future) historians. More than 7500 photos and drawings have already been gathered by this project which has been going on since 1971, under the auspices of IAU commission 41 (History of Astronomy).

However, it appears that many astronomers are unaware of the existence of this catalogue, that is at least my impression after having talked to some colleagues here in Munich. This is confirmed by Prof. Herrmann’s difficulties in acquiring portraits of now living astronomers. He therefore asked whether it would be possible to place a small note in the *ESO Messenger* for this effect, at the same time hoping for reaction from our readers. I am happy to provide this space for this useful purpose.

So Messenger readers beware: here is your best chance ever to make your image known to future generations! I am told that portraits can be sent as gifts or on loan only; in the latter case, they will be returned within a month after having been copied. Subject to any restrictions imposed by the donors, the Archenhold Observatory is prepared to supply on request copies of portraits held by them and will issue lists of their holdings from time to time. That is a most useful offer for all who have to write an article or give a talk about the past of their observatory, etc.

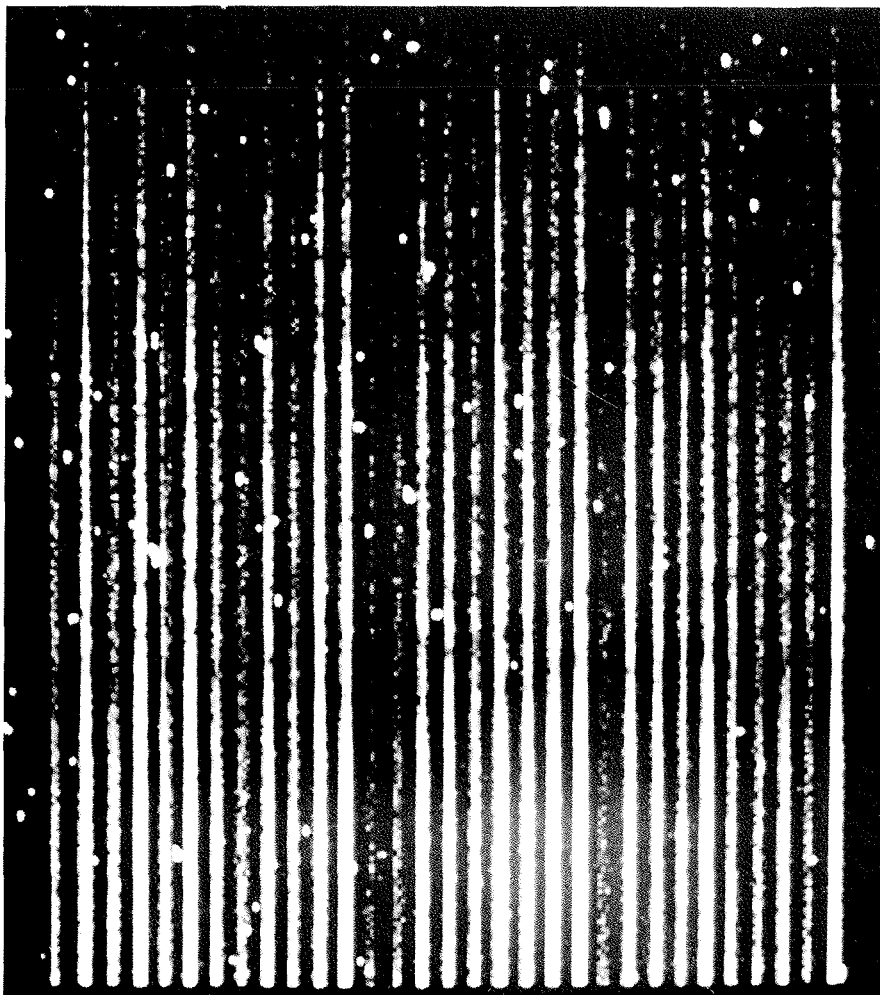
The address is: Prof. Dr. D.B. Herrmann, Archenhold-Sternwarte, Alt-Treptow 1, DDR-1193 Berlin, German Democratic Republic. They will be happy to hear from you. *The editor*

Jacques Beckers Elected to Dutch and Norwegian Academies

On August 28, Queen Beatrix of the Netherlands confirmed the election of ESO staff member Jacques Beckers as "Correspondent" of the Division for Sciences of the Royal Academy of Sciences of the Netherlands. Corresponding members are researchers with a degree from a university in the Netherlands, residing abroad.

Jacques Beckers, who joined ESO in 1988 to become Head of the Interferometry Group, also became a foreign member of the Mathematics-Physics Sciences Division of the Norwegian Academy of Sciences last year.

Our best congratulations to Jacques at the time of these well-deserved honours!



The Efficiency of OPTOPUS

This is part of an OPTOPUS frame resulting from an exposure of galaxies in the cluster Abell 3158, as obtained during the first run (in September 1989) of the ESO Key Programme on "Structure and Dynamics of Rich Clusters of Galaxies".

Note that only the blue parts of the 31 spectra (of 28 galaxies and 3 "skies") are shown in this picture, which covers the wavelength range from ~ 383 nm (top) to ~ 440 nm (bottom). The bluest CaII doublet (about one third of the way down) is from sky; the redder CaII doublet (about two thirds of the way down) is from the galaxies, and visually displays the dispersion of the radial velocities of the galaxies in the cluster.

In total, 37 exposures were obtained during the run, which yielded a total of about 1000 galaxy spectra. *P. Katgert (Leiden)*

An Accurate Wavelength Calibration of CCD CASPEC Echelle Spectra

H. HENSBERGE¹, W. VERSCHUEREN²

¹*Koninklijke Sterrenwacht van België, Brussels, Belgium*

²*Theoretical Mechanics and Astrophysics, University of Antwerp (RUCA), Belgium*

Introduction

In December 1986 and January 1988 we obtained with CASPEC at the 3.6-m telescope spectra of early-type member stars of the young stellar cluster NGC 2244 with the main purpose of deter-

mining accurate radial velocities. We focused our attention on the blue wavelength region (3700–4700 Å) and used CCD # 3 in combination with the 52 l/mm echelle grating.

For the study of the internal kinema-

tics of the cluster and dealing with relatively few lines in early-type stars, it is evidently of primary interest to achieve high precision in the wavelength calibration, particularly avoiding systematic errors with wavelength. Th-Ar calibra-

tion spectra were obtained before and after every stellar exposure, in the corresponding telescope position. The internal consistency obtained from comparing measured line positions on subsequent calibration frames, after allowance was made for a small shift of the spectrum over the CCD (of the order of a few 10^{-2} pixel in the wavelength direction), is roughly 0.03 pixel in agreement with Monte Carlo simulations taking into account photon noise and read-out noise.

However, in a first reduction using standard MIDAS procedures we noticed that the r.m.s. of the residuals between fitted and theoretical wavelengths was much larger, of the order of 0.15 pixel (0.02 \AA) in accordance with the results mentioned by D'Odorico and Ponz (1984). These residuals are obviously not representing random errors, but systematic trends as one might check by comparing the residuals for a given line on various frames. This contribution points out the origin of these systematic errors and describes our solution to the problem.

Analysis of Standard MIDAS Wavelength Calibration Procedure

The standard MIDAS procedure defines the actual position of the Th-Ar lines in the extracted orders by default as the centre of gravity of the two brightest pixels relative to the third brightest. (The more experienced user can use gaussian fitting by specifying his choice in the MIDAS procedure ECHSEAR.) It then identifies the lines, after elimination of resolved doublets, and in the case of theoretical close doublets with components of comparable strength, it couples the line position to a weighted mean wavelength. Finally, it predicts $\lambda_m(x)$ as a function of position x in order m for each order independently by fitting a third degree polynomial in x . If less than 4 lines are identified in a given order, a lower degree polynomial is chosen or, when less than 2 lines are identified, ultimately a global first approximation fit with 6 coefficients is used.

Two kinds of systematic errors are introduced by using the standard calibration method, one associated with the actual definition of line centre, the other with the inadequate treatment of line blending. Depending on the desired wavelength accuracy, one might consider these errors either negligible or inadmissible.

In order to illustrate the kind of systematic error introduced by the "gravity" method used to determine line centre, we calculated the theoretical difference between the exact and the "gravity" pre-

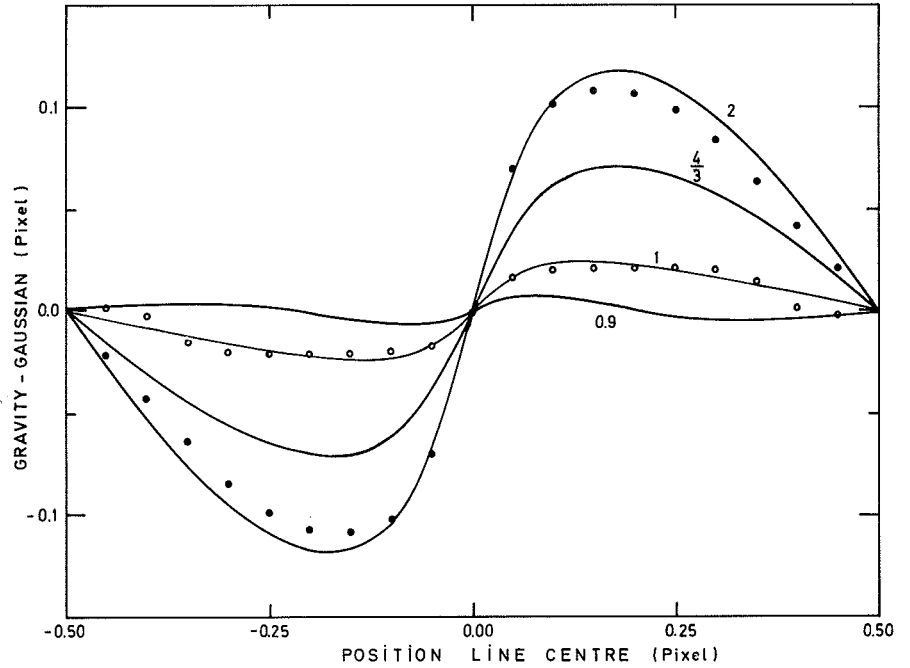


Figure 1: Systematic errors induced by the "gravity" method depending on true line centre-to-pixel centre position. Curves labelled with FWHM refer to theoretical calculations for gaussian lines. Dots resp. circles refer to empirical relations deduced from blue 52 l/mm resp. red 31 l/mm echelle CASPEC data on CCD # 3.

dicted line centre position for gaussian lines as a function of the position of the exact line centre relative to the centre of the pixel on which the line was found. Figure 1 shows that the usefulness of the "gravity" method strongly depends on FWHM, producing systematic errors of order 10^{-2} pixel for FWHM = 1 pixel

but of order 10^{-1} pixel for FWHM = 2 pixels. The global effect of "gravity" is that the line is seen closer towards the pixel edge than is actually the case (FWHM > 0.9), an effect that might be empirically illustrated by forming a histogram of the "gravity" measured line centre-to-pixel centre positions (Fig. 2).

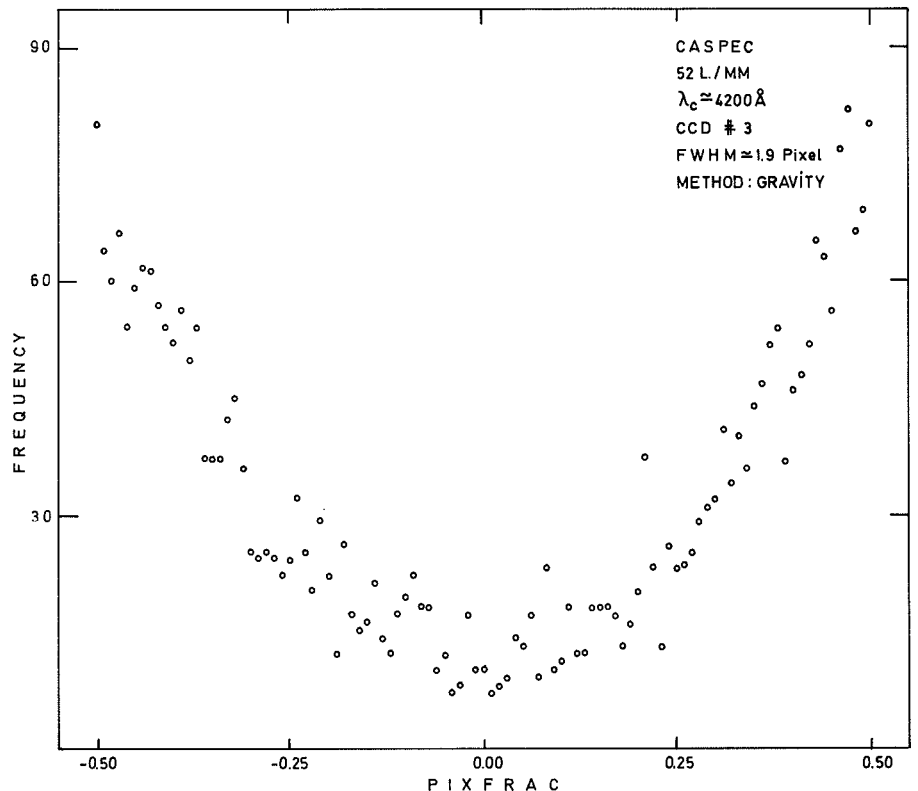


Figure 2: Distribution of "gravity" measured line positions relative to pixel centre (0.0), summed over 18 calibration frames.

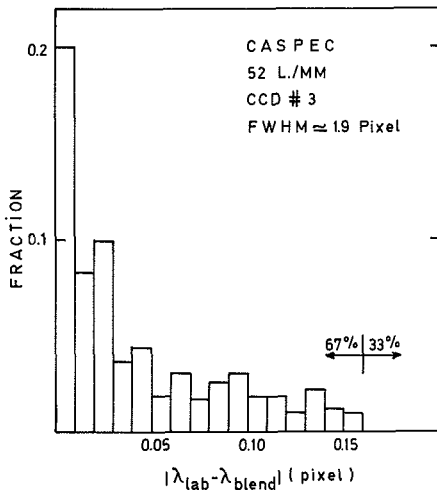


Figure 3: Distribution of the offsets caused by line blending in the thorium spectrum between 3700 and 4700 Å for gaussian fitting over 5 pixels at the indicated instrumental configuration. Only lines strong enough to be detectable with CASPEC were retained as primary component.

The thorium spectrum is rich in spectral lines, especially in the blue. When aiming at position accuracies of a few 10^{-3} Å, even weak blends should be taken into account. Convolution of the laboratory thorium spectrum (Palmer and Engleman, 1983) with a point-spread function (PSF) representative for our data and subsequent gaussian line fitting shows that two third of the measured line positions for lines detectable in the CASPEC calibration spectra differ by more than 0.025 pixel (0.003 Å) from their theoretical position (Fig. 3). One third of all lines give offsets larger than 0.15 pixel (0.02 Å). Only a very small fraction of these blends is avoided in the current procedure. Effects of the order of 0.1 pixel are commonly caused by spectral lines one order of intensity fainter than the line they disturb.

It is obvious that line blending and "gravity" line fitting cause errors of the order of the r.m.s. measured using the standard MIDAS wavelength calibration procedure. Thus this r.m.s. does not reflect information on the ultimately obtainable accuracy. More seriously, these approximations have impact on the final wavelength calibration, on the order of a few km s^{-1} . We will not develop here the statistical arguments in support of this statement, but we will illustrate it at the end of the next section (Fig. 6) when discussing one of our calibration frames.

An Improved Wavelength Calibration Procedure

There is no essential argument against the definition of the actual line position of the Th-Ar lines by gaussian

(or PSF) fitting. The possibility of gaussian fitting is available in MIDAS, except for the fact that the standard gauss fitting routines in the current echelle package are not intended to deal with under-sampled gaussians, nor to treat all kinds of input data substantially differing from pure gaussians. We removed these limitations by an extension of the convergence criteria, an improvement of the initial guesses for the fit parameters and the introduction of the finite pixel size in the computation of the gaussian fit function and its derivative.

The line blending problem calls for a scrutiny of the available calibration tables (LINCAT tables in the MIDAS environment). With the majority of the lines more or less seriously affected by blends, the choice is somewhere in between adopting corrections to the laboratory wavelengths according to the instrument's characteristics and the applied reduction procedure, or selecting a relatively small number of almost unblended lines. The weak points of the first choice are the dependence of the corrections on line strengths (which may vary with age, temperature, internal pressure, etc. of the lamp) as well as on measurement and reduction parameters (PSF, line centre-to-pixel centre position, window used in fitting). The selection possibility on the other hand reduces the number of available calibration lines substantially and creates the need for a global wavelength calibration in order to prevent errors from fitting small numbers of lines in each order to become the major error source (in our set-up the frame includes 21 orders i.e.

84 coefficients to be determined in the standard MIDAS procedure).

We performed theoretical and empirical tests, fully independent from r.m.s. considerations, to build a system for calibration line selection that allows as much freedom as possible to the potential user. On the one hand, we degraded the laboratory thorium spectra according to our instrumental set-up and calculated blend-induced offsets $\delta\lambda$ for several line centre-to-pixel centre positions by gaussian fitting using windows including up to 7 pixels. On the other hand, we searched empirically for evidence of blends by exploiting the different sensitivity for asymmetries of the "gaussian" and the "gravity" methods. The latter test has been performed on 3 complementary frames i.e. each shifted by $\frac{1}{3}$ pixel in order to achieve optimal results (the detection sensitivity for a particular blend depends strongly on line centre-to-pixel centre position). The test is inherently insensitive to close blends (separation much less than one pixel) and is noise-limited. If one wants to be reasonably confident that the final r.m.s. is not dominated by uncertainties in the corrected laboratory wavelengths, the range of allowed corrections $\delta\lambda$ should be not much larger than the expected r.m.s. and its associated uncertainty ϵ certainly not larger than half that value. In our case, we selected about 85 lines using $|\delta\lambda| < 5 \cdot 10^{-3}$ Å, $0 \leq \epsilon \leq 1.5 \cdot 10^{-3}$ Å to have a reasonable frame coverage (Fig. 4) and checked a posteriori that relaxing the criteria up to $|\delta\lambda| < 2 \cdot 10^{-2}$ Å and $0 \leq \epsilon \leq 2 \cdot 10^{-3}$ Å did not change the wavelength calibration solu-

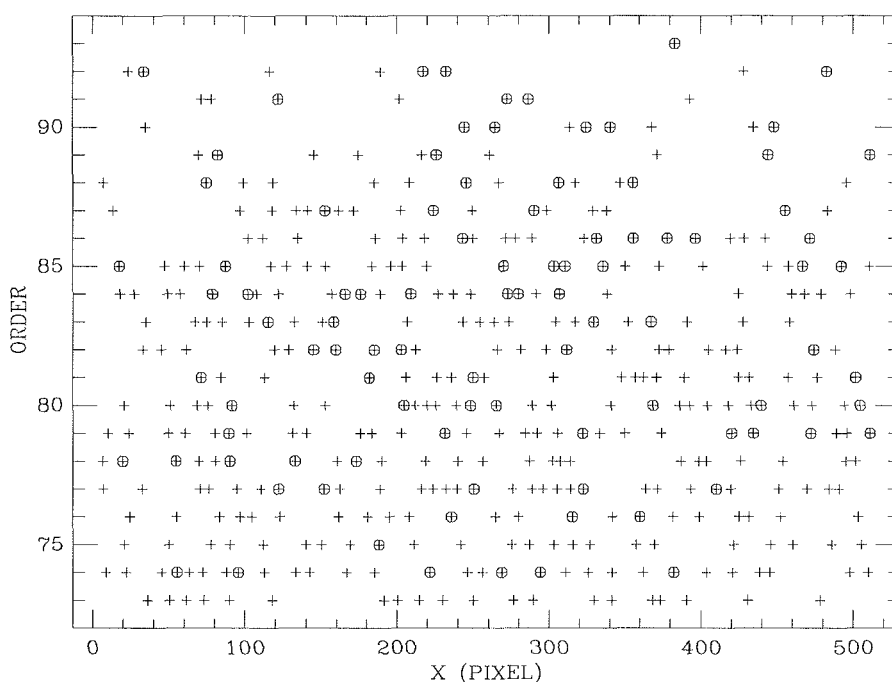


Figure 4: Distribution of identified (+) and selected lines (encircled).

tion discussed hereafter although the inclusion of about 25 additional lines did enhance slightly the r. m. s. of the fit. The calibration solution itself remained stable with respect to the line selection as long as it was stringent enough to exclude lines whose assumed (blend)-wavelength is presumably wrong by at least 4 to 5 times the noise-expected uncertainty. The information content of the computed r. m. s. however does depend more critically on the selection and the r. m. s. rises strongly when the conditions on ϵ are further relaxed.

The calibration has been made finally using a *global fit* of the form

$$\lambda(x, m^*) = \frac{a_0 + (a_1 + b_1 m^*)x + a_2 x^2 + a_3 x^3}{1 + c_1 m^*}$$

with $m^* = \text{constant} - m$, conform to the MIDAS order renumbering, equal to 1 for the highest observed order (the constant being 94 in our case) and x running from 1 to 520 (CCD # 3) defining the actual position of the line centre along the extracted order m^* . Table 1 lists approximate values for the coefficients obtained for two frames taken in different runs. Notice that the term in m^* in the nominator reduces the r. m. s. of frame 2 very significantly, while it is more or less insignificant in the fit of frame 1.

Figure 5 compares the residuals relative to this global fit with selected lines against the residuals obtained using the standard MIDAS procedure, however with the “gravity” method already replaced by gaussian fitting. It illustrates the dominant contribution of line blending to the r. m. s. Moreover, notice in Figure 5a the correlation between low residuals and small numbers of lines for $m \geq 88$, characteristic for overfitting of the data.

Figure 6 shows the wavelength differences generated by these fits at corresponding positions in the frame. Differences of 1 to 2 km s⁻¹ are very common, while the r. m. s. of almost un-

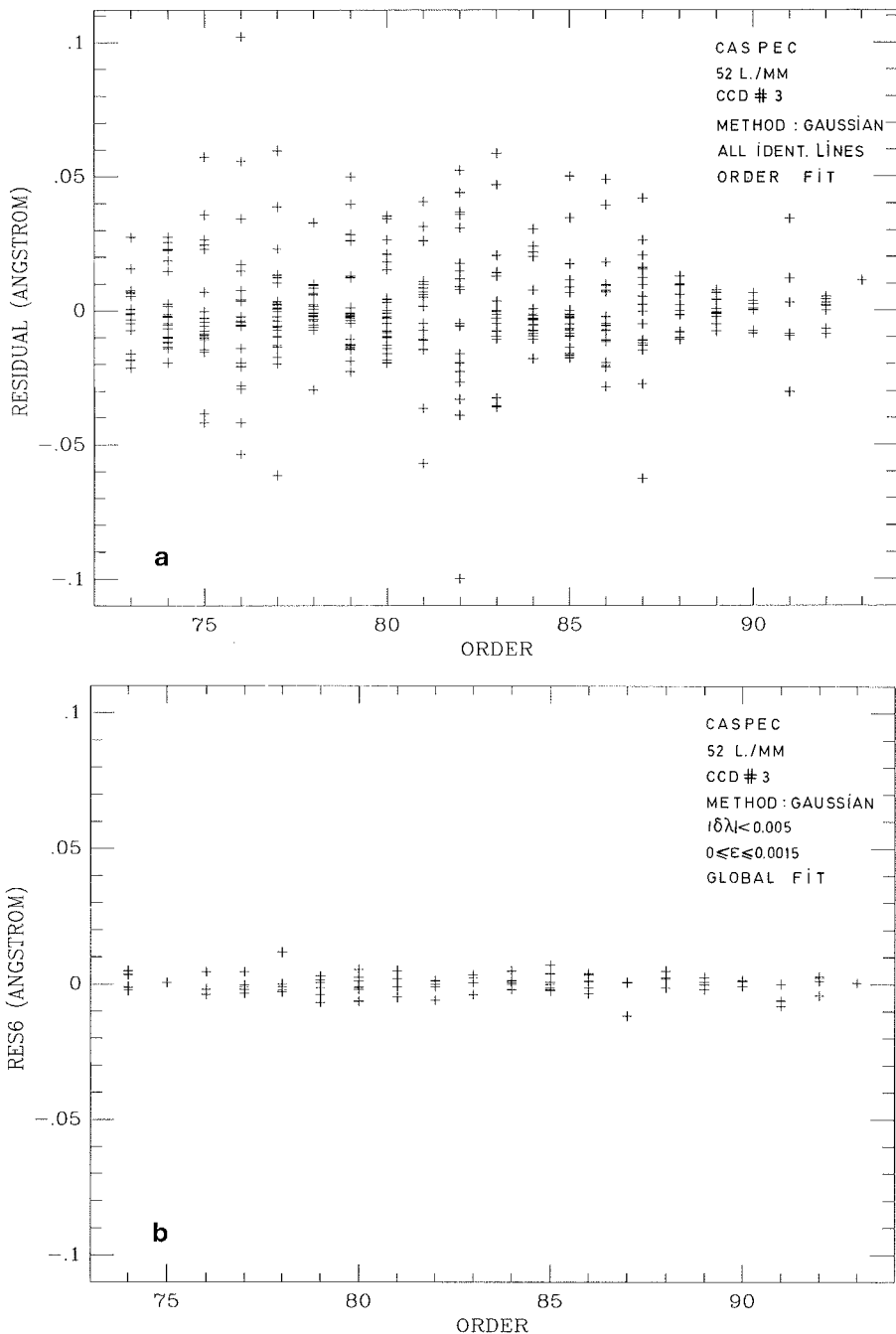


Figure 5: Residuals in the wavelength calibration for the standard MIDAS procedure with gaussian fitting on all identified lines (5a) and in case of the proposed global fit using selected lines (5b).

Table 1. Approximate fit coefficients and the maximal contribution in absolute value of the corresponding terms. Last rows give r. m. s. of residuals with b_1 included as free parameter or fixed to 0.

| Coeff. | Frame 1 (Dec. 86) | Frame 2 (Jan. 88) | Max. contr. (Å) |
|---------------------|-----------------------|-----------------------|-----------------|
| a_0 | 3637.2 | 3635.6 | constant |
| a_1 | 0.118 | 0.118 | 61.4 |
| a_2 | $-0.86 \cdot 10^{-5}$ | $-0.86 \cdot 10^{-5}$ | 2.3 |
| a_3 | $-0.08 \cdot 10^{-8}$ | $-0.16 \cdot 10^{-8}$ | 0.23 |
| b_1 | $-0.16 \cdot 10^{-5}$ | $-0.55 \cdot 10^{-5}$ | 0.06 |
| c_1 | -0.010749 | -0.010742 | — |
| r. m. s. | | | |
| $b_1 = 0$ | $4.6 \cdot 10^{-3}$ | $5.2 \cdot 10^{-3}$ | |
| $b_1 = \text{free}$ | $4.5 \cdot 10^{-3}$ | $3.3 \cdot 10^{-3}$ | |

blended lines relative to the global fit is only 0.3 km s⁻¹.

Figure 7 finally illustrates the adverse effect of the “gravity” method, showing the residuals to our global fit when this “gravity” method is used to define the actual line position. The residuals are plotted to the line centre-to-pixel centre position rather than to order number to show its (expected) dependence on that quantity.

Discussion and Conclusions

The effects of line blending and, to a lesser extent, the definition of line centre

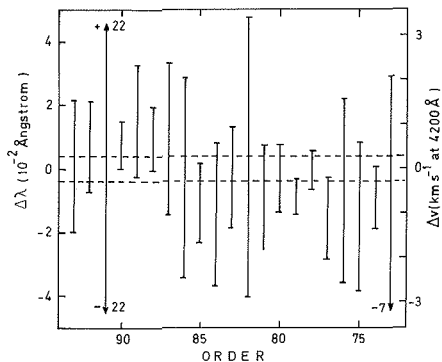


Figure 6: Range of differences between the wavelength predicted by our global fit and that predicted by the standard MIDAS order-per-order fit. Labels indicating the larger ranges refer to the ordinate scale at the left ($\Delta\lambda$). The horizontal broken lines indicate \pm one standard deviation of the residuals in the global fit.

by the “gravity” method, give dominant contributions to the residuals between predicted and measured line positions. They affect the wavelength calibration increasingly with the number of parameters allowed in the calibration fit. The global calibration fit $\lambda = \lambda(x, m^*)$, deduced empirically from the regularities seen in provisionally made bivariate polynomial fits, has given excellent results i.e. residuals of about 0.03 pixel. Additional support for its validity comes from the fact that it predicted better than bivariate polynomials the wavelengths of the best (relatively weakly blended) not-selected lines, even when the polynomials were allowed to have up to 24 parameters.

Both the questions whether there is any theoretical support for this formula and whether it is (more) generally applicable to other echelles remain to be investigated. Since the mathematical form of $\lambda(x, m^*)$ should be obviously invariant for linear transformations in x and m^* (i.e. for scaling and zero-point changes), the formula to be actually tested should contain at least an additional term in m^* in the nominator,

$$\lambda(x, m^*) = \frac{(a_0 + b_0 m^*) + (a_1 + b_1 m^*)x + a_2 x^2 + a_3 x^3}{1 + c_1 m^*}$$

In our case b_0 appeared to be indistinguishable from 0, but it would not have been with any zero point definition.

Goodrich and Veilleux (1988) recently proposed a somewhat similar global formula, a bivariate polynomial in x and $1/m$ that might be conveniently written as

$$\Lambda(x, m) = - \sum_{k=0}^2 (A_k + B_k m) x^k$$

They claim much higher residuals, 0.2 to 0.5 pixel. Since part of it might be due

to line blending effects (they start with about 600 calibration lines per frame and reject in up to 5 iterations outliers (residual $> 5\sigma$), but Figure 3 shows that such procedure is relatively inadequate (as statistically the probability that a blending line causes a given wavelength offset decreases smoothly with the size of the offset), we also tried to fit our selected data with this type of calibration formula. However, we did not obtain lower residuals, so that its usefulness is at best limited to the particular kind of echelle discussed by Goodrich and Veilleux (1988) for which it was intended. The main difference with our formula is the denominator, where we have $m + \text{constant}$ instead of m , the constant being near to 1 in our case. It turns out that optimization of this constant is a necessary condition to obtain an accurate solution for CASPEC.

Our main conclusions are, that

(i) in order to achieve high precision in the wavelength calibration of CCD echelle spectra, a careful selection of reference lines is required, and the method “gaussian” should be used in the definition of line centre.

(ii) a global calibration model $\lambda(x, m)$ describes accurately the measured line positions in the case of “blue” CCD CASPEC echelle spectra.

The success of the global model is essential with respect to (i) in so far that it permits to apply a stringent selection on the thorium-argon reference lines.

MIDAS users interested in an accurate wavelength calibration will find already part of the possibilities discussed here available in MIDAS. Presently, the portable MIDAS version already includes “gaussian” as default method. A catalogue of thorium-argon lines including indications on the blending of the lines in the wavelength range 3700–9000 Å is also available in Garching. This catalogue will be updated end 1989 to include our theoretical study of blending due to argon based on a wavelength list compiled by Norlén (1973). This reference contains accurate wavelengths for a large sample of the ArI and ArII lines seen in the CASPEC calibration spectra (it may also be useful to improve some argon wavelengths in the LINCAT tables) as well as for weaker lines that may nevertheless perturb thorium lines. The catalogue is an extension of the LINCAT tables in the sense that columns specifying our parameters $\delta\lambda$ and ϵ are added. The user might create his own selection from this catalogue by applying the SELECT/TAB command on the added columns and by adding the corrections $\delta\lambda$ to the (uncorrected) wavelengths in the first column. Although compiled for one specific dispersion, it remains useful at higher dispersion (e.g. smaller pixel size) when the selection is limited to almost unblended lines. It is believed that the definition of the risk factor through $\delta\lambda$ and ϵ leaves

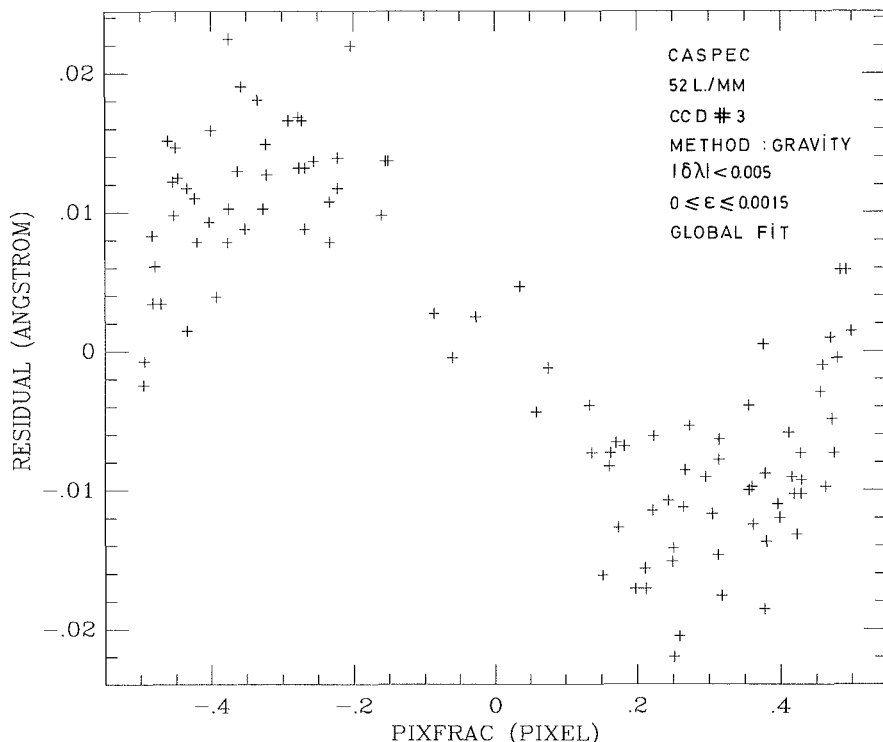


Figure 7: Influence of the “gravity” method on the residuals in the wavelength calibration (global fit using selected lines). PIXFRAC is the “gravity” computed pixel fraction position of line centre.

room for interpretation and generalization whenever necessary. Presently, ϵ includes uncertainties due to line centre-to-pixel centre position, window choice in the gaussian fitting (up to 7 pixels), FWHM of the PSF (up to 2 pixels). ϵ is provisionally set to a predefined code when there is empirical evidence for blending with argon lines. Blends with weaker argon lines undoubtedly remained unrecognized, especially above 4700 Å where the empirical test turned out to be less sensitive (among others due to the undersampling of the lines in the available frames).

At present, however, the user will have to specify his (own) global dispersion fit function using the possibility

offered by MIDAS to define user functions, and he will himself have to take care of the transport of the coefficients in the system during the further reductions. Nevertheless, ESO is looking into the possibility to include the alternative of global dispersion formulae in future versions of the echelle package.

Acknowledgements

We gratefully acknowledge the cooperation of ESO staff. In particular, this work benefited from discussions and correspondence with D. Baade and D. Ponz. The calibration spectra in the red were provided by J. Melnick. The MIDAS reductions were performed

using the facilities at ESO-Garching. H. Van Diest (KSB) helped in introducing software changes in IHAP for test purposes in Brussels. The Belgian Nationaal Fonds voor Wetenschappelijk Onderzoek is acknowledged for a grant in connection to this work (nr. S2.0091.88).

References

- D'Odorico, S., Ponz, D.: 1984, *The Messenger* **37**, 24.
 Goodrich, R.W., Veilleux, S.: 1988, *Publ. Astron. Soc. Pacific* **100**, 1572.
 Norlén, G.: 1973, *Physica Scripta* **8**, 249.
 Palmer, B.A., Engleman, R.Jr.: 1983, *Atlas of the Thorium Spectrum*, Los Alamos National Laboratory, ed. H. Sinoradzky.

Pushing CASPEC to the Limit

E. J. WAMPLER, ESO

Recent CASPEC users will have noticed that there is a continuing programme to upgrade the capabilities of the spectrograph. Together with electromechanical modifications of the spectrograph itself, there have been changes in the data reduction procedures. In addition, there is now substantially more experience with the biases that ESO reduction techniques introduce into the data. These improvements and the increased understanding of the critical processes can lead to a substantial increase in the limiting magnitude of CASPEC over that obtained in the past. Here I want to discuss some of the important choices to be made if good signal-to-noise (S/N) ratios, together with high resolution, is needed for faint objects. A general description of CASPEC has been given by D'Odorico et al. (1983).

The detector now used with CASPEC is RCA CCD number 8. This CCD has a readout noise equal to about 25 e⁻ when it is used with its controller operating at high gain. When observing faint objects, the CCD controller should be operated at the highest possible gain since faint sources do not tax the dynamic range of the system and a small step size in the analogue to digital conversion of the data reduces quantization errors when working at low signal levels.

CCD number 8 has several cosmetic and operational problems that affect its ability to detect weak signals. Between columns numbers 1 and 40 the background drops with increasing column number. Column numbers 40–45, 161 and 201 are always bright and must

be discarded. For approximately 48 hours after the CCD has first been turned on, the dark current is high, initially as much as one hundred times the 2–3 e⁻ pix⁻¹ hour⁻¹ that is reached after a few days of operation. Therefore, observational programmes that are directed to the spectra of objects fainter than about mag 15 should be scheduled after programmes for brighter stars. CCD number 8 has some UV sensitivity but the sensitivity below about 4300 Å drops rapidly. It is possible to reach magnitude 14 or 15 at 3700 Å with a S/N ratio of about 50 after an integration time of several hours. At 5000 Å the gain in limiting magnitude over that at 3700 Å is about 2 magnitudes.

Even though the readout noise of CCD number 8 is lower than that of ESO's other RCA CCDs, this readout noise is still the dominating noise source when faint objects are observed. Therefore, the S/N ratio that can be achieved is directly proportional to the integration time rather than the square root of the integration time as is the case when the limiting noise source is not the detector noise. I have used integration times as long as 5 hours when observing faint sources. Such long integration times do result in a large number of cosmic ray events. However, the situation is not as bad as it may first appear; CCD number 8 is a high resolution CCD and the small, 15 μm square, pixel format greatly aids the identification and removal of cosmic ray events. Figure 1 shows the results of removing cosmic ray noise from CCD exposures on the 16.5-mag quasar UM402 = Q 020207-003. Figure 1 a

shows a three-hour frame before cleaning. In Figure 1 b the lower threshold of the image was set to 280 DN, just above the highest level reached by the quasar signal. In Figure 1 b nearly all the cosmic ray events are seen. Despite the large number of cosmic ray events seen in the figure, only about 1% of all image pixels are affected by these cosmic rays. Filtering programmes, if used with a fixed threshold set to 280 DN (just above the highest level of the quasar signal), can be very effective in removing the cosmic ray tracks seen in this image. The cosmic ray impacts on the CCD generate a large number of electrons but these do not migrate very far in the Si substrate. The influence of a cosmic ray impact is confined to only a few pixels. Because these pixels are small, the contrast between the cosmic ray events and the photon signal from the spectrum is large. Leach (1988) has measured the cosmic ray e⁻ generation in CCDs. He finds that the differential pulse height distribution of cosmic ray generated electrons has a peak at about 400 e⁻. This distribution is very skewed to high energy events; only a small fraction of all events produce fewer than 400 e⁻.

The ESO RCA CCDs also show events caused by a local source of radioactivity. At least for CCD number 8, the local source has a pulse height distribution that is similar to that of the cosmic rays. An examination of the detected radiation events seen on long exposure frames taken with CCD number 8 indicates that aside from differences in the total counting rate, the cosmic ray model of Leach (1988) ade-

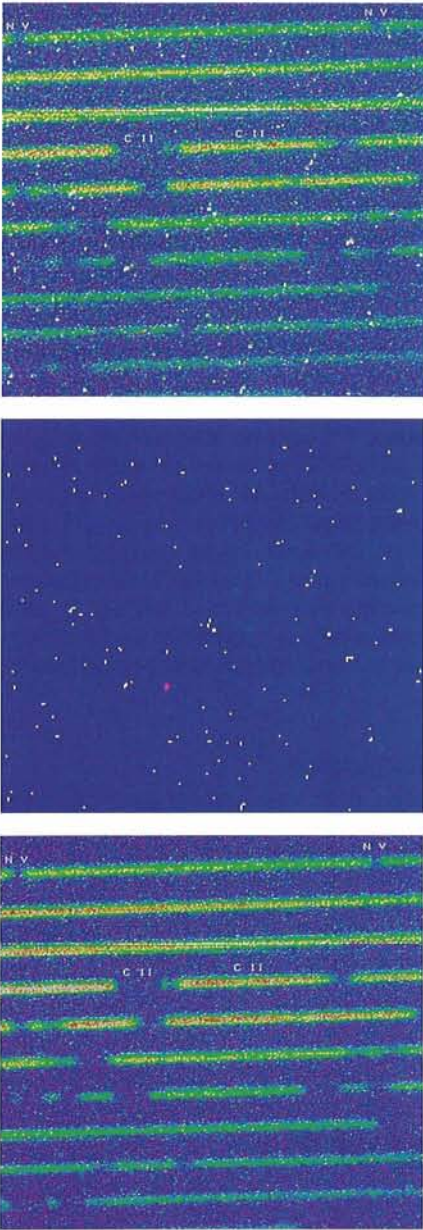


Figure 1: **a** (upper) A three-hour exposure of the 16.5-mag quasar UM 402. The intensity scale of this frame is in the range $200 < DN < 260$. **b** (middle). The same frame as the upper one but with the intensity scale in the range $280 < DN < 290$. This image clearly shows the cosmic rays "hits" accumulated during the three-hour exposure. **c** (bottom). The average of two three-hour exposures after the images were cleaned as described in the text. Several absorption lines are identified.

quately describes the radiation events found in CCD number 8 images. After experimenting with alternative programmes for removing these events from the image, the MIDAS programme called "MEDIAN/FILTER" was used since, with a suitable choice of parameters, this programme is effective in removing the cosmic ray events while doing minimal damage to the underlying data.

Figure 1c shows the average of two three-hour integrations; clearly, the

effects of the cosmic rays have been largely suppressed. The location of strong features due to C II and NV lines are indicated together with the weak C II fine structure transition. It is noticeable that the residual intensity in the centre of the C II line is very low. After data reduction this intensity was found to be less than 5%. Figure 2 shows a plot of the data in the neighbourhood of the C II line after extraction and wavelength calibration but before any correction for the sky or scattered light background was made. The scattered light properties of CASPEC are quite reasonable.

In order to improve the stabilization of CASPEC, a mechanical grip has been installed to clamp the cross disperser, which in the past has been held in position by an active servo system that had a small amount of jitter.

When CCD number 8 is used with CASPEC, a single pixel corresponded to 0.36 arcsec perpendicular to the dispersion and 0.56 arcsec along the dispersion. With the $31.6 \text{ groove mm}^{-1}$ grating the spectral resolution represented by a single pixel was about $R \equiv \lambda/\Delta\lambda = 65,000$. Although the optics of the spectrograph are nearly good enough to actually achieve this resolution, atmospheric seeing, guiding errors and the need to oversample the image reduced the resolution. For the UM 402 observations a 1.8 arcsec wide slit was used, but the seeing during the observing period was equal to, or less than, one arcsec. This gave a resolution approaching $R = 30,000$. The narrowest lines seen in the spectrum of UM 402 suggest that the velocity resolution exceeded 15 km s^{-1} ($R = 20,000$).

The 3.6-metre telescope was guided using a TV guiding system locked to an offset guide star. To monitor the guiding, a mirror was periodically inserted behind the spectrograph slit to relay transmitted light to a second camera that gave a display of the quasar image in the slit. The position of the offset guider was adjusted from time to time to remove the effects of differential flexure between the guide probe and the spectrograph and to accurately maintain the centring of the quasar image in the spectrograph slit. For faint objects, wide slits should be used in order to pass as much starlight as possible into the spectrograph. It is important to check the centring of a faint star by seeing the light transmitted through the slit. The CASPEC slit jaws do not have good edges. If the star is slightly off centre, it is possible to lose a substantial amount of light on the rounded edge of the slit jaw without seeing the lost light when viewing the image of the slit face.

Experiments showed that for observations in the declination range $+10 > \delta > -40$ and with the entrance slit oriented along the East-West direction, the principal component of internal spectrograph flexure displaces the spectrum perpendicular to the dispersion. The amount of this flexure can be reduced by rotating the spectrograph 180 degrees at meridian passage. Differential atmospheric refraction can shift the position of the blue image of the quasar in the slit relative to that of the green image detected by the TV camera system. Systematic shifts of several km s^{-1} between the two ends of the spectra are possible. If the spectro-

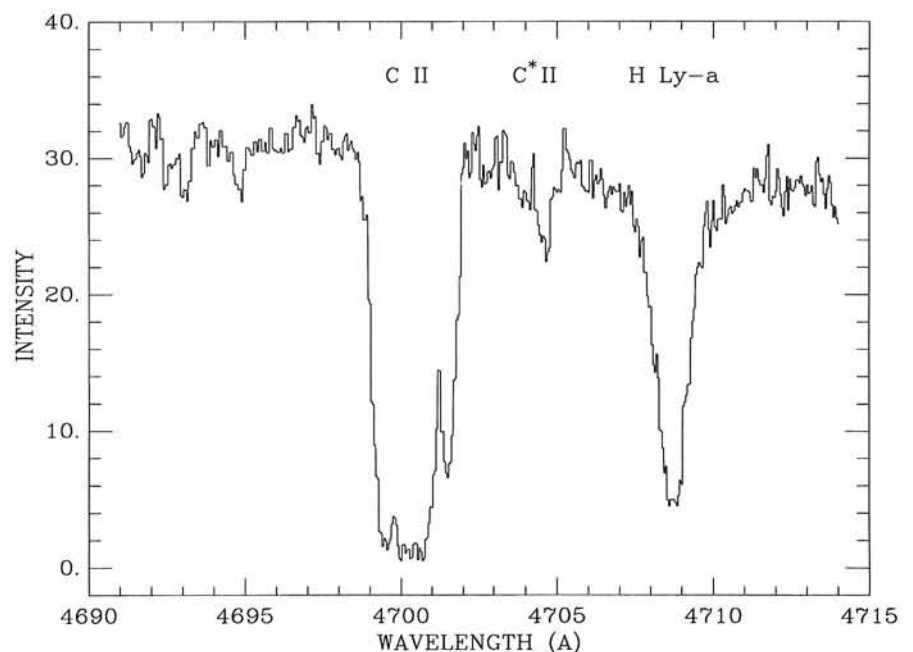


Figure 2: An extracted portion of the spectrum shown in Figure 1c. Note the residual intensity from scattered light in the bottom of the saturated C II line.

graph is rotated at meridian passage in order to reduce the total flexure, and if the observations are centred on meridian passage the principal result of this shift is to smear the violet end of the spectrum, rather than to create a systematic wavelength dependent velocity shift.

The wavelength calibration is obtained from observations of a Th-Ar lamp. In the reduction process 50 to 70 spectral lines were used to determine the calibration of each echelle order. (Over 10^3 lines are used for wavelength calibrations in the blue green spectral regions). The use of many lines strongly constrains the two dimensional wavelength fit and, to some extent, reduced the calibration errors caused by line blends and misidentifications in the Th-Ar wavelength table. The wavelength calibration process is an iterative one: the first step is to obtain an initial calibration using only the strongest lines. This initial calibration is then used to constrain a second calibration that uses much weaker spectral lines. If the weak lines are used initially, the programme usually finds an incorrect solution for the line fit. But if the wavelength calibration is done correctly, the mean residuals to the fits are about $9 \text{ m}\text{\AA}$ in the blue and $12 \text{ m}\text{\AA}$ in the yellow. In each case this is about $\frac{1}{2}$ pixel or about 0.7 km sec^{-1} .

The motion of the earth can also result in a differential velocity shift of several

km s^{-1} between the beginning and the end of a long integration. The principal effect on the spectrum of the observatories changing velocity vector in space is a reduction of the spectral resolution. A careful choice of the time of observation can mitigate this problem.

If it is intended to convert the observed wavelengths to vacuum values, the formula given by Allen (1964) for the refractive index of air can be used. His formula is valid for standard temperature and pressure and is not strictly correct for the high altitude conditions at La Silla. The difference can amount to about 20 km s^{-1} . The differential effect is approximately 400 m s^{-1} between 4000 \AA and 6000 \AA .

An important feature of the MIDAS extraction programme is that it rebins the raw image pixels to a uniform wavelength scale before merging individual spectral orders. In order not to degrade the spectral resolution of the extracted spectrum, software bin widths of 0.05 \AA can be chosen for the blue spectrum, and for the red 0.10 \AA bin widths were used. Both of these choices result in bins that are narrower than the wavelength span of a single CCD pixel. Unfortunately, the rebinning substantially increases the apparent noise in the spectrum. A discussion of "pattern noise", but in a slightly different context, is given in a paper by Dick et al. (1989). The reduction procedure could be im-

proved if the original CCD pixel width was retained. This would result in a non-uniform wavelength spacing of the pixels. At present, with the available software, this is not possible. Rebinning to a coarser grid than the CCD pixel smooths the data but at the expense of lowering the resolution of the spectrum. I think that some of the even pixel, odd pixel jitter in the spectrum seen in Figure 2 is due to this rebinning pattern noise.

I hope that some of these comments prove useful to the CASPEC user community. A total system efficiency of about 4% can be obtained when using CASPEC! This is rather good for the present state of instrument development. New detectors are on the way, and new instruments and telescopes will make our existing facilities seem modest. But for now CASPEC, if used intelligently, is a powerful tool for widening our understanding of the Universe.

References

- Allen, C.W. 1964, *Astrophysical Quantities* (London: The Athlone Press), p. 144.
 Dick, J., Jenkins, C. and Ziabicki, J. 1989, *Pub. Astron. Soc. Pac.*, **101**, 684.
 D'Odorico, S., Enard, D., Lizon, J.L., Ljung, B., Nees, W., Ponz, D., Raffi, G. and Tanné, J.F. 1983, *The Messenger*, **33**, 2.
 Leach, R.W. 1988, *Pub. Astron. Soc. Pac.*, **100**, 853–858.

More Light Through the Fibre: an Upgrading of the Link 3.6-m – CES

S. D'ODORICO, G. AVILA and P. MOLARO, ESO

1. The Configuration of the Fibre Link Today

Different types of commercial fibre optics find useful application in modern astronomical instruments. ESO has been particularly interested in the use of fibres as "light pipes" to feed spectrographs at a distance from the telescope. This is the case of the Coudé Echelle Spectrograph (CES) fed through a 35 m long fibre from the Cassegrain focus of the 3.6-m telescope, alternatively to the standard use with the CAT telescope. The gain one can achieve by using the larger telescope can be as large as two magnitudes over a wide spectral range and this difference opens the way to an entirely new class of observations that at the CAT would be photon limited. Obviously, would-be observers have to be aware that when the link operates,

both the CAT and the 3.6-m need to be "booked". As a consequence, the OPC checks with special care whether the use of the larger collecting area is indeed absolutely necessary. A very convincing case and an outstanding scientific justification are a must for these programmes.

ESO observers have access to this new observing mode as of April 1988. A complete description of the set-up had been given in the article by Avila and D'Odorico in the Proceedings of the ESO Conference on "Very Large Telescopes and their Instrumentation", p. 1121 (1988). In March 1989 the system was upgraded and we report here on the options which are now available and on the overall efficiency. This information complements what can be found in the March 1989 version of the Operating Manual of the CES.

There are now four fibres permanently installed between the Cassegrain cage of the 3.6-m telescope and the entrance to the CES. Table 1 summarizes the characteristics of the four fibres. Two types of lenses are used on different fibres to image the pupil of the telescope on the fibre input face and change the input ratio from F/8 to around F/3. The rod lenses have a better transmission below 4000 \AA , the self-foc lenses are slightly more efficient between 5000 and 10000 \AA . The transmission of the Polymicro and GFO fibres are approximately equivalent (see Fig. 1); both are used with a 3.4 arcsec diaphragm at their entrance. The smaller core diameter QSF fibre is used with a 2.4 arcsec diaphragm: it has no transmission below 4000 \AA , but it is more efficient than the other two types above 7000 \AA . Three new image slicers are

also available. They are built from silica with transmission around 90% over the entire spectral range. The output end of the working fibre is coupled by a field lens and a triplet to the input face of one of the image slicers. In March 1989 the triplet was also substituted with one made of UV transparent glass with high efficiency over the entire spectral range. The optical system converts the F/3 beam from the fibre to the F/32 beam accepted by the CES collimator. The image slicers "reformat" the image of the fibre into an artificial, narrow long slit. The properties of the different slicers and their optimal coupling to the different fibres and cameras of the CES are also given in Table 1. The resolution on the spectra is determined by the projected width of the slices on the detector. In the March run, using the image slicer #2, we measured an average resolution of 55,000 with the short camera and of 75,000 with the long one.

At the beginning of an observing run with the fibre link, the OPTOPUS adapter is mounted at the Cassegrain focus of the 3.6-m. The fibre of choice is mounted on a special OPTOPUS plate in the central hole of a small mirror, which is used to reflect the light not entering the fibre to the guiding TV. This is normally sufficient to operate the autoguider. On the other end, at the level of the coudé room floor, the fibre, the projection optics and the image slicer replace the mechanical slit at the entrance of the CES. The adjustment of the fibre at the centre of the guiding mirror and at the other end the coupling of the fibre to the image slicer are relatively simple operations which however require time and skill. For this reason they cannot be done during the night.

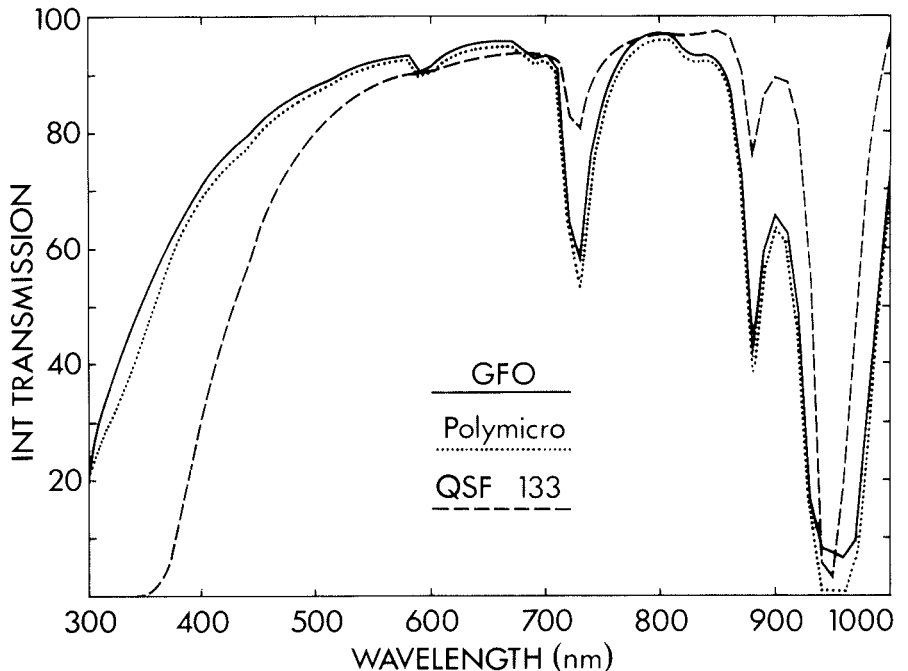


Figure 1: Measured internal transmission of three 35-m fibres used in the link.

Observers are actually asked to identify a single configuration of the link they want to use with a given CES camera to minimize the intervention of the La Silla staff.

2. The Efficiency of the CES Fed by the CAT or by the 3.6-m

The paper by Avila and D'Odorico quoted above included an estimate of the overall efficiency of the link and a measurement in the visible. The internal transmission of the 35-m fibres identified in Table 1 is shown in Figure 1. Additional losses are introduced by the absorption in the various optical com-

ponents of the link and in their interfaces. In order to obtain a set of reliable values, four standard stars were measured in March 1989 both through the link and with the CAT at 6 different wavelengths: 3636, 4030, 5020, 5520, 6460 and 8080 Å. These values were chosen close to the centres of different echelle orders of the CES. The efficiencies at wavelengths far from the blaze can be substantially lower (see Table 2.1 of the CES Operating Manual). The observations in the UV-blue were obtained with the short camera, those in the visible-red region with the long one. For the fibres from the 3.6-m the 3.4-arcsec entrance aperture was used; for the observations with the CAT the entrance slit of the spectrograph was widened to 5 arcsec. The observations were distributed over different nights, all of excellent photometric quality. With both cameras the detector was the standard CES CCD, a double density RCA (ESO #9). The results of this comparative test are shown in Figure 2. The limiting magnitude plotted on the y-axis is defined as the magnitude of a star which at that wavelength produces one photoelectron/Å/sec on the detector. The values were measured for an average seeing of 1.5–2 arcsec and the scatter in the measurements of the different stars was better than ± 0.3 magnitudes. From these numbers the observers can easily estimate the exposure times needed to reach a given signal-to-noise ratio. The gain of the 3.6-m over the CAT is consistently around 1.8 magnitude at all wavelengths longer than 5000 Å, it is 1.5 mag at 4000 Å and drops to .65 mag in the UV where the

TABLE 1: Options Available at the Fibre Link

| Fibres | | | | |
|---------------|------------------|--------------------|---|-----------------|
| Type | Core diameter | Input ¹ | Coupling lens | Recommended use |
| GFO | 200 μ | 3.4 | rod lens/UBK7 | Blue wavel. |
| GFO | 200 μ | 3.4 | self-foc lens | Red wavel. |
| Polymicro | 200 μ | 3.4 | rod lens/UBK7 | Blue wavel. |
| QSF | 133 μ | 2.3 | self-foc lens | Red wavel. |
| Image Slicers | | | | |
| ESO # | Number of slices | Width ² | Recommended use | |
| # 1 | 4 | 360 | Short Camera + QSF fibre | |
| # 2 | 7 | 300 | Short and long Camera + GFO or Pol fibres | |
| # 4 | 10 | 270 | Long Camera + GFO or Pol fibres | |

¹ Diameter of the entrance aperture on the sky in arcsec.

² Approximate width of slices at the entrance of CES in micron.

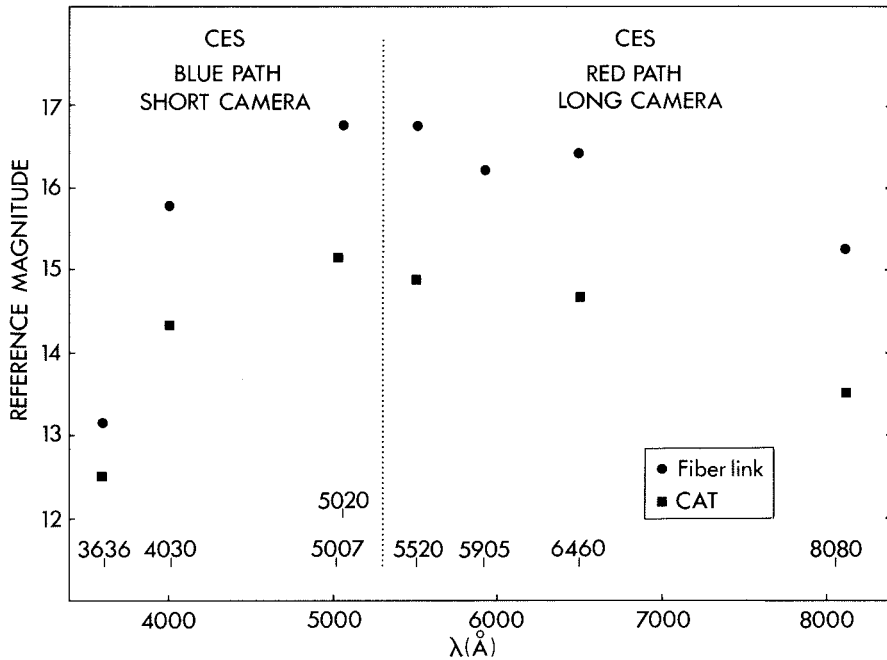


Figure 2: The efficiency of the CES at different wavelengths when fed by the CAT and when used with the fibre link from the 3.6-m telescope. The reference magnitudes on the Y-axis are for stars which give one detected photoelectron/Å/sec.

absorption in the fibre itself is important. The CAT observations were obtained with a 5 arcsec wide slit. The actual gain in a science exposure can be larger than that shown in Figure 2. In medium-poor seeing the narrow slit of the CES will admit less light than the fibre. As an example, with a stellar image of 2 arcsec

FWHM, a typical slit of the CES (1.5 arcsec width, 10 arcsec length) transmits 55% of the light while in the same condition the 3.4 arcsec circular diaphragm transmits 70% of the stellar light.

The measurements have also been used to derive the absolute efficiencies, that is the ratio between the detected

photons and the number of photons falling on the unit surface of the telescope. These numbers take into account the effect of all of the telescope and instrument optics and of the detector. For the measurements with the CAT, these average efficiencies are 0.5, 3.4, 8.6, 9, 7.7 and 2.9 at 3636, 4030, 5020, 5520, 6460 and 8080 Å respectively. The agreement with the values given in the CES Operating manual at slightly different wavelengths is reasonable. The corresponding values from the observations with the 3.6-m and the link are 0.26, 2.1, 6.4, 7, 6 and 2.3 respectively. At wavelengths longer than 4000 Å, the CAT+CES combination is on average 1.3 times more efficient. This advantage is however fully lost when the seeing is 2 arcsec or worse. In those nights the link works at its best and the gain of the larger collecting area is fully realized.

Finally, it is important to call attention to the problems related to the long slit format of the spectra that one obtains with the link. At the beginning of an observing run, the artificial slit produced by the image slicer must be well aligned with the rows of the CCD to avoid a loss of resolution. The use of CCD binning in the direction normal to the dispersion is recommended for those observations where the read-out noise of the CCD (around 30 e/pixel) is a limiting factor. However, binning cannot be too strong if the cosmic ray events which accumulate on the CCD over long integrations have to be identified and corrected for.

A Programme to Simulate Observations with EFOSC2 and EMMI

S. D'ODORICO, J.-L. PRIEUR, G. RUPPRECHT, ESO

Introduction

Every astronomer appreciates the importance of preparing accurately an observing run to optimize the use of the time assigned at the telescope. The preparation implies, among other things, the selection of the observing mode which is best suited to the needs of the scientific programme and the computation of the signal-to-noise ratios (SNRs) one can achieve in a given observing time on the selected targets.

Instrumental models have been developed especially for space instruments to simulate the data obtainable at the telescope and to help in the detailed planning of the sequence of the observations. The possibility of a full simulation is relatively less common with

ground-based telescopes. At ESO, would-be observers have still to rely on the information of the Operating Manuals and do their own computations. This has the disadvantage that the parameters of the instruments are not available in digital form, that a change in the instrument configuration or in the detectors cannot be taken promptly into account and that the results of the computation of the final SNRs come in as many flavours as the number of astronomers.

As a first step in building a set of models which will describe the behaviour of the mostly used instruments at ESO one of us (J.L.P.) has developed in MIDAS a simulation programme for observations with EFOSC2 and EMMI,

two new ESO instruments which are about to come into general use at the NTT. EFOSC2 (eventually to be assigned to the 2.2-m telescope) has the same operating modes as EFOSC, the well-known focal reducer at the Cassegrain focus of the 3.6-m. EMMI is a more complex device which offers the possibility to select in real time among several observing modes. A description is attached to the ESO Call for Applications for Observing Time for period 45. The properties of EFOSC2 (such as the transmission of the optics, of the grisms, etc.) have been fully measured in the laboratory and can be used in the simulation. In the case of EMMI the data set is not complete and a realistic simulation will be working from March 1990

Imaging mode

When finished press CTRL/Z and then on R

| | | | | | |
|-----------|-------------|------------|---------------|-------------|-------------------------|
| Channel | <i>R</i> | Filter | <i>ESO585</i> | Obj spect | <i>EM\$D:EGAL</i> |
| F/D cam | <i>6.7</i> | V obj | <i>25.0</i> | Sky spect | <i>EM\$D:ESKY</i> |
| Detector | <i>CCD1</i> | V sky | <i>22.0</i> | Zenith dist | <i>20.0</i> |
| Prefl. e- | <i>0.0</i> | Seeing | <i>1.0</i> | Out. image | <i>OUT_SIMU</i> |
| Binn in x | <i>1</i> | Exp time | <i>300.0</i> | | |
| Binn in y | <i>1</i> | | | | |
| DETECTOR: | | | | | |
| ESO ident | <i>CCD1</i> | Scale in x | <i>0.167</i> | Full name | <i>THX 31156 coated</i> |
| Ncol. | <i>1024</i> | Scale in y | <i>0.167</i> | Dark e-/s | <i>0.00800</i> |
| Nrows | <i>1024</i> | Bias ADU | <i>100.0</i> | Satur. e- | <i>200000.0</i> |
| ADU e- | <i>2.0</i> | RON e- | <i>6.0</i> | | |

Spectroscopic mode

When finished press CTRL/Z and then on R

| | | | | | |
|-----------|---------------|------------|--------------|-------------|-------------------------|
| Channel | <i>R</i> | Filter1 | <i>CLEAR</i> | Filter2 | <i>CLEAR</i> |
| F/D cam | <i>6.7</i> | V obj | <i>25.0</i> | Obj spect | <i>EM\$D:EGAL</i> |
| Detector | <i>CCD1</i> | V sky | <i>22.0</i> | Sky spect | <i>EM\$D:ESKY</i> |
| Prefl. e- | <i>200.0</i> | Seeing | <i>1.0</i> | Zenith dist | <i>20.0</i> |
| Exp time | <i>3600.0</i> | Disperser | <i>GRIS1</i> | Slit width | <i>0.8</i> |
| Binn in x | <i>1</i> | Slit displ | <i>0.0</i> | Slit length | <i>20</i> |
| Binn in y | <i>1</i> | Dichroic | <i>N</i> | Dispersion | <i>0.856</i> |
| Lambda1 | <i>500.0</i> | Lambda2 | <i>600.0</i> | Lambda3 | <i>700.0</i> |
| DETECTOR: | | | | | |
| ESO ident | <i>CCD1</i> | Scale in x | <i>0.167</i> | Full name | <i>THX 31156 coated</i> |
| Ncol. | <i>1024</i> | Scale in y | <i>0.167</i> | Dark e-/s | <i>0.00800</i> |
| Nrows | <i>1024</i> | Bias ADU | <i>100.0</i> | Satur. e- | <i>200000.0</i> |
| ADU e- | <i>2.0</i> | RON e- | <i>6.0</i> | | |

Figure 1: The appearance of the screen at the beginning of a session of the programme is shown. The various parameters which are needed in a simulation of a direct image or of a spectroscopic observation are displayed and can be edited in an interactive way.

only. The programme is written in MIDAS command language (version 89NOV), and uses MIDAS tables, but the user does not need to be familiar with MIDAS to be able to run it. It works in interactive mode using part of the STARCAT interface. A preliminary User Manual is available with J. L. Prieur, and astronomers at Garching and La Silla are encouraged to experiment with it.

The ST-ECF Space Telescope Model (Rosa, M., Baade, D., 1986, *The Messenger*, 45), was used as a starting point and adapted to our needs and to the portable version of Midas. Although we have not yet tested its portability on work stations and its use on other systems than VAX VMS, it is expected that this should be possible without a major effort. When that step will be completed, the simulation programme will be made part of the official MIDAS software as a new CONTEXT.

Description of the Programmes

For the time being the programme handles stellar-like targets only. The case of a diffuse object of constant brightness will be implemented together with the full EMMI simulator. The computation starts from the spectrum of the

target outside the atmosphere and then takes into account the effect of atmosphere, telescope, instrument optics and detector, to compute the observed data, these being direct images or spectra.

At the beginning of a session, the default parameters for one observation (or those from the previous session) are displayed and the user can change them by moving around the screen with the arrows. An example of the screen with the default parameters for imaging, spectroscopy and the detector with EFOSC2 is shown in Figure 1. The input parameters are checked for consistency, and the transmission and efficiency curves for the telescope, instrument, filter, grism and detector are loaded from tables in the EFOSC2 data base. The user can also modify the detector properties and check in this way whether a different device is better suited for his/her programme.

In the next stage, the input spectra of the object and the sky are normalized to the V magnitudes given by the user. All the tables are resampled to a common scale in wavelength. This requires some computer time, but has the advantage of a higher flexibility. The user can use his own tables for the object and the sky

spectra. The only requirement is to have the wavelength in nm in the first column, and the relative flux in photons in the second column. Standard spectra and an average sky spectrum are available in the programme data base.

With this input the format and the quality of the final data are computed. In the case of spectroscopy, the programme will give the spectral range, the transmission of the slit, the average dispersion and resolution and will compute at three different wavelengths chosen by the users the SNRs of the extracted sky-subtracted spectrum. For imaging, the SNR computation assumes an integration of the total flux of the star-like object, down to a 1% level for a gaussian point spread function.

Four sources of noise are taken into account in the SNR computation: the read-out-noise of the detector, the shot noise coming from the object, the sky, the preflash (if any) and the dark current, and the error in the calibration of the detector pixel-to-pixel sensitivity (taken as 1% of the total level for a given pixel in the default case). These errors are added quadratically and assumed to be independent from one pixel to another.

The main results of the simulation are written in a logfile (SIMU.LOG) which is automatically printed on a laser printer. Curves of the spectral input and output for a given object, sky spectra, and the overall efficiency can be displayed on a graphic terminal, and then sent to a laser printer within the programme.

There is also a possibility of simulating a 2D output image, or an output spectrum (Fig. 2). In the first case the Pleiades cluster as seen at 30 kpc (250 times further than in reality) is used as reference image. The brightest star is placed in the middle of the frame, and normalized to the magnitude given by the user for the object. The relative brightness of the other stars is maintained and the stellar images are scaled according to the seeing and the scale at the detector. A visual impression of the angular resolution and limiting magnitude in the field is then possible.

For spectroscopy, an extracted spectrum is computed from the addition of the brightest rows in the simulated 2D CCD frame down to a 1% level relative to the peak value. The starting point is always the spectral energy distribution of a standard object in the data file scaled at the desired magnitude and including the contribution of the sky over the same aperture. The output spectra from the object alone and sky alone are also available.

The simulation programme includes also parameters which are peculiar to

ground-based observations, that is the average seeing and airmass at the time of the observations.

Conclusion

Even at this early stage of implementation, the EFOSC2 simulator appears as a useful tool to plan and optimize the observations at the NTT. In addition to the planned extension to EMMI, the programme could be easily extended to other, similar instruments by modifying the initial parameters. This can be done using a simple MIDAS procedure to write the desired values in the corresponding MIDAS keywords. The integration into the MIDAS environment makes it possible to display, edit, and print easily the characteristics of the different components which enter in the computation. If this updating is done in a systematic way, the programme will also provide on line an accurate description of the status of a given instrument. One can envisage that in the future potential users will check by a remote login whether the actual status of the instrument corresponds to the version recorded on their local workstation, introduce the upgraded parameters, if any, and then go on with the planning of their observing programme.

It is of course clear that the results of these first simulations need to be systematically compared with the output of real observations to refine the model. This interactive process will start when the first data with EFOSC2 will become available. As the model will become rel-

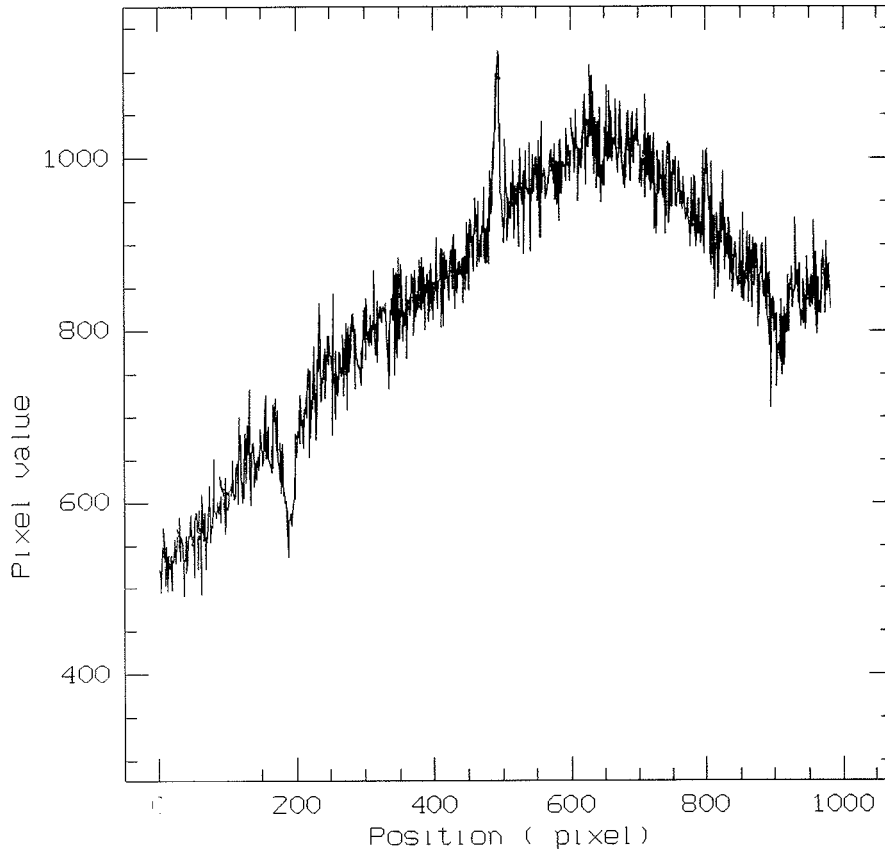


Figure 2: A simulated spectrum of an A5 star of $m(v) = 20$ obtained in 1 hr exposure with EFOSC2 and grism # 4, which gives on the detector (a 1024×1024 CCD with 19μ pixels) the wavelength range 4100–7200 Å. The seeing was assumed 0.5 arcsec (FWHM). The slit width was also 0.5 arcsec. The various sources of noise and the sky spectrum have been added to the stellar continuum.

atively stable and the results fully reliable, one could also think to use the quantitative information that it provides

into the programmes which in the not-too-far future will optimize the use of the telescope by flexible scheduling.

MIDAS Memo

ESO Image Processing Group

1. Application Developments

The FIT package is now available in the portable MIDAS for both VMS and UNIX systems. It was upgraded in a number of areas. Some deficiencies of the old VMS version were corrected, in particular the methods applied to problems with constraints. The implementation is still using some NAG library routines.

A new context LONG has been implemented for the reduction of Long-Slit spectra. This first version provides only basic tools for calibration and analysis. It is planned to perform major upgrades for the spectral packages e.g. ECHELLE and LONG when the final archive tape format has been implemented as output format from instruments. This will en-

able a much more automated reduction sequence than is possible today.

A new context STATIST has been developed for statistical tests on tables. This includes specifically the comparison of empirical distribution with theoretical distribution, the comparison of independent data samples, the measurement of correlation. The Multivariate Analysis package (previously named STATIST) has been renamed to MVA.

In the stellar photometry package ROMAFOT, a major part of the code has been rewritten in order to integrate the software completely within MIDAS environment. In the new version the various file extensions for the different intermediate files (e.g. .Q, .F, .R) are no longer used: ROMAFOT now uses exclusively the MIDAS table file system for storing intermediate and final results. Obviously, with the introduction of the MIDAS tables in the ROMAFOT pack-

age the user is offered greater flexibility since MIDAS commands can now be used to manage the (intermediate) results.

The display parts of the new version of ROMAFOT are either directly based on the Image Display Interfaces or have been rewritten in the MIDAS Command Language (MCL). Hence, ROMAFOT can be used on all systems (VMS and UNIX) with display devices supported by MIDAS. For workstations this implies that an implementation of the X11 windowing software should be available.

2. System Development: Astronet Graphic Library

A new version of the AGL software has been completed. Besides several small improvements, a major effort has been made to improve the management of the graphic window on workstations.

Whereas in the previous implementation of AGL the graphics display in MIDAS was controlled by a separate server, in the new version the graphic display and the image display use a common server. This possibility became available by building an additional IDI driver. As a positive side effect the interaction of the user with the graphics window using mouse and keyboard will now be identical to the interaction with the display window. The new driver will also open possibilities to integrate the graphics and display software more on the level of application software. The new IDI driver for AGL was written by L. Fini during his two weeks at ESO in the autumn. We would like to thank him for this effort.

With the introduction of the IDI driver, installation of AGL for MIDAS graphics is now possible on all workstations supporting X11. Since, for the graphics window MIDAS will only use the IDI driver, all the different server options for the various workstation models are no longer needed. Therefore, we have decided to strip the AGL distribution kit of the parts not used by MIDAS and to integrate the stripped version into the MIDAS directory structure. As a result of this, starting from the 89NOV release of MIDAS a separate implementation of the graphics software will not be needed. The complete distribution kit of AGL, if one wants AGL as a stand alone package, is available from the Italian Astronet Group.

3. MIDAS Support for GNU Software

MIDAS has been ported to the GNU C-compiler and will now compile without warnings under both UNIX and VMS. This is the first strict ANSI C compiler under which MIDAS has been thoroughly tested and we do not expect problems with other ANSI C compilers.

The major advantage of the GNU C-compiler is that it's free. It was developed by the GNU project which aims to provide high quality UNIX system software free of charge. The final goal is to provide a full implementation of UNIX with all utilities for any 32-bit machine. The man behind the GNU project is Richard Stallman, a former MIT AI-expert, who wants to promote software sharing between programmers and fight against the restriction placed on software preventing others from using it without paying. Other software available from the GNU project today is the 'emacs' editor, a source-level debugger and numerous utilities in beta-release.

In addition, the GNU C-compiler ('gcc') is fast and produces good code. We have made some rudimentary tests on our main development machines,

Sun SPARC-stations and a VAX 8600 running VMS, and have found some interesting results. On the Sun, 'gcc' is virtually as fast as 'cc' when compiling without optimization, but twice as fast when compiling with optimization. The code produced is virtually the same quality, both in terms of code size and execution time. Under VMS, only the execution time of the code produced by 'gcc' has been tested and found to be slightly worse, say 10–20%, than the code produced by the VAX11 C-compiler. For MIDAS, however, this is not a major concern since most of the CPU intensive code is written in FORTRAN 77.

The MIDAS developing team encourages the use of the GNU 'emacs' editor, since it, unlike 'vi' and EDT (and derivatives), runs under both UNIX and VMS and also can emulate both 'vi' and EDT.

How do I get GNU software? The software is available in tar-tape format with anonymous 'ftp' from several sources on the Internet. The latest versions are available from 'pre.ai.mit.edu'. Both tar-tapes and VMS backup tapes are available from 'Free Software Foundation' (address below). They take a nominal distribution fee and only accept orders with payment. However, since the software may be distributed freely, you may acquire it from any source where you may have heard that the software is being installed. The computer science department of your local university may be worth a try. Note that the GNU C-compiler cannot be compiled by the VAX11 C-compiler, so the VMS version

must be obtained in compiled form from a VMS source.

Free Software Foundation
675 Massachusetts Avenue
Cambridge, MA 02139
USA

4. Personnel

The Image Processing Group deeply regrets to announce that Daniel Ponz has left the Group to take up a position in ESA. Daniel participated very actively in the MIDAS project from its start in 1981 and developed since then many important packages such as the Table File system and most major spectral reduction packages. We wish him all the best in his new position and will try to minimize the effects for MIDAS of this significant loss.

5. MIDAS Hot-Line Service

The following MIDAS support services can be used to obtain help quickly when problems arise:

- EARN: MIDAS @DGAESO51
- SPAN: ESOMC1::MIDAS
- Tlx.: 52828222 eso d, attn.: MIDAS HOT-LINE
- Tel.: +49-89-32006-456

Users are also invited to send us any suggestions or comments. Although we do provide a telephone service we ask users to use it only in urgent cases. To make it easier for us to process the requests properly we ask you, when possible, to submit requests in written form through either electronic networks or telex.

Manuel Cartes V. (1952–1989)

The departure of Manuel Cartes on September 19th was received with a profound impact at La Silla. Manuel was highly esteemed and appreciated as a colleague and a friend.

He first came to La Silla as a summer student in 1976 and 1977 before joining the ESO staff as a graduated electronics engineer in 1978. Within the electronics section he demonstrated a great enthusiasm and a first rate dedication to his work. He personified a style of commitment which proved to be the base of a successful technical operation. Often Manuel could be seen late at night at the telescopes ready to assist, sparing neither time nor efforts.

In 1982 he went to Europe with the challenge to interface the MPI 2.2-m telescope controls to our environment. It is largely thanks to him that the 2.2-m telescope electronics could be brought in line with our maintenance facilities.

In 1987 he was assigned to the NTT project and started his involvement in Garching. Then came a terrible sickness. At La Silla we had to witness his courageous fight to face this sickness which would eventually overcome his will.

We wish to assure his wife Sylvia, his sons Manuel and Patricio that the memory of his kindness, dedication and friendship will never leave our observatory.

ESO, the European Southern Observatory, was created in 1962 to . . . establish and operate an astronomical observatory in the southern hemisphere, equipped with powerful instruments, with the aim of furthering and organizing collaboration in astronomy . . . It is supported by eight countries: Belgium, Denmark, France, the Federal Republic of Germany, Italy, the Netherlands, Sweden and Switzerland. It operates the La Silla observatory in the Atacama desert, 600 km north of Santiago de Chile, at 2,400 m altitude, where thirteen optical telescopes with diameters up to 3.6 m and a 15-m submillimetre radio telescope (SEST) are now in operation. A 3.5-m New Technology Telescope (NTT) will become operational soon and a giant telescope (VLT=Very Large Telescope), consisting of four 8-m telescopes (equivalent aperture = 16 m) is under construction. Eight hundred scientists make proposals each year for the use of the telescopes at La Silla. The ESO Headquarters are located in Garching, near Munich, FRG. It is the scientific-technical and administrative centre of ESO, where technical development programmes are carried out to provide the La Silla observatory with the most advanced instruments. There are also extensive facilities which enable the scientists to analyze their data. In Europe ESO employs about 150 international Staff members, Fellows and Associates; at La Silla about 40 and, in addition, 150 local Staff members.

The ESO MESSENGER is published four times a year: normally in March, June, September and December. ESO also publishes Conference Proceedings, Preprints, Technical Notes and other material connected to its activities. Press Releases inform the media about particular events. For further information, contact the ESO Information Service at the following address:

EUROPEAN
SOUTHERN OBSERVATORY
Karl-Schwarzschild-Str. 2
D-8046 Garching bei München
Fed. Rep. of Germany
Tel. (089) 32006-0
Telex 5-28282-0 eo d
Telefax: (089) 3202362
Bitnet address: IPS@DGAESO51

The ESO Messenger:
Editor: Richard M. West
Technical editor: Kurt Kjær

Printed by Universitäts-Druckerei
Dr. C. Wolf & Sohn
Heidemannstraße 166
8000 München 45
Fed. Rep. of Germany

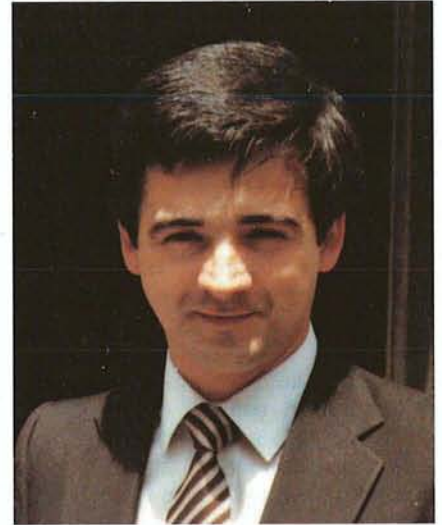
ISSN 0722-6691

Manuel Cartes V. (1952–1989)

El fallecimiento de Manuel Cartes el día 19 de septiembre causó un profundo impacto en La Silla. Era una persona muy estimada y apreciada por todos, tanto como colega y como amigo.

Sus primeros contactos con la ESO los tuvo en los veranos de 1976 y 1977 cuando realizó su práctica profesional como estudiante universitario. En 1978 pasó a formar parte del personal de planta de la organización como ingeniero civil electrónico. Desde un principio demostró gran entusiasmo y una dedicación total a su trabajo dentro del laboratorio de electrónica. Personificaba un estilo muy propio de compromiso en el cumplimiento de sus obligaciones, estilo que demostró ser el fundamento del éxito en las diversas operaciones técnicas. A menudo se podía ver a Manuel, tarde en algún telescopio, siempre dispuesto a cooperar, sin prestar atención ni al tiempo ni al esfuerzo requeridos.

En 1982 fue enviado a Europa con el desafío de participar en la implementación de la interfase entre el telescopio de 2.2 m del MPI y nuestros sistemas. Gracias, en gran parte, a su trabajo la electrónica del telescopio pudo conectarse en línea con nuestros sistemas de mantención.



En 1987 fue asignado al proyecto del telescopio de nueva tecnología (NTT) y debió dirigirse nuevamente a Garching para participar en dicho proyecto. Luego fue víctima de una terrible enfermedad. En La Silla fuimos testigos de su valiente lucha contra el mal que lo aquejaba, el cual, finalmente, doblegó su voluntad.

Deseamos asegurar a su esposa Silvia y a sus hijos Manuel y Patricio que el recuerdo de su bondad, dedicación y amistad perdurará en nuestro observatorio.

Contents

| | |
|---|----|
| F. Merkle et al.: Successful Tests of Adaptive Optics | 1 |
| M. Tarenghi: Astronomical Observations With the NTT During Commissioning | 4 |
| J. Melnick: The First Observations With the NTT | 5 |
| A. Moneti: Spatially Resolved Images of the Optical Counterpart to Circinus X-1 | 7 |
| R. Falomo and J. Melnick: The Nebulosity Around BL Lac Objects | 8 |
| H.E. Schwarz: Possible Transition Objects Discovered with the NTT | 9 |
| B. Jarvis: Narrow-Band Imaging of M87 with the NTT | 10 |
| G. Gouiffes et al.: NTT Images of SN 1987 A | 11 |
| S. Prat: Axial Support Prototypes for the VLT | 14 |
| 2nd ESO/OHP Summer School in Astrophysical Observations | 15 |
| The ESO Research Student Programme: Change of Deadline | 16 |
| First Announcement of the 2nd ESO/ST-ECF Data Analysis Workshop | 17 |
| R. M. West: ESO Exhibition Opens in Copenhagen's New Tycho Brahe Planetarium | 18 |
| ESO Publications | 21 |
| New ESO Scientific Preprints | 21 |
| C. Barbieri et al.: Profile of a Key Programme: A Homogeneous Bright Quasar Survey | 22 |
| A. Blaauw: ESO's Early History, 1953–1975. V. Earliest Developments in Chile; 24 March 1966: The Road on La Silla Dedicated | 24 |
| Second Extension of ESO Headquarters | 31 |
| The R Corona Australis Cloud | 31 |
| H. W. Duerbeck: V 745 Sco – a New Member of the Elusive Group of Recurrent Novae | 34 |
| C. Chavarría et al.: Photometry of Two Southern T Tauri Stars | 35 |
| Staff Movements | 37 |
| M. Heydari-Malayeri: Discovery of a Low Mass B[e] Supergiant in the SMC | 37 |
| P.E. Nissen: CASPEC Observations of the Most Metal-Deficient Main-Sequence Star Currently Known | 40 |
| B. Barbuy et al.: The Peculiar Colour-Magnitude Diagrams of the Metal-Rich Globular Cluster NGC 6553 | 42 |
| A. Acker et al.: On the Theoretical Ratio of Some Nebular Lines | 44 |
| F. Paresce et al.: EFOSC Observations of the Inner Echo Around SN 1987 A | 46 |
| E. Cappellaro et al.: "Deep" Rotation Curves of Edge-on S0 Galaxies | 48 |
| International Portrait Catalogue | 50 |
| Jacques Beckers Elected to Dutch and Norwegian Academies | 51 |
| P. Katgert: The Efficiency of OPTOPUS | 51 |
| H. Hensberge and W. Verschueren: An Accurate Wavelength Calibration of CCD CASPEC Echelle Spectra | 51 |
| E. J. Wampler: Pushing CASPEC to the Limit | 56 |
| S. D'Odorico et al.: More Light Through the Fibre: an Upgrading of the Link 3.6-m – CES | 58 |
| S. D'Odorico et al.: A Programme to Simulate Observations with EFOSC2 and EMMI | 60 |
| ESO Image Processing Group: MIDAS Memo | 62 |
| Manuel Cartes V. (1952–1989) | 63 |